



SPMT

SPMT Conceptual Design Pre PDR

Project Code: TRP/TELE/001-R

Issue: 1.C

Date: 24/06/2014


No. of pages: 153

INSTITUTO DE ASTRONOMIA – UNIVERSIDAD NACIONAL AUTONOMA DE MEXICO

Apartado Postal 70-264 Cd. Universitaria 04510 MEXICO D.F. – Phone: 525556223907 – Fax: 525556160653


URL : <http://www.astro.unam.mx>

E-mail : beatriz@astro.unam.mx

	<p>SPMT</p> <p>SPMT Conceptual Design Pre PDR</p>	<p>Code: TRP/TELE/001-R</p> <p>Issue: 1.C</p> <p>Date: 24/06/2014</p> <p>Page: 2 of 152</p>
---	--	---

Approval control

<p>Prepared by</p>	<p>Jorge Uribe</p> <p>Diana Lucero</p> <p>Alberto Rodríguez</p> <p>Berenice Rodríguez</p> <p>Rogelio Manuel</p> <p>César Martínez</p> <p>CIDESI</p>	
<p>Approved by</p>	<p>Alan Watson</p> <p>Beatriz Sánchez</p> <p>Jesús González</p> <p>IAUNAM</p>	
<p>Authorized by</p>	<p>William Lee</p> <p>IAUNAM</p>	<p>Date: 30-06-2014</p>


	<p>SPMT</p> <p>SPMT Conceptual Design Pre PDR</p>	<p>Code: TRP/TELE/001-R</p> <p>Issue: 1.C</p> <p>Date: 24/06/2014</p> <p>Page: 3 of 152</p>
---	--	---

Applicable documents

Nº	Document title	Code	Issue
A.1	SPMT Specifications	GEN/SYEN/0004-F	Draft
A.2	SPMT Alternatives Evaluation and Budget	GEN/SYEN/0005-F	Draft
A.3	MMT Analysis	GEN/SYEN/0002-F	1.A
A.4	Magellan Analysis	GEN/SYEN/0003-F	1.A
A.5	Site and Geotechnical Study for the SPMT	GEN/SYEN/0001-F	1.A
A.6	Conceptual Design	GEN/SYEN/0006-F	1.A
A.7	Mass Budget,Center of Mass and Moments of Intertia of SPMT Telescope	TEN/TELE/001-F	1.B
A.8	SPMT High Level Requierements	SPMT/HLREQ-001	1.D


Reference documents

Nº	Document title	Code	Issue
R.1			

	<p>SPMT</p> <p>SPMT Conceptual Design Pre PDR</p>	<p>Code: TRP/TELE/001-R</p> <p>Issue: 1.C</p> <p>Date: 24/06/2014</p> <p>Page: 4 of 152</p>
---	--	---


List of acronyms and abbreviations

MMT	Multi Mirror Telescope
SPMT	San Pedro Mártir Telescope
SPM	San Pedro Mártir
OAN	Observatorio Astronómico Nacional
IA-UNAM	Instituto de Astronomía – Universidad Nacional Autónoma de México
CIDESI	Centro de Ingeniería y Desarrollo Industrial


	<p>SPMT</p> <p>SPMT Conceptual Design Pre PDR</p>	<p>Code: TRP/TELE/001-R</p> <p>Issue: 1.C</p> <p>Date: 24/06/2014</p> <p>Page: 5 of 152</p>
---	--	---

CONTENTS


1.	SUMMARY	9
2.	SPMT GENERAL REQUIREMENTS	9
2.1	GENERAL SPECIFICATIONS	9
2.2	GENERAL SITE CHARACTERISTICS	10
3.	OPTICAL DESIGN GENERAL DESCRIPTION.....	11
3.1	F/5 CASSEGRAIN	12
3.2	F/5 NASMYTH.....	12
3.3	F/11 NASMYTH	15
4.	SAN PEDRO MARTIR TELESCOPE GENERAL CHARACTERISTICS	16
4.1	PRODUCT TREE	16
4.2	TELESCOPE STRUCTURE MASS BUDGET	16
4.3	GENERAL KINEMATIC AND MECHANIC CONSIDERATIONS	20
5.	SAN PEDRO MARTIR TELESCOPE MECHANICAL DESIGN DESCRIPTION.....	23
5.1	ALT-AZIMUTH MOVEMENT	24
5.1.1	<i>Elevation and azimuth motor speeds</i>	<i>25</i>
5.1.2	<i>Elevation and azimuth motor acceleration</i>	<i>26</i>
5.1.3	<i>Rotators and field rotation</i>	<i>29</i>
5.1.4	<i>Azimuth rotation torque</i>	<i>29</i>
5.1.5	<i>Elevation torque</i>	<i>33</i>
5.1.6	<i>Nasmyth rotator calculations.....</i>	<i>35</i>
5.1.7	<i>Cassegrain Rotator Calculations.....</i>	<i>37</i>

	<p>SPMT</p> <p>SPMT Conceptual Design Pre PDR</p>	<p>Code: TRP/TELE/001-R</p> <p>Issue: 1.C</p> <p>Date: 24/06/2014</p> <p>Page: 6 of 152</p>
---	--	---

5.1.8	<i>Elevation hydrostatic shoe bearing</i>	39
5.1.9	<i>Azimuth hydrostatic shoe bearing</i>	40
5.1.9.1	Hydrostatic principle.....	41
5.2	PRIMARY MIRROR DESCRIPTION	46
5.2.1	<i>Primary Mirror support system</i>	49
5.2.2	<i>Hardpoints</i>	51
5.2.3	<i>Pneumatic suspension system</i>	59
5.2.4	<i>Primary mirror thermal system</i>	66
5.2.5	<i>Thermocouple mirror temperature measurement</i>	68
5.3	TELESCOPE STRUCTURE.....	69
5.4	TELESCOPE COUNTERWEIGHTS.....	70
5.5	SECONDARY MIRROR	71
5.5.1	<i>Vane system</i>	71
5.5.1.1	Description	72
5.5.1.2	Mechanisms of the vanes	72
5.6	TERTIARY MIRROR.....	77
5.7	TELESCOPE BUILDING	78
5.8	F/5 INSTRUMENTS	80
5.8.1	<i>Hectochelle and Hectospec</i>	80
5.8.1.1	Hectospec and Hectochelle mounting considerations on the SPMT	82
5.8.2	<i>MMIRS</i>	83
5.8.2.1	MMIRS overview.....	85

	<p>SPMT</p> <p>SPMT Conceptual Design Pre PDR</p>	<p>Code: TRP/TELE/001-R</p> <p>Issue: 1.C</p> <p>Date: 24/06/2014</p> <p>Page: 7 of 152</p>
---	--	---

5.8.2.2	3D Model	87
5.8.3	<i>Megacam</i>	91
5.8.3.1	Megacam mounting considerations on the SPMT	97
5.8.4	<i>Binospec</i>	97
5.8.4.1	Instrument Overview	97
5.8.4.1.1	Support Structure	97
5.8.4.1.2	Calibration System	99
5.8.4.1.3	Calibration / Derotator Assembly	100
5.8.4.2	Telescope Envelope and instrument Mass Constraints	103
5.8.4.3	Interface Connections.....	106
5.8.4.3.1	Cable Connection to the Telescope	106
5.8.4.4	Binospec mounting considerations on the SPMT	108
6.	TELESCOPE FINITE ELEMENT MODEL (FEM)	108
6.1	STRUCTURAL AND MODAL ANALYSIS REPORT OF SPMT TELESCOPE	108
6.1.1.1	Analisis objective.	108
6.1.1.2	Analisis description.	108
6.1.1.3	Analisis procedure for SPMT.....	109
6.1.1.4	Model FEM description.	109
6.1.1.4.1	BEAM4 ⁽¹⁾	113
6.1.1.4.2	SHELL93 ⁽¹⁾	113
6.1.1.4.3	MASS21 ⁽¹⁾	114
6.1.1.5	Boundary conditions zenith position:	114
6.1.1.6	Boundary conditions horizon position:.....	121
6.1.2	<i>Modal analysis</i>	128

	<p>SPMT</p> <p>SPMT Conceptual Design Pre PDR</p>	<p>Code: TRP/TELE/001-R</p> <p>Issue: 1.C</p> <p>Date: 24/06/2014</p> <p>Page: 8 of 152</p>
---	--	---

6.1.3 *Conclusions from Analysis* 133

7. SAN PEDRO MARTIR TELESCOPE CONTROL ARCHITECTURE **134**

7.1 NETWORK RELIABILITY..... 138


7.2 SITE DIMENSIONS..... 148

LENGTH: 6 METERS, CONTEMPLATING THREE RACKS AND AISLES 1.5 METERS LATERALS 148

WIDTH: 5 METERS, CONTEMPLATING OPENING RACK AND 1.5 METERS HALL, FRONT AND BACK..... 148

HEIGHT: 3.20 METERS, CONTEMPLATING FALSE CEILING 0.50 CM AND 0.50 CM FALSE FLOOR, ALLOWING 2.20 METERS HEIGHT WORKING AREA..... 148

8. APPENDIX 1..... **152**

	<p>SPMT</p> <p>SPMT Conceptual Design Pre PDR</p>	<p>Code: TRP/TELE/001-R</p> <p>Issue: 1.C</p> <p>Date: 24/06/2014</p> <p>Page: 9 of 152</p>
---	--	---

1. SUMMARY

During the feasibility study for the construction of the SPMT were evaluated the different options of design the MMT Telescope and the Magellan Telescope and as result were obtained references for the mechanical design, for the control architecture and the network infrastructure of the telescope.

This document describes the conceptual design (at Pre-PDR stage) of the telescope and its subsystems to show about the level of detail of the design until stage. This stage gives us the information in order to see wich requeriments are needed for future design and interfases.

Here is included the results of an structural analysis and a modal analysis for the structure of the telescope to have reference values for the next stages of project.


2. SPMT GENERAL REQUIREMENTS

2.1 General specifications

Then are listed the general requirements and specifications provided by IA UNAM (A.8) where the code under parentheses (P1, P1.2 etc.) means the priority scale for each requirement.

Development:

- SPMT project shall construct a new 6.5-m telescope at SPM. (P1) (A.8)
- SPMT shall be suitable for general science projects (A.8)
- SPMT shall use the existing 6.5-m primary mirror owned by INAOE and UA. (A.8)
- Telescope must be operational on a short time Scale (P1.2) (A.8)
- SPMT should be operational on a short time scale. (A.8)
- SPMT shall minimize risks by following existing and proven reference designs (e.g., the MMT and Magellan) where appropriate and possible. (A.8)
- The SPMT primary mirror shall be manufactured and polished to the same optical specifications as the MMT and Magellan primaries. (A.8)
- The SPMT design and development shall explicitly consider operations and operation costs. (A.8)
- The development of SPMT shall take place in Mexico, by Mexican institutions and companies, where appropriate and possible. (A.8)
- The concept should allow the use of the f/5 instruments like: Binospec, MMIRS, MEGACAM, MAESTRO, Hectospec and Hectochelle (P1) (A.8)
- Ability to use multiple instruments in one night (more than 2) (P1.5)

	SPMT	Code: TRP/TELE/001-R
	SPMT Conceptual Design Pre PDR	Issue: 1.C
		Date: 24/06/2014
		Page: 10 of 152

- Risk mitigation:

- Construction time (P1.1)
- Financial costs for development and operation (P1)
- Technical Feasibility (P1)
- Scientific efficiency (P1.5)


2.2 General site characteristics

The Site characteristics in detail are described on the document Site and Geotechnical Study for SPMT GEN/SYEN/0001-F (A.5). Tables 2.1 to 2.3 shows the main site characteristics to be considered during the telescope structure mechanical concept development.

Latitude	31° 02' 40" N
Longitude	115 ° 29'
Elevation	2830 m (over sea level)
Average Temperature	- 1.5°C
Atmospheric Pressure	542 mm Hg
Wind Speed	8.5 m/s
Photometric Nights	57%
Spectroscopic Nights	80%
Sky brightness	B= 22 mag/arcsec ²
Optical Turbulence (seeing)	0.5 arcsec at 15 m
Atmospheric water vapor	2.5 mm H ₂ O
Relative Humidity	54%
Atmospheric inversion layer height	1000 m (over sea level)

Table 2-1 General characteristics OAN, SPM

The survival limits characteristics are described on the document SPMT High Level Requirements (A.8).

	SPMT	Code: TRP/TELE/001-R
	SPMT Conceptual Design Pre PDR	Issue: 1.C
		Date: 24/06/2014
		Page: 11 of 152

Temperature	-25°C to 35°C (A.8)
Humidity	100% (A.8)
Maximum wind	120 Km/h (about 700 N/m ²) (A.8)
Snow loads	400 kg/m ²
Aceleration	Horizontal acc. 0.4 g , vertical 0.2 g (A.8)
Electric storms	(A.8)
Hail storms	(A.8)

Table 2-2 Survival conditions OAN, SPM

3. OPTICAL DESIGN GENERAL DESCRIPTION

For SPM Telescope three optical configurations are considered:

- f/5 Cassegrain
- f/5 Nasmyth
- f/11 Nasmyth

The following figure shows the three optical configurations.

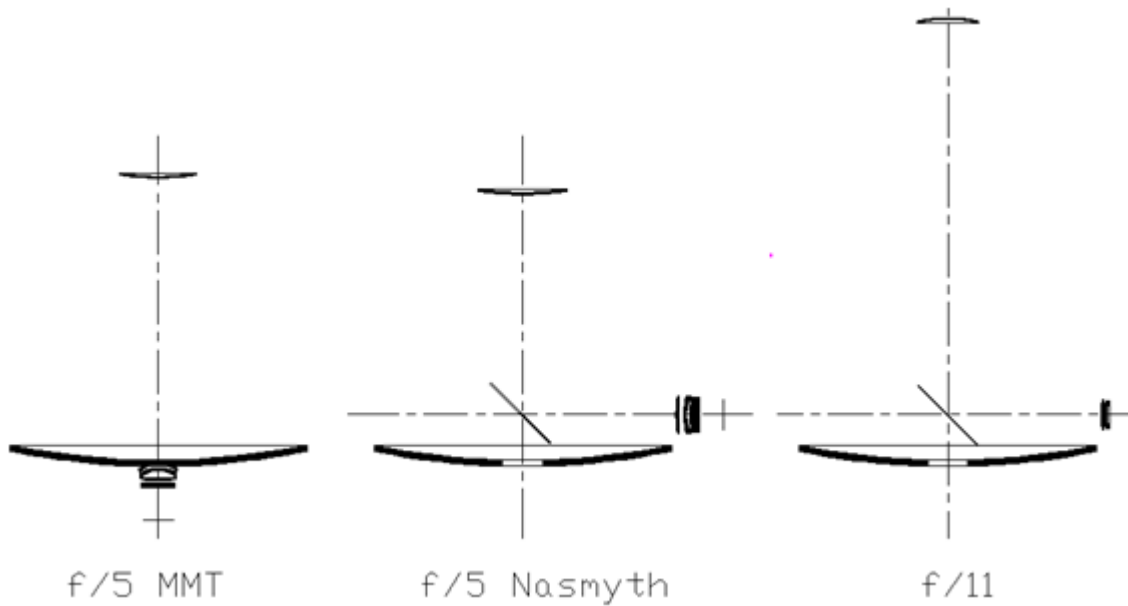



Figure 3-1 SPMT optical configurations

	<p>SPMT</p> <p>SPMT Conceptual Design Pre PDR</p>	<p>Code: TRP/TELE/001-R</p> <p>Issue: 1.C</p> <p>Date: 24/06/2014</p> <p>Page: 12 of 152</p>
---	--	--

3.1 f/5 Cassegrain

The configuration of SPMT should have use the instruments from the MMT, Hectochelle, Hectospec, and the Magellan Clay instruments like Binospec, MMIRS and Megacam. All the instruments mentioned will be the first light instruments for the SPMT to accomplish the specification mentioned on 2.1.

3.2 f/5 Nasmyth

The design of SPMT have wider field (aprox. 1 meter in SPMT), due to a longer distance between the primary mirror and the Elevation axis. This allow to mount bigger instruments and also new wide field spectroscopy instruments on the Nasmyth platform, also to accomplish the specification of th ability to use more han one instrumen per night **Figure 3-2**.

The f/11 will be implemented too, for new instrument aplicaciones, and to use instruments with more field scales **Figure 3-2**

To implement the optical configurations on the mechanical design of the telescope structure, after evaluation is possible to implement the three focal ratios in one secondary cage without any change on the secondary spider.

Figure 3-2 and **Figure 3-3** shown the front and lateral views of the telescope three focal ratios implemented.

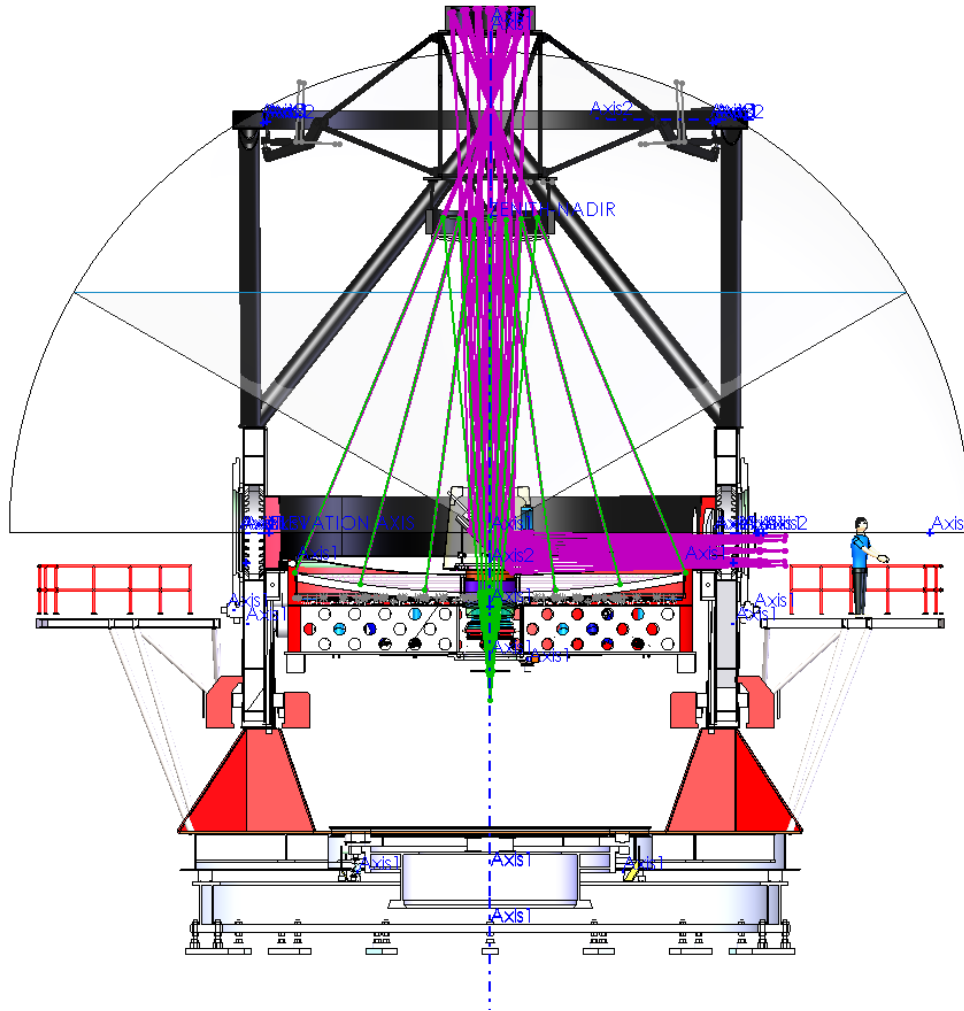



Figure 3-2 SPMT front view with f/5 Cassegrain (green) and f/5 Nasmyth (purple) f/11 (purple)

	<p>SPMT</p> <p>SPMT Conceptual Design Pre PDR</p>	<p>Code: TRP/TELE/001-R</p> <p>Issue: 1.C</p> <p>Date: 24/06/2014</p> <p>Page: 14 of 152</p>
---	--	--

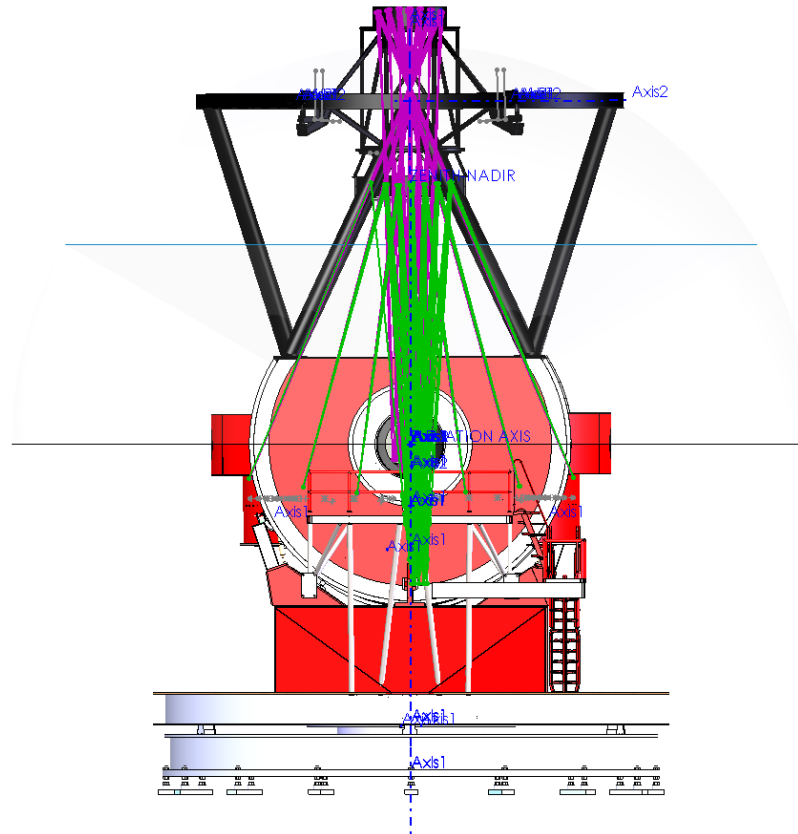



Figure 3-3 SPMT lateral view with f/5 Cassegrain (green) and f/5 Nasmyth (purple) f/11 (purple)

This solution has several benefits in terms of cost and mechanical implementation:

- The Secondary Mirror Cage and the spider are the same for three focal configurations (f/5 MMT, f/5 Nasmyth and f/11, reducing cost on the spider and the secondary mirror and the same positioning system.
- It allows installation of a hexapod if is needed wider movements than the vane ends allow.
- Using vane end configuration during the engineering activities for “f” change only is necessary to dismount the f/5 Cassegrain and Nasmyth configurations, and the tertiary mirror.
- The software, the actuators and the wiring harness are the same for all configurations, reducing the cost, maintenance and the commissioning times during the “f’s” change.

	<p>SPMT</p> <p>SPMT Conceptual Design Pre PDR</p>	<p>Code: TRP/TELE/001-R</p> <p>Issue: 1.C</p> <p>Date: 24/06/2014</p> <p>Page: 15 of 152</p>
---	--	--

3.3 f/11 Nasmyth

f/11 secondary mirror can remain installed during the f/5 modes operation reducing risk; only during the f/11 use the f/5 mirrors must be removed **Figure 3-4**.

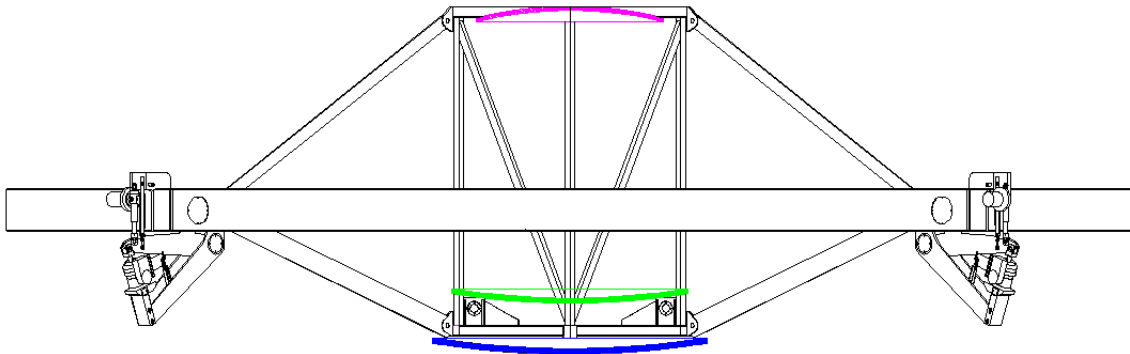


Figure 3-4 f/5 MMT, f/5 Nasmyth and f/11 installed on the cage

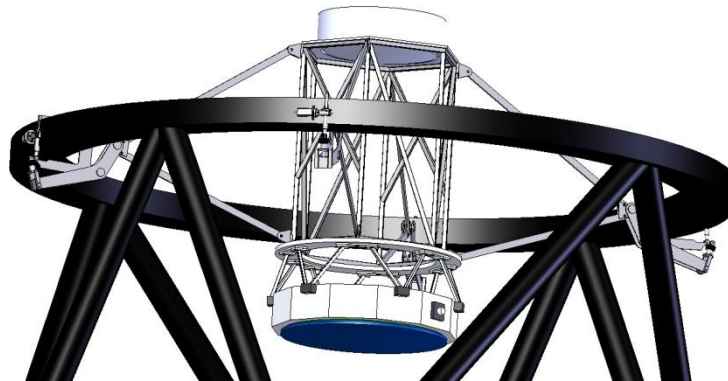



Figure 3-5 .f/5 MMT, f/5 Nasmyth and f/11 installed on the cage

In the same way we will implement the four vane Secondary positioning system instead of the hexapod system (Steward Platform) to reduce cost. The use of hexapod positioning system can be only implemented using two hexapod systems, one for the f/5's and another for the f/11. In case that the Hexapod is provided, can be considered the change from vane end to hexapod design but these cases are being analyzed.

	SPMT	Code: TRP/TELE/001-R
	SPMT Conceptual Design Pre PDR	Issue: 1.C
		Date: 24/06/2014
		Page: 16 of 152

For the Pre- PDR design is considered the f/5 Cassegrain and in future chapters of this document is described.

4. SAN PEDRO MARTIR TELESCOPE GENERAL CHARACTERISTICS

4.1 Product Tree

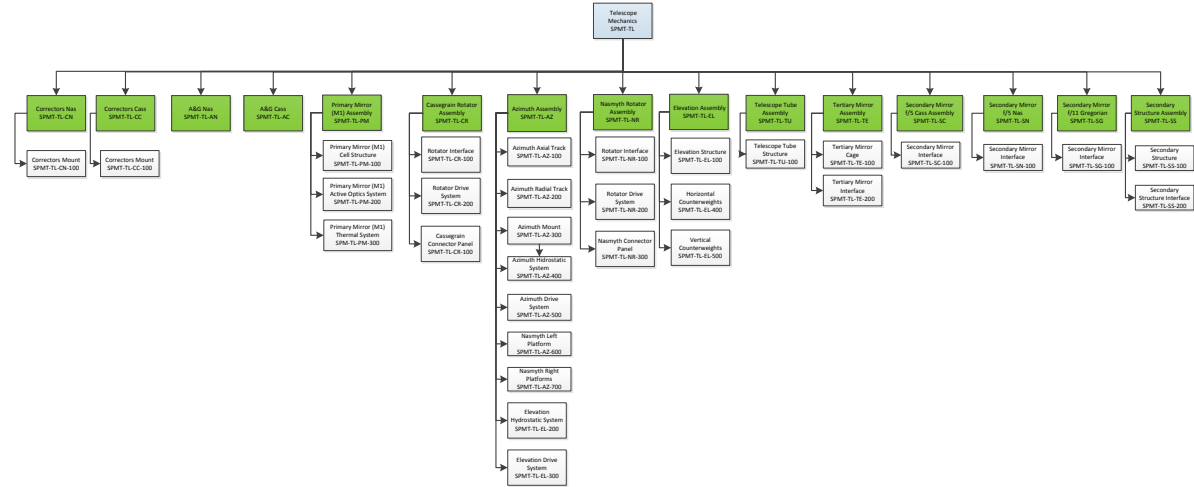
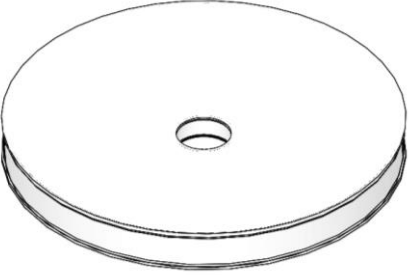



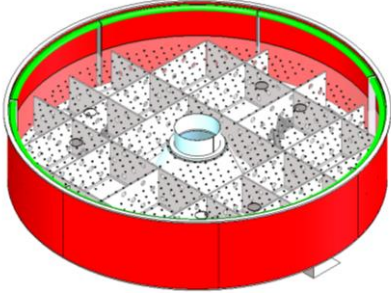
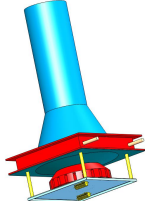
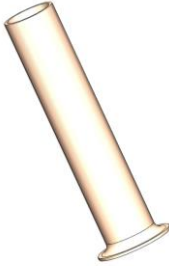
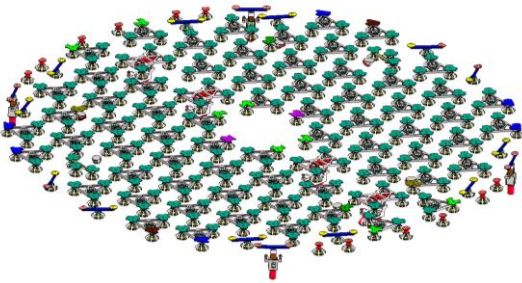
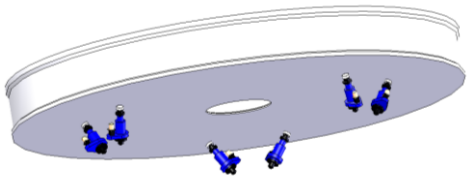
Figure 4-1 Product Tree


4.2 Telescope structure mass Budget (A.7)



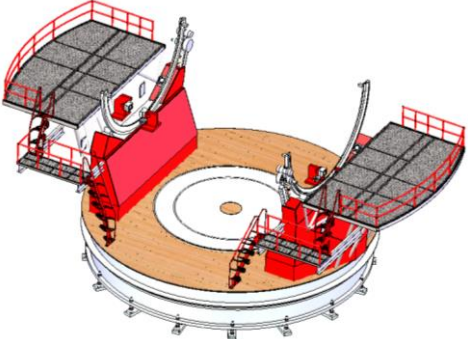
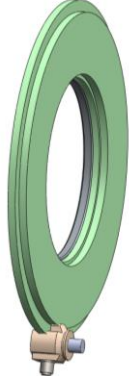
The following table shows the estimated mass budget for SPMT (A.7).


Component	Reference	Estimated weight (kg)	Figure
Primary mirror (M1)	Active supports and force optimization for the MMT primary mirror (1998)	8780 (TBC)	

	<p>SPMT</p> <p>SPMT Conceptual Design Pre PDR</p>	<p>Code: TRP/TELE/001-R</p> <p>Issue: 1.C</p> <p>Date: 24/06/2014</p> <p>Page: 17 of 152</p>
---	--	--


<p>Primary Mirror Cell Structure</p>	<p>SPMT-TL-PM-100-000</p>	<p>21748.56</p>	
<p>Fans and coolers (56)</p>		<p>1680 (TBC)</p>	
<p>Nozzles pattern</p>	<p>SPMT-TL-PM-300-000</p>	<p>152.29</p>	
<p>Loadspreaders, pucks and flexible spring supports</p>	<p>SPMT-TL-PM-200-000</p>	<p>1011.17</p>	
<p>Hardpoints system (steward platform) (6 actuators)</p>		<p>480 (TBC)</p>	

	<p>SPMT</p> <p>SPMT Conceptual Design Pre PDR</p>	<p>Code: TRP/TELE/001-R</p> <p>Issue: 1.C</p> <p>Date: 24/06/2014</p> <p>Page: 18 of 152</p>
---	--	--

<p>Floating support actuators (70 double, 30 single)</p>		<p>8436 (TBC)</p>	
<p>Cassegrain rotator</p>	<p>MMTO217</p>	<p>706</p>	
<p>Azimuth Assembly</p>	<p>SPMT-TL-AZ-000-000</p>	<p>106879.13</p>	
<p>Nasmyth Rotator (2)</p>	<p>SPMT-TL-NR-000-000</p>	<p>3178.41</p>	

	<p>SPMT</p> <p>SPMT Conceptual Design Pre PDR</p>	<p>Code: TRP/TELE/001-R</p> <p>Issue: 1.C</p> <p>Date: 24/06/2014</p> <p>Page: 19 of 152</p>
---	--	--

Elevation System	SPMT-TL-EL-000-000	38032.56	
Telescope Tube	SPMT-TL-TU-000-000	10168.10	
Tertiary Mirror Structure	SPMT-TL-TE-000-000	1277.67 (TBD)	
Secondary mirror assembly	SPMT-TL-SC-000-000	5112.45	

	SPMT	Code: TRP/TELE/001-R
	SPMT Conceptual Design Pre PDR	Issue: 1.C Date: 24/06/2014 Page: 20 of 152

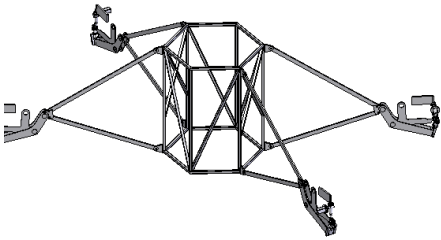
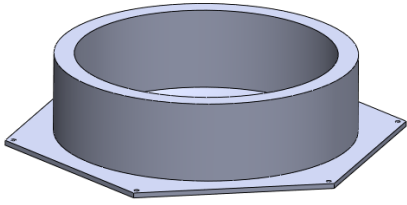

Secondary Structure	SPMT-TL-SS-000-000	365.64	
Secondary Mirror Gregorian Structure	SOMT-TL-SG-000-000	649.22	
Tertiary mirror		400 (TBD)	
Nasmyth rotator bearings Rothe Erde 110 diam 1450 mm (2)		400	
Counterweights		2000 (TBD)	
Rotators power traction system (3)		300	
Wiring harness, pipes and hoses		500	
Cassegrain and Nasmyth instruments max. load capacity		3(4000) 4(1000)	2 Nasmyth 1 Cassegrain 4 Folded Cassegrain (TBD)

Table 4-1 SPMT mass budget (A.7)


4.3 General kinematic and mechanic considerations

The following table shows the general kinematic considerations resume from SPMT.

Characteristic	Value
Azimuth turn	255°(TBC)
Elevation	From 0 to 90 ° (Horizon to Zenith) (TBC)

	SPMT	Code: TRP/TELE/001-R
	SPMT Conceptual Design Pre PDR	Issue: 1.C Date: 24/06/2014 Page: 21 of 152


Elevation Speed	0.8° /s(TBC)
Elevation acceleration	0.1° /s ² (TBC)
Azimuth speed	2°/s(TBC)
Azimuth acceleration	0.05 °/s ² (TBC)
Structure first primary mode	Above 10 Hz(TBC)
Elevation Motion	Preloaded friction drive(TBC)
Elevation preload force (estimated)	1662 kg (two Systems) (TBC)
Elevation motor torque (estimated)	233.36 Nm (two systems) (TBC)
Azimuth Motion	Preloaded friction drive
Elevation Bearings	Hydrostatic bearings (SKF) 4 radial (225x290 mm, r=3223.76 mm) and 4 supports lateral. Axial stiffness 6.8x 10 ⁶ , radial 0.9x 10 ⁷ (TBC)
Azimuth preload force (estimated)	3644 kg (two Systems) (TBC)
Azimuth motor torque (estimated)	516.26 Nm (two systems) (TBC)
Azimuth Bearings	Hydrostatic bearings (SKF) 6 axial (225x290 mm) and 4 radial (225x290 mm r= 2085 mm) on the center above the pier. Axial stiffness 0.98 x10 ⁷ , radial 6.8 x10 ⁶
Elevation position measurement	Dual type with tape encoder and encoder mounted direct on the motor (resolution 1µm)
Azimuth position measurement	Dual type with tape encoder and encoder mounted direct on the motor (1 µm)
Tertiary mirror movement	Preloaded friction drive
Tertiary position measurement	Dual type with tape encoder and encoder mounted direct on the motor (1 µm)

	SPMT	Code: TRP/TELE/001-R
	SPMT Conceptual Design Pre PDR	Issue: 1.C
		Date: 24/06/2014
		Page: 22 of 152

Tertiary preload force (estimated)	110 kg
Tertiary motor torque (2) (estimated)	20 Nm
Nasmyth Rotators movement (2)	Preloaded friction drive
Nasmyth rotators bearings (2)	Rotek 5000 Cross roller heavy duty Slewing ring R9-59E3
Nasmyth rotators position measurement (2)	Dual type with tape encoder and encoder mounted direct on the motor (1 μ m)
Nasmyth rotators preload force (estimated) (2)	2178 kg
Nasmyth rotators motor torque (2) (estimated)	325.41 Nm
Cassegrain Rotator movement	Preloaded friction drive
Cassegrain rotator bearings	Rotek 5000 Cross roller heavy duty Slewing ring R8-39E3
Cassegrain rotator position measurement	Dual type with tape encoder and encoder mounted direct on the motor (1 μ m)
Cassegrain rotator preload force (estimated) (2)	2398 kg
Cassegrain rotator motor torque (2) (estimated)	342.23 Nm
Secondary mirror positioning	Four vanes system with two actuators per vane
Vane stroke	Axial 50.8 mm, radial 25.4 mm
Secondary mirror resonant frequency (estimated)	Above 8 Hz (TBC)

Table 4-2 SPMT kinematic and mechanic general characteristics resume

The values shown on the Table 4-2 are developed on the next chapters.

	<p style="text-align: center;">SPMT</p> <p style="text-align: center;">SPMT Conceptual Design Pre PDR</p>	<p>Code: TRP/TELE/001-R</p> <p>Issue: 1.C</p> <p>Date: 24/06/2014</p> <p>Page: 23 of 152</p>
---	--	--

5. SAN PEDRO MARTIR TELESCOPE MECHANICAL DESIGN DESCRIPTION

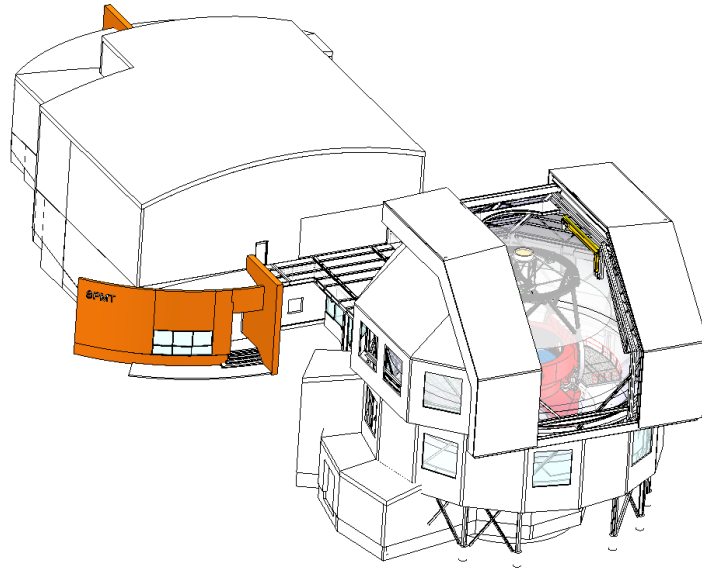


Figure 5-1 Building Isometric view

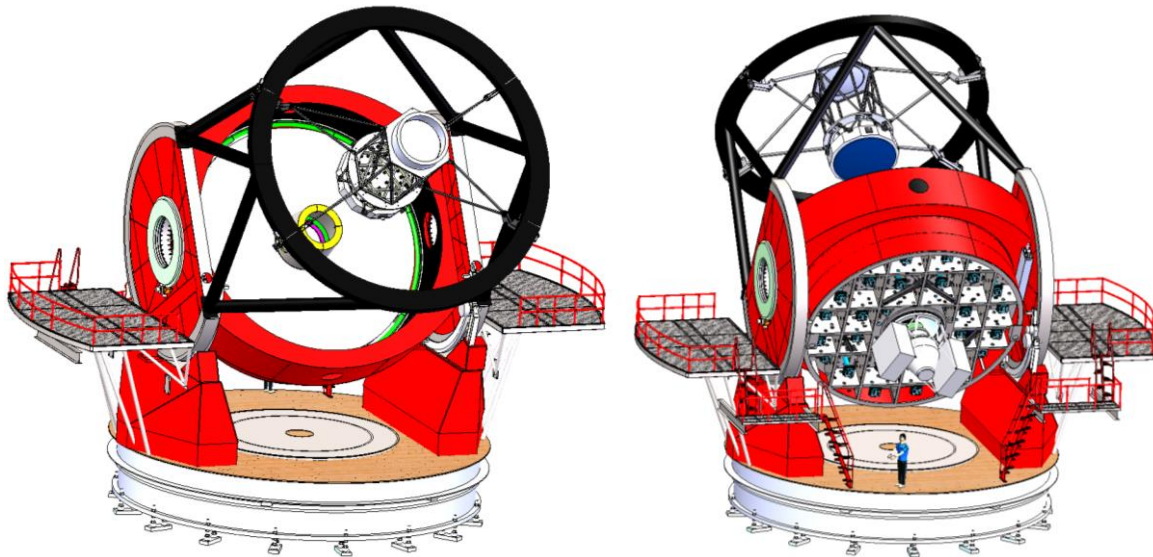



Figure 5-2 Left mirror side in isometric view. Right.Cass Instruments isometric view.

	<p>SPMT</p> <p>SPMT Conceptual Design Pre PDR</p>	<p>Code: TRP/TELE/001-R</p> <p>Issue: 1.C</p> <p>Date: 24/06/2014</p> <p>Page: 24 of 152</p>
---	--	--

5.1 Alt-azimuth movement

SPMT is an alt-azimuth telescope; the coordinate system will be an altitude-azimuth with the local horizon as a fundamental plane. This plane divides the sky into upper and lower hemispheres. The pole of the upper hemisphere is the zenith. (*Figure 5-3 SPMT zenith position*)

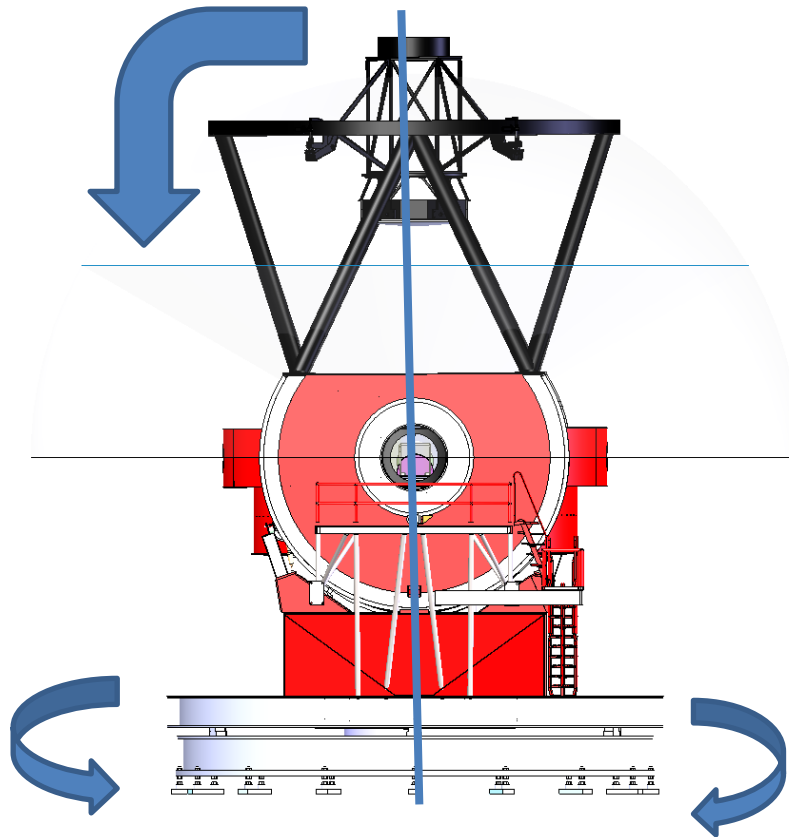



Figure 5-3 SPMT zenith position

The alt-azimuth coordinates are respectively, elevation or altitude, measured from the horizon, and the azimuth, measured eastward from the north. The star elevation position measured from the zenith point is the zenith angle. The transformation from equatorial coordinates into alt-azimuth ones is:

$$\tan A = \frac{\sin t}{-1 \sin \phi \cos t + \cos \phi \tan \delta}$$

$$\cos Z = \sin \phi \sin \delta + \cos \phi \cos \delta \cos t \quad (5.1)$$

	SPMT SPMT Conceptual Design Pre PDR	Code: TRP/TELE/001-R Issue: 1.C Date: 24/06/2014 Page: 25 of 152
---	---	---

with:

$A = azimuth\ angle$

$Z = zenith\ distance$

$\varphi = geographical\ latitude\ of\ the\ observatory$

$\delta = declination$

$t = the\ local\ hour\ angle\ of\ the\ celestial\ object$

During the star tracking for the control system programming, both the azimuth angle and the zenith distance vary as defined in equation 5.1.

5.1.1 Elevation and azimuth motor speeds

The corresponding velocities of two alt-azimuth coordinates to define the elevation and azimuth motor speeds are:

$$\frac{dZ}{d\tau} = \cos\varphi \sin A$$

$$\frac{dA}{d\tau} = \frac{\sin\varphi \sin Z + \cos Z \cos A \cos\varphi}{\sin Z} \quad (5.2)$$

Equation 5.2 indicates that the absolute elevation velocity is never faster than that of the local hour angle, while the azimuth velocity may reach arbitrarily high values as the celestial object close to the zenith point (see figure 5.2 a). For stars, the transitional azimuth velocity over the local meridian plane equals to:

$$\frac{dA}{d\tau} = \cos\delta / \sin(\varphi - \delta)$$

For the SPMT the elevation and azimuth design speeds are:

Elevation speed: 0.8°/s

Azimuth speed: 2°/s

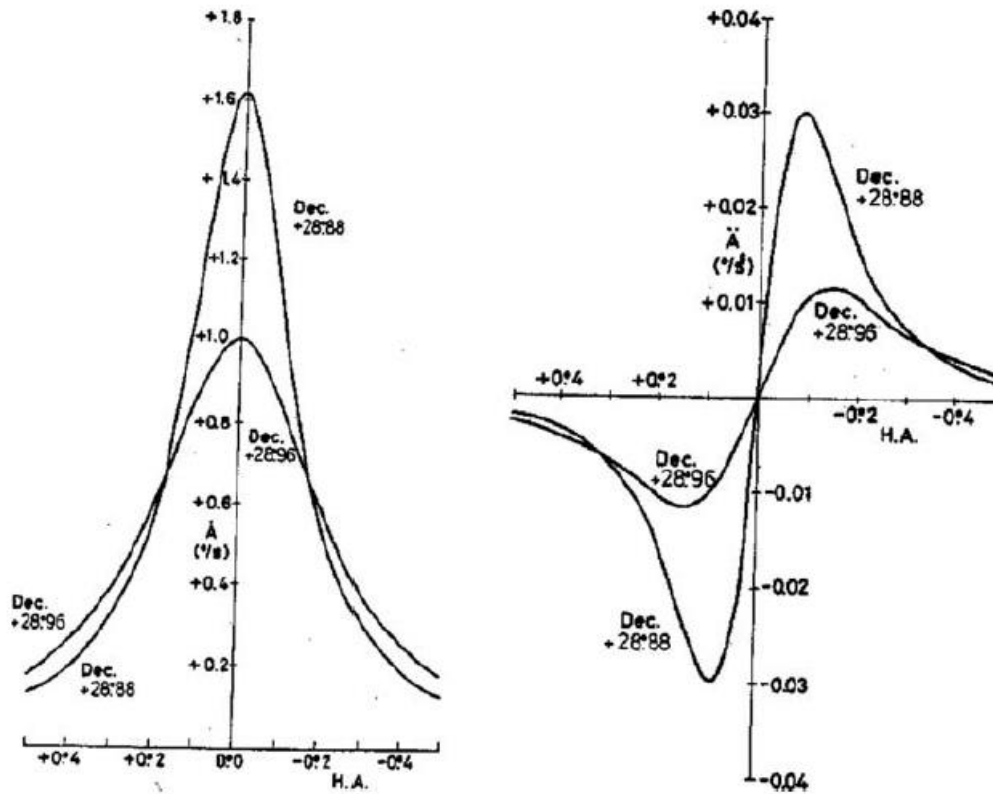


Figure 5-4 The azimuth velocity (a) and the azimuth acceleration (b) for celestial objects with 0.1° and 0.2° zenith distances at a latitude of 28.75° (Watson, 1978).


5.1.2 Elevation and azimuth motor acceleration

The corresponding accelerations of the two alt-azimuth coordinates during star tracking are:

$$\frac{d^2Z}{dt^2} = \cos\phi \cos A \left[\sin\phi + \frac{\cos\phi \cos A}{\tan Z} \right]$$

$$\frac{d^2A}{dt^2} = -\frac{\cos\phi \sin A}{\sin^2 Z} [\sin Z \cos Z \sin\phi + \cos\phi \cos A (1 + \cos^2 Z)] \tag{5.3}$$

For the SPMT the elevation and azimuth design accelerations are:

	SPMT SPMT Conceptual Design Pre PDR	Code: TRP/TELE/001-R Issue: 1.C Date: 24/06/2014 Page: 27 of 152
---	---	---

Elevation acceleration: $0.1^\circ/s^2$

Azimuth acceleration: $0.05^\circ/s^2$

From the equation 4.3, the azimuth acceleration has a sign change at the transit and it reaches a high value when the star is near the zenith point (see figure 5.2b).

SPMT computerized control system, will point and track a star if the maximum azimuth velocity and acceleration ($2^\circ/s$ and $0.05^\circ/s^2$) allow it, more bigger speeds will be analyzed on the definitive control system design. A small inaccessible blind spot will exist around the zenith point as the azimuth angle will suddenly change sign when celestial body crosses the meridian. The telescope will track the star until a point, east of the meridian, where dA/dt of equation 5.2 reaches its maximum allowable azimuth velocity. Using the actual star azimuth velocity at the meridian, the tracking limitation happens for stars whose declination lies in range (Borowski, 1987):

$$\phi - \arctan \frac{\cos\phi}{|V| - \sin\phi} < \delta < \phi + \arctan \frac{\cos\phi}{|V| + \sin\phi} \quad (5.4)$$

Where V is the maximum azimuth tracking velocity. This formula determines the north-south limits of the blind spot. The blind spot at the zenith is also determined by the maximum azimuth acceleration and the slewing velocity. The contours of maximum azimuth tracking velocity can be calculated from (Watson, 1978):

$$\tan Z = \frac{\cos\phi}{\frac{A}{\omega} + \sin\phi} \cos A \quad (5.5)$$

Where ω is the angular velocity of a star in the polar coordinate system. Figure 4.3a shows the contours for various maximum azimuth tracking velocities. These contours contain east-west and nearly south-north symmetry. When the maximum azimuth tracking velocity is a constant, the zenith angles of the maximum contour are different for different site latitude ϕ . For $\phi = 0$, $Z = \tan^{-1}(\cos A \cdot \omega / \dot{A})$.

The contour for the maximum azimuth tracking acceleration is given by:

$$\sin(2A) \cos^2\phi \cos^2 Z - \frac{1}{2} \sin A \sin(2\phi) \cos Z + \frac{1}{2} \sin(2A) \cos^2\phi + \frac{\ddot{A}}{\omega^2} = 0 \quad (5.6)$$

Figure 5.3b shows the contours for various maximum azimuth accelerations. However, to derive a precise shape of the blind spot, the slewing limitation effect (maximum azimuth velocity) will be considered during the definitive control design.

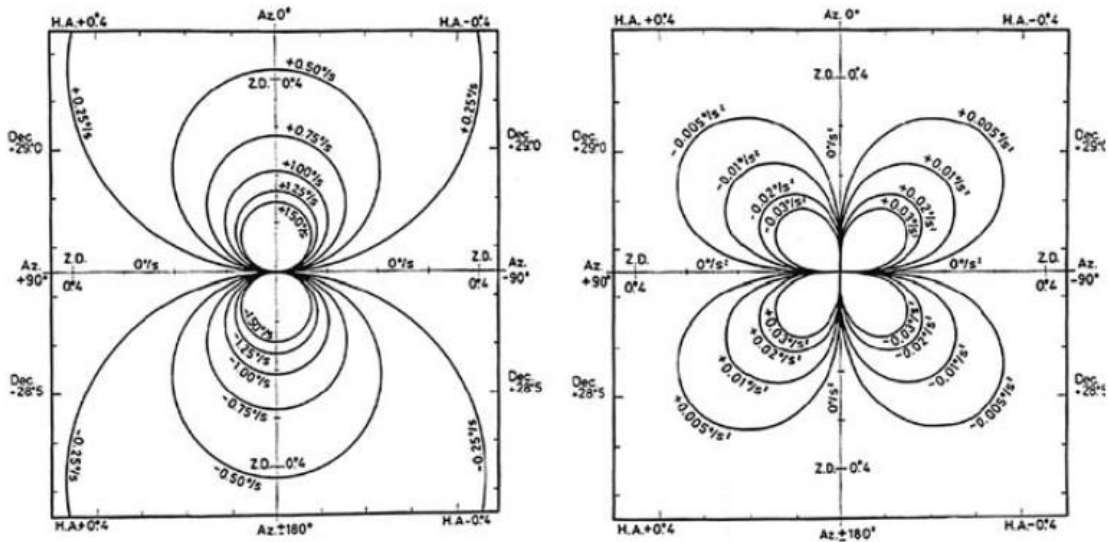



Figure 5-5 The Contours of various maximum azimuth tracking velocities (left) and tracking accelerations (right) at a latitude of 28.75° (b, right) (Watson, 1978).

The blind spot due to the slewing limitation is formed in the following way: as the telescope is trying to follow a celestial object through the blind spot at the zenith, it accelerates from tracking velocity to the slewing limit with a maximum acceleration and it slews over the blind spot. Then in the last stage, it decelerates to the tracking velocity and meets the celestial object on the other side of the meridian plane (see figure 5.4). This movement must be performed by the control system with the motors and the feedback of the encoder tape on the structure and the rotatory encoder (or tachometer) direct on the motor shaft. Assuming the change of the hour angle inside the blind spot is H , the formula for the maximum slewing velocity is:

$$\frac{H}{\omega} = \frac{A}{\dot{A}_{max}} + 2 \frac{\dot{A}_{max} - A}{\dot{A}_{max}} - \frac{\dot{A}_{max}^2 - A^2}{\dot{A}_{max} \dot{A}_{max}} \quad (5.7)$$

Or approximately

$$\cos Z = \cos A \tan \phi + \sin A \sec \phi \cot \left(\frac{A\omega}{\dot{A}_{max}} \right) \quad (5.8)$$

	SPMT SPMT Conceptual Design Pre PDR	Code: TRP/TELE/001-R Issue: 1.C Date: 24/06/2014 Page: 29 of 152
---	---	---

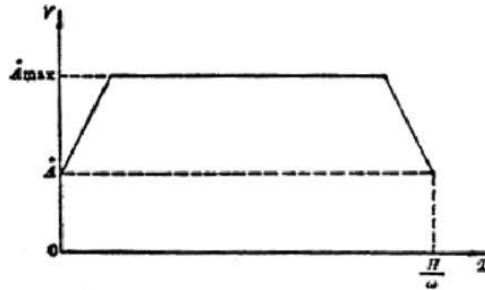


Figure 5-6 Azimuth velocity curve while a telescope crosses the blind zenith spot.

5.1.3 Rotators and field rotation

When the telescope is tracking a celestial object, the orientation of its field will change with time. The field angle, or parallactic angle, and its rate of change are given by:

$$\tan p = \frac{\sin t}{\tan \phi \cos \delta - \sin \delta \cos t} \quad (5.9)$$

$$\frac{dp}{d\tau} = - \frac{\cos \phi \cos A}{\sin Z}$$

For SPMT de design base data for rotators are:

Nasmyth and Casserain rotators conceptual speed and acceleration:

Velocity= 2.1 °/s

Acceleration = 0.05 °/s

Slewing Speed=4 °/s

These values will be definitively established on de Definitive Design stage of the project.

5.1.4 Azimuth rotation torque


Fa=284729 lb.

Ma=(1470lbs)(24.26ft) = 35662.2 lb-ft

Where

Fa= Is the weight of structure.

Mo: Is the moment of the upper structure at the horizon position.

	<p>SPMT</p> <p>SPMT Conceptual Design Pre PDR</p>	<p>Code: TRP/TELE/001-R</p> <p>Issue: 1.C</p> <p>Date: 24/06/2014</p> <p>Page: 30 of 152</p>
---	--	--

The average tuning torque is:

$$TR = \frac{\mu}{2} \left(Mo + \frac{Fa(Dt)}{12} \right)$$

Where

μ = Is he friction coefficient of the track (0.001).

Dt= Diameter of the track (371.47 in).

$$TR = \frac{0.001}{2} \left(35.662.2 \text{ lb} - ft + \frac{248729 \text{ lb}(371.47 \text{ in})}{12} \right)$$

TR=4424.84 lb-ft

Friction torque

TF= 0.05(4424.84 lb-ft)= 221.24 lb-ft

Wind torque

Tw=(0.08)(4424.84 lb-ft) = 353.98 lb-ft

Inertia Torque


$$TI = \frac{Mo * n}{9.55 \eta}$$

Where

n= rpm of the structure

η = efficiency of the system

$$TI = \frac{35662.2 * 1}{9.55 (0.9)}$$

	SPMT SPMT Conceptual Design Pre PDR	Code: TRP/TELE/001-R Issue: 1.C Date: 24/06/2014 Page: 31 of 152
---	---	---

$T_I = 4149.179 \text{ lb-ft}$

Total slewing torque.

$$T_T = T_R + T_F + T_W + T_I$$

$$T_T = 4424.84 + 221.24 + 353.98 + 4149.179 = 9149.23 \text{ lb-ft}$$

At the center of the telescope.

Now

$D =$ Diameter of the propulsion track (driven) = 169.33 in

$d =$ Diameter of the traction wheel = 5.9 in

$w =$ width of the traction wheel = 4 in

$$l = \frac{D}{d} \approx 24$$

Then the torque at the driven wheel is

$$T_D = 381.21 \text{ lb-ft or } 516.26 \text{ N-m.}$$

Now the power is

$$P = \frac{n * T_D}{5252 * \eta}$$

Where $n =$ rpm driven wheel

$T_D =$ Torque driven wheel (lb-ft)


$\eta =$ efficiency

$$P = \frac{24(381.21 \text{ lb-ft})}{5252(0.9)}$$

$$P = 1.9 \text{ HP}$$

$$P = (1.9 \text{ HP}) (745.7) = 1443.38 \text{ Watts.}$$

Now the preload force for transmission is

	<p>SPMT</p> <p>SPMT Conceptual Design Pre PDR</p>	<p>Code: TRP/TELE/001-R</p> <p>Issue: 1.C</p> <p>Date: 24/06/2014</p> <p>Page: 32 of 152</p>
---	--	--

$$PF = \frac{33000(12 \text{ HP})}{3.1416 d * n * w * \mu} \text{ (in lbs)}$$

Where μ = friction coefficient steel-steel =0.09

$$PF = \frac{33000(12 \text{ HP})}{3.1416 (6.4)(24)(4)(0.09)}$$

PF=4017.307 lbs

PF= 1822 Kg

With a safety factor of 2

PF=3644 Kg

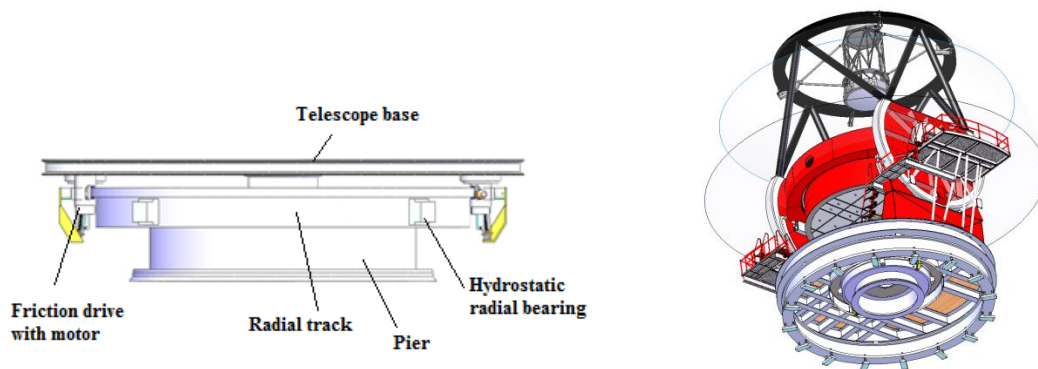



Figure 5-7 Azimuth motors and lower view of azimuth track and pier

The azimuth traction system will consist in a set of two gear reducer motors with a torque of 516.25 Nm and a preload force of 3644 Kg. The azimuth track material is structural steel heat treated for wear resistance. The system will be supported by a set of hydrostatic bearings with a film oil clearance of 50 μm . Six hydrostatic bearings (SKF HSBM 325X240 mm) running in a 9425.89 mm diameter track and four radial bearings HSBM 325X240 mm running in a 4175.19 mm diameter track. The estimated axial stiffness for the bearings is 0.98×10^7 N/mm and for the radial 6.8×10^6 N/mm.

	<p>SPMT</p> <p>SPMT Conceptual Design Pre PDR</p>	<p>Code: TRP/TELE/001-R</p> <p>Issue: 1.C</p> <p>Date: 24/06/2014</p> <p>Page: 33 of 152</p>
---	--	--

5.1.5 Elevation torque

Fa=169996 lbs

Mo=35662.2 lbs-ft

The average running torque is:

$$TR = \frac{0.001}{2} (35662.2 \text{ lb} - \text{ft} + \frac{169996 \text{ lbs} (253.8 \text{ in})}{12})$$

TR=1815.538

Friction torque

TF=0.05(1815.538) = 90.77 lb ft

Wind torque

T_w=0.08(1815.538) = 145.24 lb ft

Inertia torque

$$TI = \frac{35662.2 * 1}{9.55 (0.9)}$$

T_i=4149.179 lb ft

Total slewing torque

T_T=1815.538+90.77+145.24+4149.179

T_T=6200.7 lb-ft at the center of elevation axis

Now

D= 253.8 in


d= 6.9 in

w= 4 in

l=36

Then the torque at the driven wheel is:

T_D=172.24 lb-ft or T_D=233.26 N-m

	<p>SPMT</p> <p>SPMT Conceptual Design Pre PDR</p>	<p>Code: TRP/TELE/001-R</p> <p>Issue: 1.C</p> <p>Date: 24/06/2014</p> <p>Page: 34 of 152</p>
---	--	--

$$P = \frac{36(172.24)}{5252(0.9)}$$

P= 1.3 HP or P= 978.22 W

The preload force is:

$$PF = \frac{33000 (12)(1.3)}{3.1416(6.9)(36)(4)(0.09)} = 1832.45 \text{ lb}$$

Pf=831 Kg with a safety factor of two

PF=1662 Kg

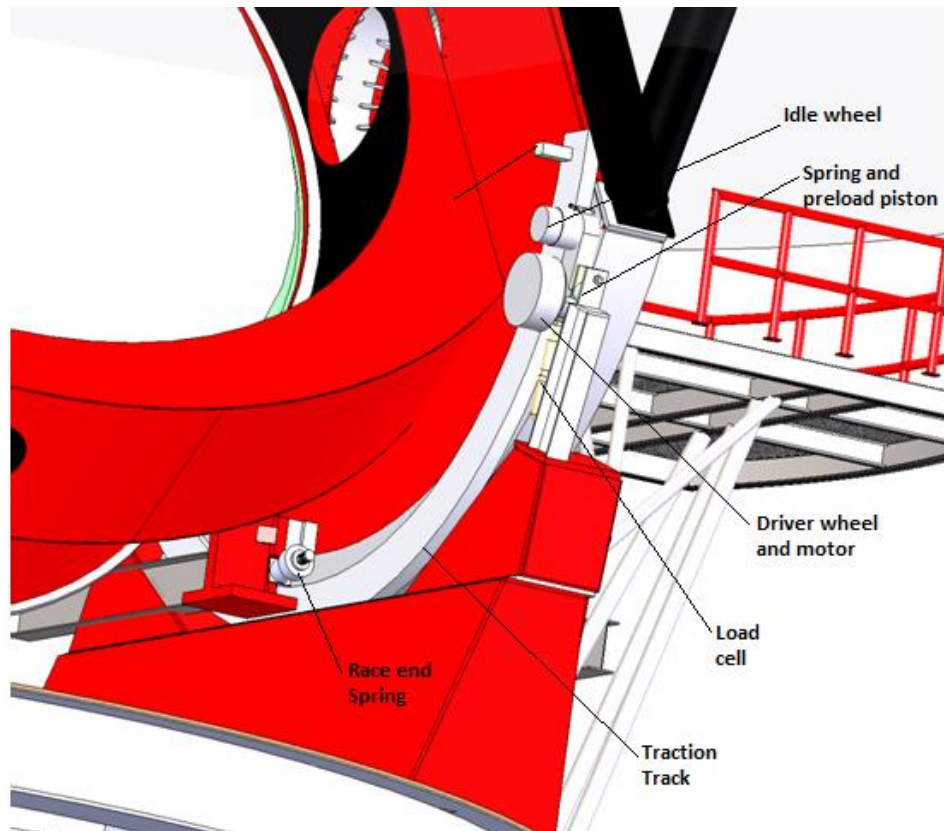



Figure 5-8 Elevation system

	SPMT SPMT Conceptual Design Pre PDR	Code: TRP/TELE/001-R Issue: 1.C Date: 24/06/2014 Page: 35 of 152
---	---	---

The elevation traction system will consist in a set of two gear reducer motors with a torque of 233.36 Nm and a preload force of 1662 Kg. The azimuth track material is structural steel heat treated for wear resistance. The system will be supported by a set of hydrostatic bearings with a film oil clearance of 50 μm. Four hydrostatic bearings (SKF HSBM 325X240 mm) running in a 6447.53 mm diameter track. The estimated axial stiffness for the bearings is 6.8X10⁶ N/mm and for the radial 0.9X10⁷ N/mm.

5.1.6 Nasmyth rotator calculations.

Max. Weight of the instrument: 2500Kg= 5511 lbs.

Nasmyth rotator Bearing Rotek 5000 R9-59E3

D_L=58.976 in

k=4.1

μ=0.004

M_k=(5511 lb)(3.3 ft) = 18370 lb – ft

Fr=4188 lbs

The average running torque is

$$TR = \frac{\mu}{2}(K * MK + \frac{k * Fr * Dl}{24})$$

$$TR = \frac{0.004}{2}(4.1)(18370) + \frac{(4.1)(4188)(58.96)}{24}$$

TR=235.02 lb-ft

Friction torque = 0.05(235.02) =11.75 lb- ft


Wind torque

Tw= 0.08(235.02) = 18.80 lb – ft

Inertia torque

$$Ti = \frac{18370 (1)}{9.55(0.9)} = 2137.28 Lb – Ft$$

The slewing torque is

	<p>SPMT</p> <p>SPMT Conceptual Design Pre PDR</p>	<p>Code: TRP/TELE/001-R</p> <p>Issue: 1.C</p> <p>Date: 24/06/2014</p> <p>Page: 36 of 152</p>
---	--	--

$$T_T = 235.02 + 1175 + 18.80 + 2137.28 = 2402.85 \text{ lb} - \text{ft}$$

D= 70 in

d=7 in

l=10

w=2

Torque at the rotator motor (driven wheel)

$$T_D = 240.28 \text{ lb-ft or } T_D = 325.41 \text{ N*m}$$

Now the power is

$$P = \frac{n * TD}{5252 * \eta} = \frac{10(240.28)}{5252(0.9)} = 0.48 \text{ Hp} = 358.59 \text{ W}$$

The preload force is

$$PF = \frac{33000 (12)(0.48)}{3.1416(7)(10)(2)(0.09)} = 4801.9 \text{ lb}$$

PF=2178 Kg

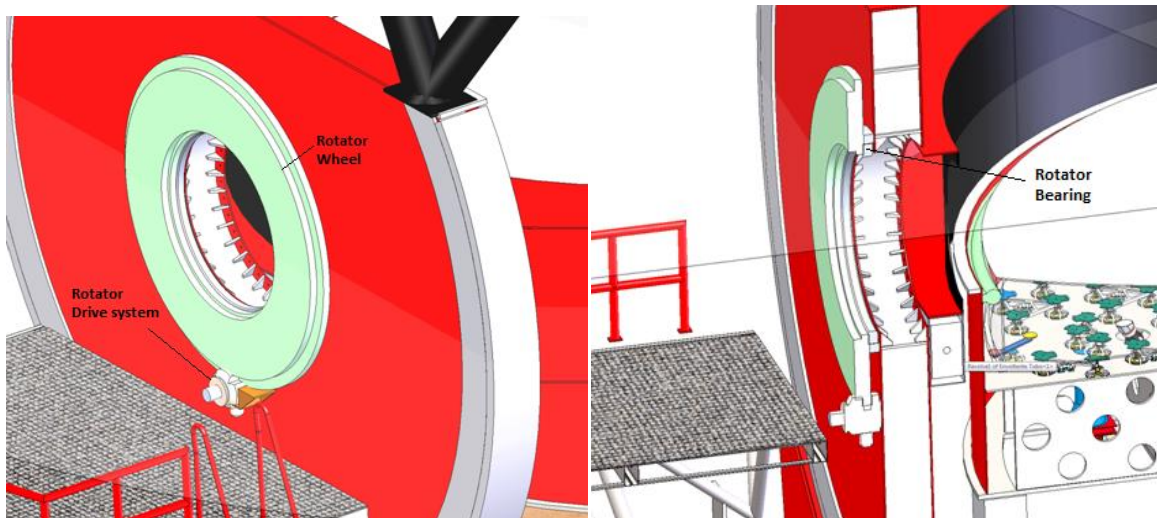


Figure 5-9 Nasmyth rotator



5.1.7 Cassegrain Rotator Calculations

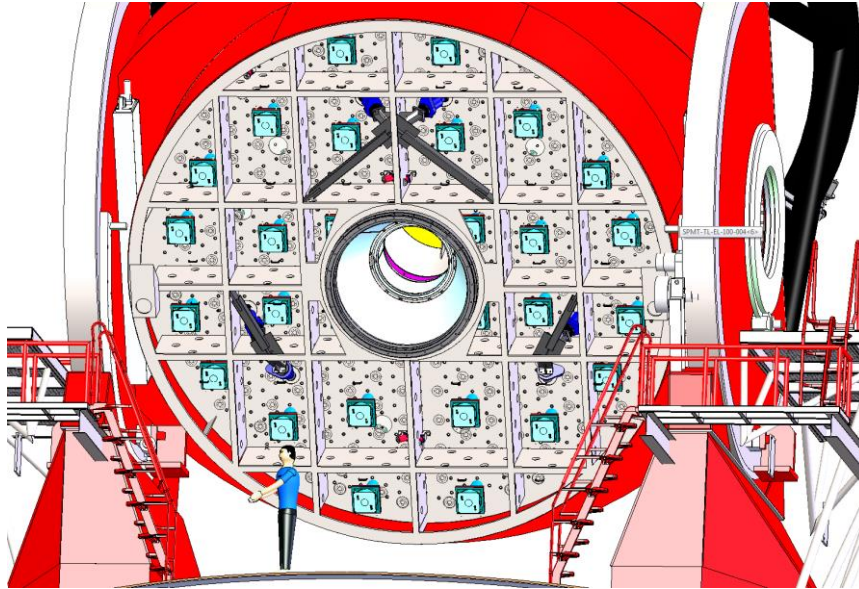


Figure 5-10 Cassegrain rotator

Maximum weight of the instrument 1900 Kg = 411 lbs

$Mk = (4188)(3.3) = 13820.4 \text{ lb-ft}$

$Fa = 4188 \text{ lbs}$

$$TR = \frac{\mu}{2} \left(k * Mk + \frac{Fa(DI)}{12} \right)$$

Bearing Rotek 500 R8-39E3


$D_L = 42.323 \text{ in}$

$k = 4.1$

$\mu = 0.004$

$$TR = \frac{0.004}{2} \left(4.1(13820.4) + \frac{4188(42.323)}{12} \right)$$

$T_R = 142.86 \text{ lb ft}$

	<p>SPMT</p> <p>SPMT Conceptual Design Pre PDR</p>	<p>Code: TRP/TELE/001-R</p> <p>Issue: 1.C</p> <p>Date: 24/06/2014</p> <p>Page: 38 of 152</p>
---	--	--

Friction torque

$$T_F = 0.05 (142.86) = 7.14 \text{ lb-ft}$$

Wind torque

$$T_W = 0.08 (148.86) = 11.142 \text{ lb-ft}$$

$$T_I = \frac{13820.4 (1)}{9.55 (0.9)} = 1607.95 \text{ lb-ft}$$

Slewing torque

$$T_T = 142.86 + 7.14 + 11.42 + 1607.95 = 1769.37 \text{ lb-ft}$$

$$D = 52 \text{ in}$$

$$d = 7 \text{ in}$$

$$l = 7$$

$$w = 2 \text{ in}$$

Torque at the driven wheel

$$T_D = 252.7 \text{ lb-ft} \text{ or } T_D = 342.23 \text{ Nm}$$

The power is


$$P = \frac{7(252.7)}{5252 (0.9)} = 0.37 \text{ HP} = 279.13 \text{ W}$$

The preload force is

$$PF = \frac{33060(12)(0.37)}{3.1416(7)(7)(2)(0.09)} = 5287.82 \text{ lbs}$$

$$PF = 2398 \text{ kg}$$

For tertiary mirror the same rotator system will be used, the tertiary mirror will be mounted on the upper part of the cassegrain rotator.

	<p>SPMT</p> <p>SPMT Conceptual Design Pre PDR</p>	<p>Code: TRP/TELE/001-R</p> <p>Issue: 1.C</p> <p>Date: 24/06/2014</p> <p>Page: 39 of 152</p>
---	--	--

5.1.8 Elevation hydrostatic shoe bearing

The total weight of structure including instruments is:

$$W_T = 77109 \text{ kg} + (2)(2500 \text{ kg}) + 1800 \text{ kg} = 83909 \text{ kg}$$

With a safety factor of 1.3:

$$W_t = 109081.7 \text{ kg} = 1069 \text{ KN}$$

The proposed configuration are 4 bearings two by elevation ring, the load per bearing is:

$$L = 267.25 \text{ KN}$$

From SKF catalog the selected model is the HSBM 325X420 with axial guiding pad 120X270 with a thrust load of 200 KN at 68 degrees of separation with a radius of 3223.7°. (see **Figure 5-11**)

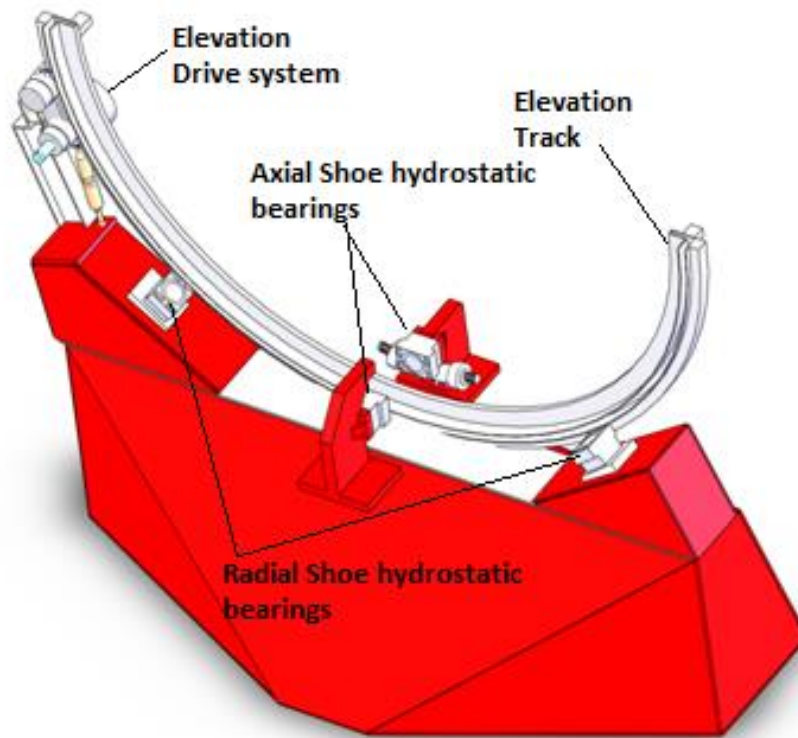



Figure 5-11 Elevation bearings

	SPMT	Code: TRP/TELE/001-R
		Issue: 1.C
	SPMT Conceptual Design Pre PDR	Date: 24/06/2014
		Page: 40 of 152

5.1.9 Azimuth hydrostatic shoe bearing

The total weight of the telescope including structure, azimuth mount and instruments with a safety factor of 1.3 is:

$$L = 177603.4 \text{ Kg} = 1741.6 \text{ KN}$$

With a set of 6 bearings equally distributed on a track of 9435.45 mm, the load for each bearing is:

$$L=290.26 \text{ KN}$$

The bearing is the SKF model HSBM 325X420, both systems operating at 10 bar of pressure.

The oil film thickness for systems, elevation and azimuth will be 50 μm. Hydraulic Oil ISO VG 32 (like Mobil DTE 24), high resistance hydraulic oil at wear and extended service interval. Oil flow 30 gpm.

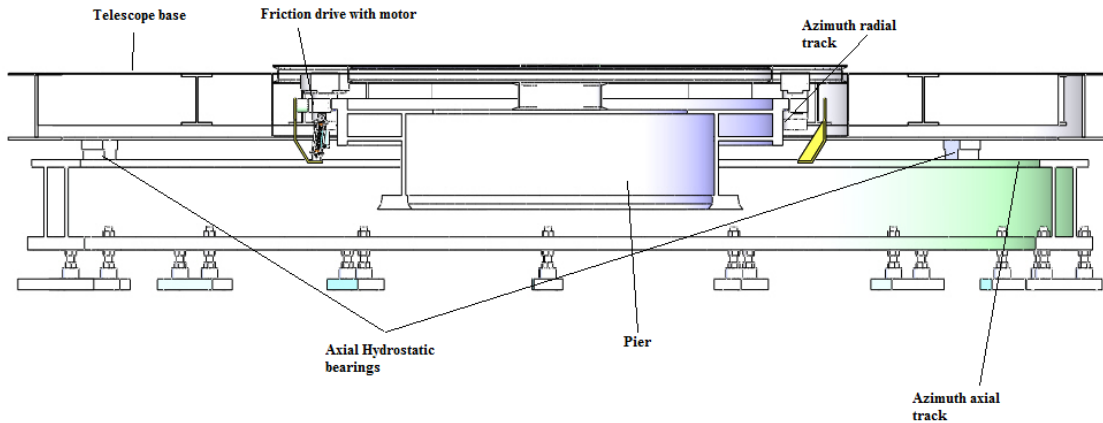


Figure 5-12 Azimuth bearings

For the lifting system and its operation we will use Hydrostatic Shoes(Hydrostatic bearings).


	<p>SPMT</p> <p>SPMT Conceptual Design Pre PDR</p>	<p>Code: TRP/TELE/001-R</p> <p>Issue: 1.C</p> <p>Date: 24/06/2014</p> <p>Page: 41 of 152</p>
---	--	--



Figure 5-13 Hydrostatic bearing.

5.1.9.1 Hydrostatic principle.

Loads of fluid in the hydrostatic shoes is supplied from an external source, oil is injected by a pump into the pocket formed between the sliding pad and the girth ring, the pressure built up in the pocket causes the girth ring to lift until a gap is created. Oil can freely escape through the gap. If the gap is sufficient to separate the shoe completely from the girth ring, the latter can rotate with low friction at any speed from very slow to high, and in either direction.

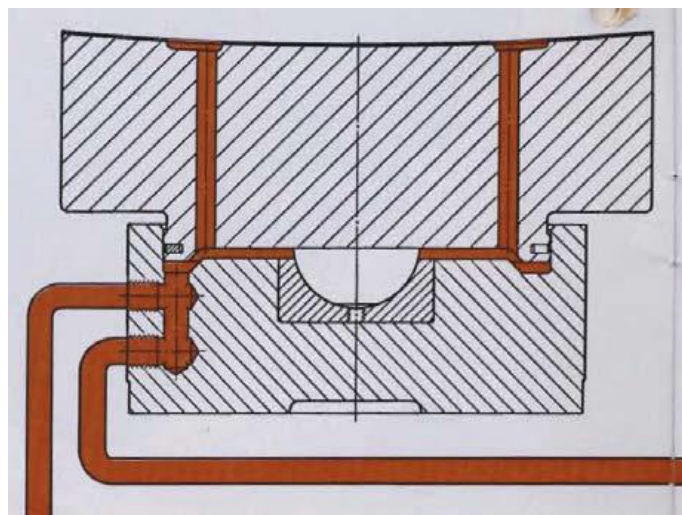



Figure 5-14 Fluid flow in the shoe.

	SPMT SPMT Conceptual Design Pre PDR	Code: TRP/TELE/001-R Issue: 1.C Date: 24/06/2014 Page: 42 of 152
---	---	---


The pocket pressure is solely dependent on the load on the girth ring and the pocket size. The height of the gap depends on the pressure, oil flow rate and viscosity, as well as the geometry of the sliding pad. The load bearing of hydrostatic bearing is a thin film of pressurized fluid, the pressure profile on the bearing surface has a triangular or trapezoidal profile of pressure, depending on the largest area exposed to into pressure, resulting in a higher load capacity and stiffness

They have a wide range of applications: high precision, miniature devices, large and heavy masses.

Some characteristics of the hydrostatic pads are:

- High carrying capacity.
- Unlimited support diameters.
- Virtually no friction or wear.
- Self-alignment to irregularities of the girth ring.
- Ability to withstand heavy shock loads.
- Independence of speed or rotational direction.
- High running accuracy and stiffness.
- We also know the advantages and disadvantages of using hydrostatic pads.

Advantages	Disadvantages
Support very large loads. The load support is a function of the pressure drop across the bearing and the area of fluid pressure action	Require ancillary equipment. Larger installation and maintenance costs
Load does not depend on film thickness or lubricant viscosity	Need of fluid filtration equipment. Loss of performance with fluid contamination
Long life (infinite in theory) without wear of surfaces	High power consumption because of pumping losses
Provide stiffness and damping coefficients of very large magnitude. Excellent for exact positioning and control	Potential to induce hydrodynamic instability in hybrid mode operation.

	<p>SPMT</p> <p>SPMT Conceptual Design Pre PDR</p>	<p>Code: TRP/TELE/001-R</p> <p>Issue: 1.C</p> <p>Date: 24/06/2014</p> <p>Page: 43 of 152</p>
---	--	--

	<p>Potential to show pneumatic hammer instability for highly compressible fluids, i. e. loss of damping at low and high frequencies of operation due to compliance and time lag of trapped fluid volumes.</p>
--	---

Table 5-1. Advantages and disadvantages of use hydrostatic shoes.

The equipment that must be available to run a hydrostatic shoe is the oil supply system and must have the following parts:

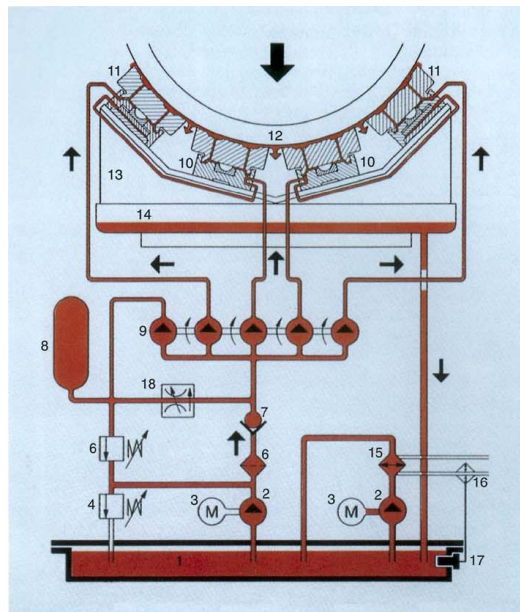




Figure 5-15 Hidraulic diagram

- Oil tank.
- Pump.
- Electric motor.
- Relief valve.
- Sequence valve.
- Oil filter.

	<p style="text-align: center;">SPMT</p> <p style="text-align: center;">SPMT Conceptual Design Pre PDR</p>	<p>Code: TRP/TELE/001-R</p> <p>Issue: 1.C</p> <p>Date: 24/06/2014</p> <p>Page: 44 of 152</p>
---	--	--

- Check valve.
- Accumulator.
- Flow divider.
- Master shoe.
- Slave shoe.
- Girth ring.
- Shoe pedestal.
- Oil sump.
- Oil cooler.
- Valve for cooling water.
- Thermostat.
- Flow control valve.

Then the hydrostatic shoes will withstand all the weight and movement of the telescope and will be placed for the lift system. The position of the hydrostatic shoes is shown in the following figure (see Figure 5-16).

	<p style="text-align: center;">SPMT</p> <p style="text-align: center;">SPMT Conceptual Design Pre PDR</p>	<p>Code: TRP/TELE/001-R</p> <p>Issue: 1.C</p> <p>Date: 24/06/2014</p> <p>Page: 45 of 152</p>
---	--	--

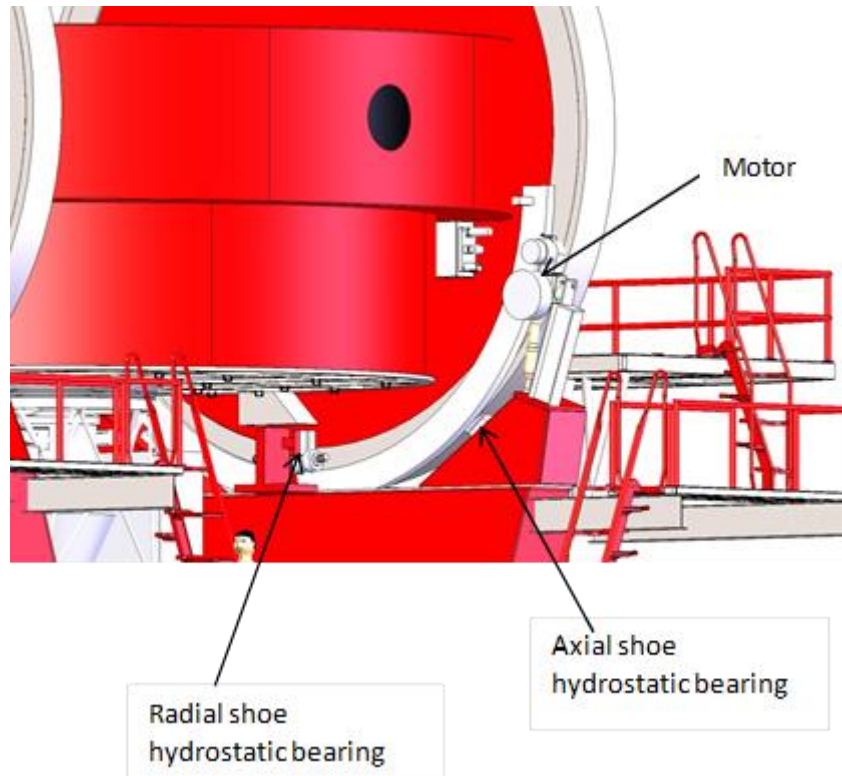



Figure 5-16 Motor and Hidrostatic shoes (Hidrostatic Bearings).

Two types of shoe hydrostatic for lifting system are selected:

1. One is to raise the system and be able to rotate.
2. The other in the transverse load to keep it in position.

	<p>SPMT</p> <p>SPMT Conceptual Design Pre PDR</p>	<p>Code: TRP/TELE/001-R</p> <p>Issue: 1.C</p> <p>Date: 24/06/2014</p> <p>Page: 46 of 152</p>
---	--	--

5.2 Primary mirror description

The primary mirror of SPMT is a borosilicate honeycomb mirror with a dimension of 6.5 m in diameter and weight of 8780kg. This mirror is located inside the primary cell, with the components of the support system and the thermal system. To prepare the conceptual design of the primary cell and its internal components was necessary to use the drawings in initial version provided by the MMT Observatory of the University of Arizona.

The primary cell is composed of two chambers, the upper chamber where the primary mirror and its support components are situated; and the lower chamber where the components of the thermal system are located. Both chambers are separated by an interface plate and an arrangement of screens which increases the rigidity of the cell. (Figure 5-17and Figure 5-18)

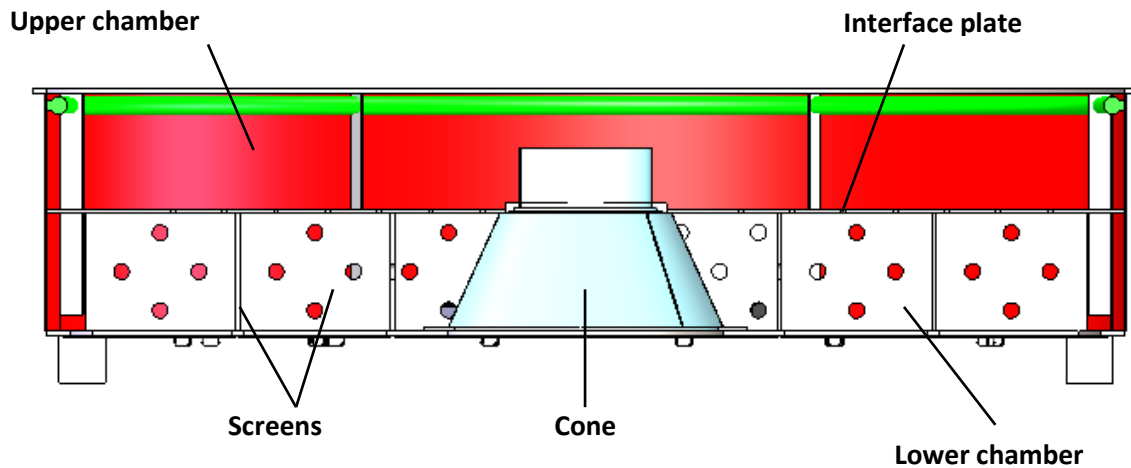



Figure 5-17 Primary cell and its chambers

	<p>SPMT</p> <p>SPMT Conceptual Design Pre PDR</p>	<p>Code: TRP/TELE/001-R</p> <p>Issue: 1.C</p> <p>Date: 24/06/2014</p> <p>Page: 47 of 152</p>
---	--	--

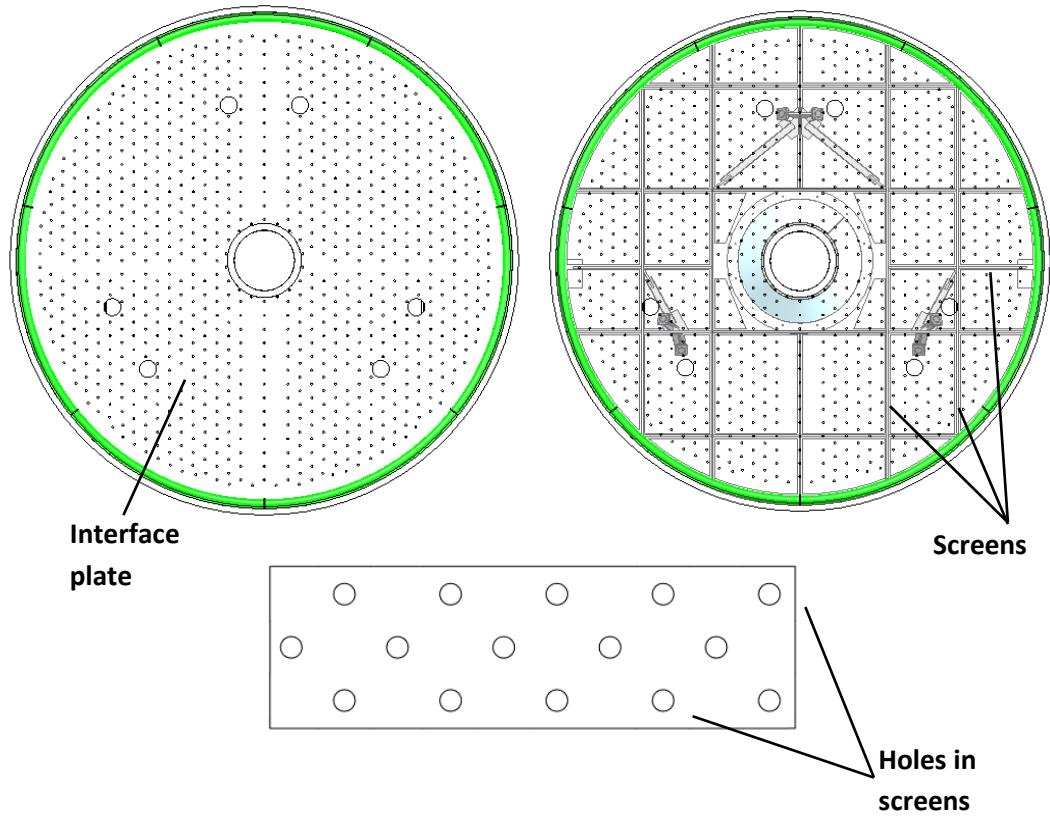



Figure 5-18 Holes pattern on interface plate, screen pattern and holes in screen

The interface plate has patterns of holes to accept the components that will be assembled on it; in the same way the screens have holes to allow air flow during the thermal process and for the supply ducts.

As shown on the next figures, in the center of the cell is placed the interface cone which will provide more space during the assembly of the corrector cell on the top of cone. Figure 5-19 and Figure 5-20

	<p style="text-align: center;">SPMT</p> <p style="text-align: center;">SPMT Conceptual Design Pre PDR</p>	<p>Code: TRP/TELE/001-R</p> <p>Issue: 1.C</p> <p>Date: 24/06/2014</p> <p>Page: 48 of 152</p>
---	--	--

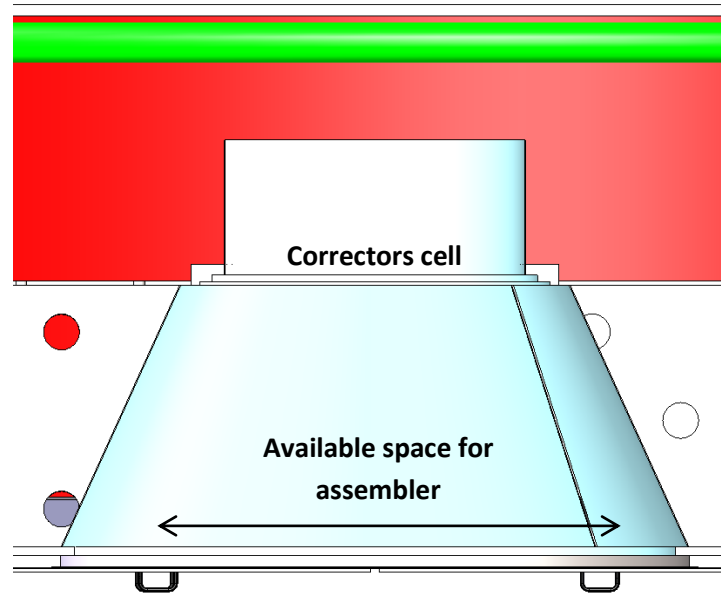


Figure 5-19 Correctors cone

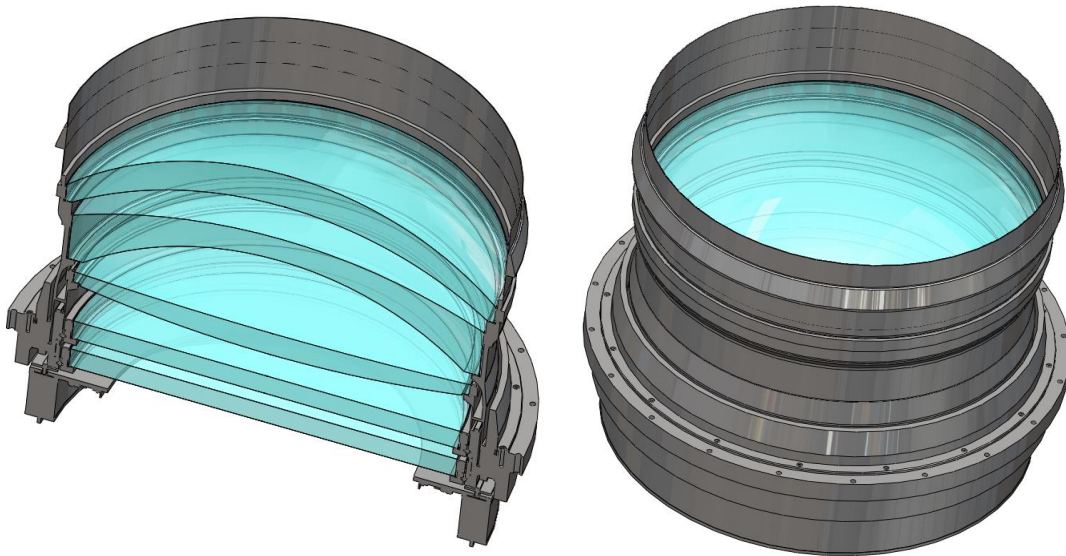



Figure 5-20 Corrector cell cuted and Isometric view of corrector cell

	<p>SPMT</p> <p>SPMT Conceptual Design Pre PDR</p>	<p>Code: TRP/TELE/001-R</p> <p>Issue: 1.C</p> <p>Date: 24/06/2014</p> <p>Page: 49 of 152</p>
---	--	--

Each of the systems in the primary cell are described in the following sections.

5.2.1 Primary Mirror support system

The support system of the primary mirror is based on the drawings that were provided with the theoretical distributions of the various components on the surface of the primary mirror like: hard points, loadspreaders, nozzles and pucks.

The next figure shows the drawing with the lay-out of the primary mirror of SPMT, where its supports are shown:

Primary mirror with hard points:

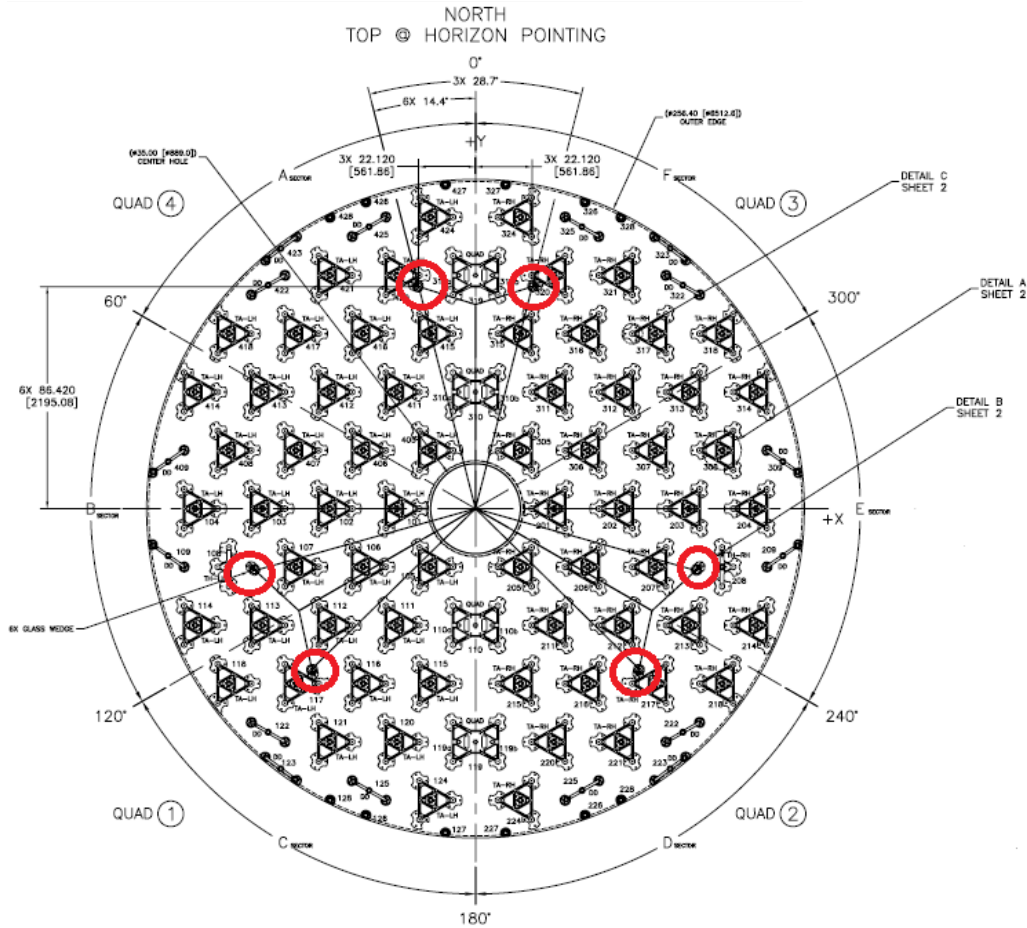



Figure 5-21 Lay-out of supports on primary mirror

	<p>SPMT</p> <p>SPMT Conceptual Design Pre PDR</p>	<p>Code: TRP/TELE/001-R</p> <p>Issue: 1.C</p> <p>Date: 24/06/2014</p> <p>Page: 50 of 152</p>
---	--	--

In the above drawing is observed in red circles the location of the "hardpoint glad wedges" where the cylinders of the Stewart platform are fixed. The others components shown are the loadspreaders in different configurations. The next figure shows the lay-out in 3D model.

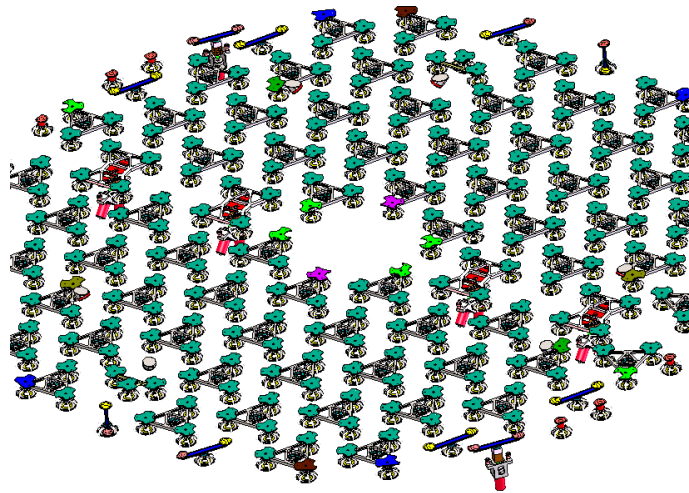
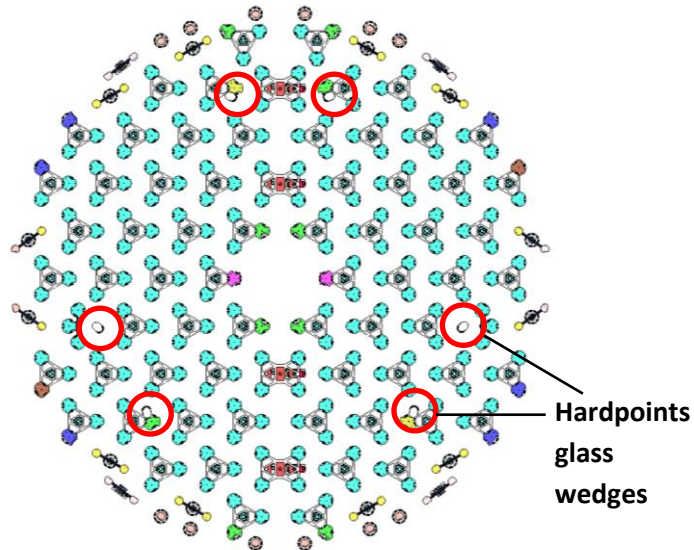



Figure 5-22 3D model with support system

The location of the subsystems are shown in the next figure, where we can observe that the loadspreaders with their pucks are fixed directly to the primary mirror and the other components are fixed to the interface plate that separates the two chambers of the primary cell.

	<p>SPMT</p> <p>SPMT Conceptual Design Pre PDR</p>	<p>Code: TRP/TELE/001-R</p> <p>Issue: 1.C</p> <p>Date: 24/06/2014</p> <p>Page: 51 of 152</p>
---	--	--

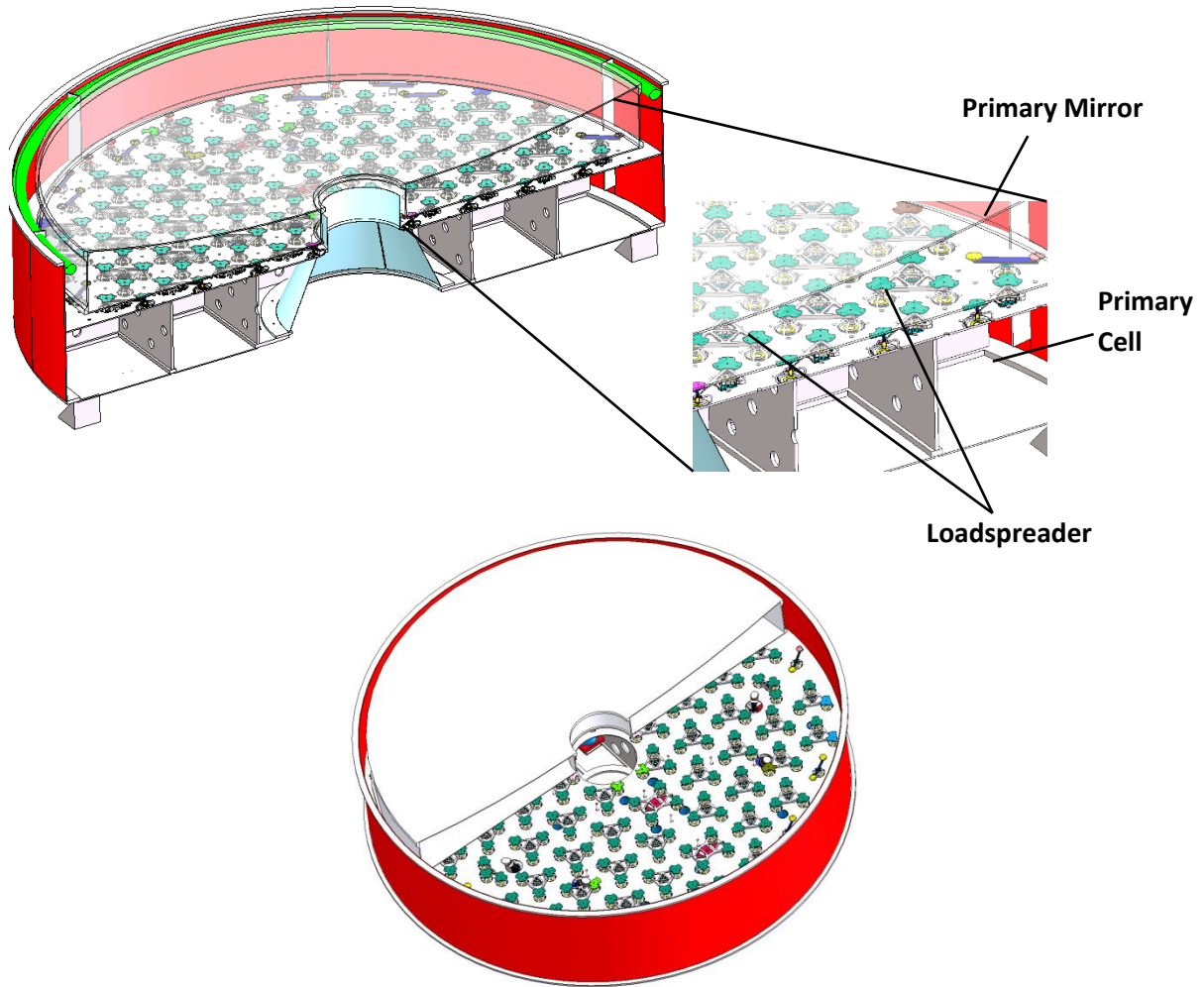



Figure 5-23 Location of the support system of the primary mirror

5.2.2 Hardpoints

The mirror support system considers a set of six linear actuators that integrate a Stewart platform. These actuators are fixed at the top side to the hardpoints wedges on the primary mirror and the lower side is attached to the primary cell with welded brackets as shown in the next figures.

	<p style="text-align: center;">SPMT</p> <p style="text-align: center;">SPMT Conceptual Design Pre PDR</p>	<p>Code: TRP/TELE/001-R</p> <p>Issue: 1.C</p> <p>Date: 24/06/2014</p> <p>Page: 52 of 152</p>
---	--	--

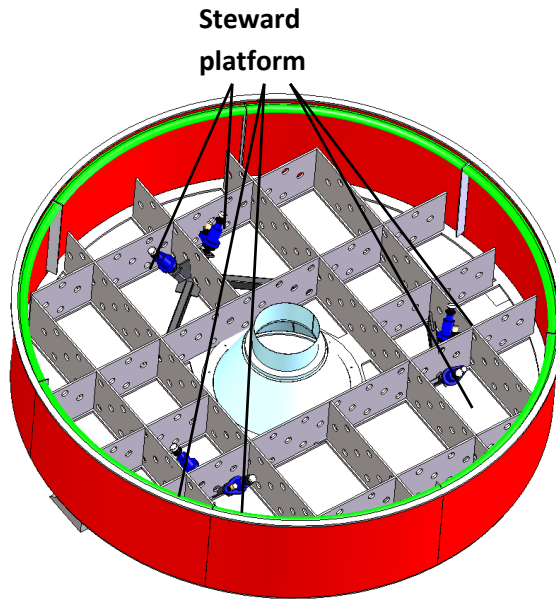


Figure 5-24 Actuators of platform Stewart

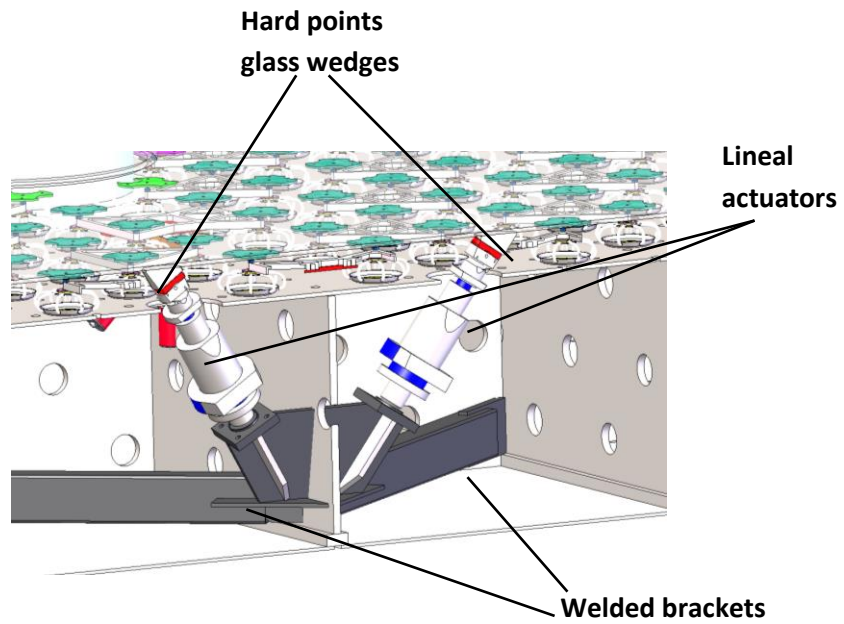



Figure 5-25 Detailed mounting of linear actuators

	<p>SPMT</p> <p>SPMT Conceptual Design Pre PDR</p>	<p>Code: TRP/TELE/001-R</p> <p>Issue: 1.C</p> <p>Date: 24/06/2014</p> <p>Page: 53 of 152</p>
---	--	--

Welded brackets have three different configurations adapted according to the positions of the actuators on the primary cell; those configurations are shown in the following figure.

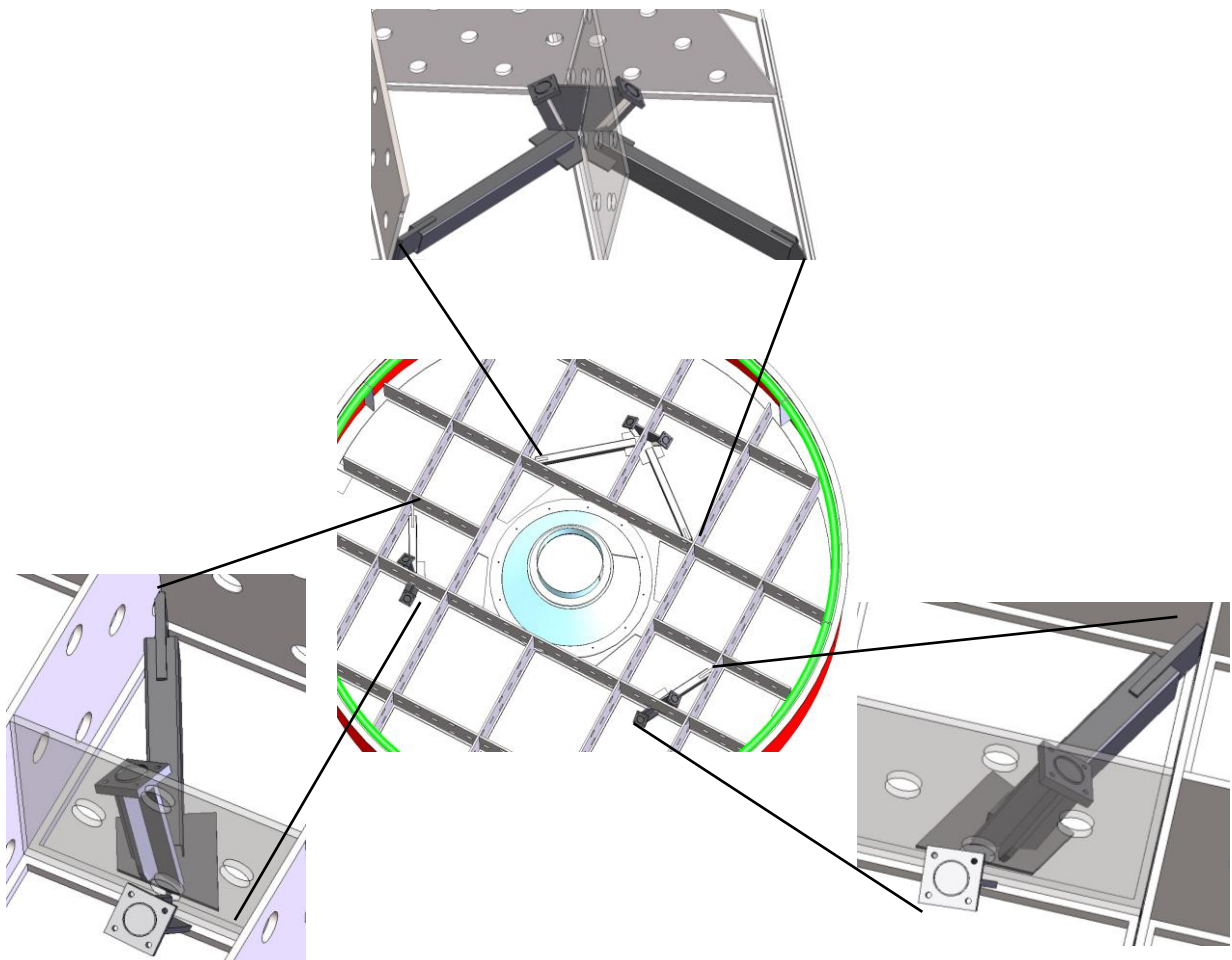



Figure 5-26 Configurations of the welded brackets

These actuators provide to the mirror all necessary degrees of freedom to align the mirror during the movements generated for the changes in the direction of the gravity vector during the elevation movement of the telescope tube deflections.

	<p>SPMT</p> <p>SPMT Conceptual Design Pre PDR</p>	<p>Code: TRP/TELE/001-R</p> <p>Issue: 1.C</p> <p>Date: 24/06/2014</p> <p>Page: 54 of 152</p>
---	--	--

According to Mirror Lab the manufacturer of the mirror, The axial stiffness of the wedge with a 0.5mm of glue thickness is 1360 KN/mm. At a maximum axial force of 3000 N applied by the hardpoint the maximum stress on the glass wedge is safely within the 0.7 MPa (100 psi) determined by the Mirror Lab. The glue is and RTV adhesive (Room Temperature Vulcanizing silicone).

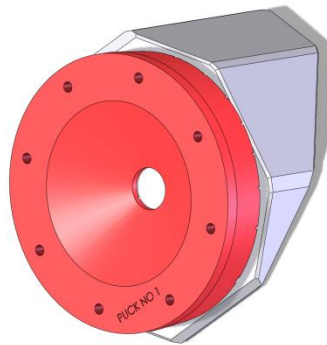



Figure 5-27 Glass Wedge

Each actuator is composed by a roller screw and a motor **Figure 5-27**. The actuator has the following general specifications:

- Number of hardpoints: 6, to constraint solid body motions.
- Support stiffness (not including the mirror cell): 80 000 N/mm.
- Force measurement range: -300 N to + 300 N.
- Force measurement resolution: 0.5 N.
- Force breakaway maintaining the above stiffness for: < 300 N.
- Maximum breakaway force: < 3000 N
- Breakaway Travel: +/- 17 mm along the mirror optical axis, and lateral/radial
- Unpredictable stray forces applied by the hardpoints to the mirror: axial < 2 N, lateral < 10 N, moment at the connections < 8 000 N mm
- Position capability:

	<p>SPMT</p> <p>SPMT Conceptual Design Pre PDR</p>	<p>Code: TRP/TELE/001-R</p> <p>Issue: 1.C</p> <p>Date: 24/06/2014</p> <p>Page: 55 of 152</p>
---	--	--

Axial and lateral motion of the mirror: (range) +/- 7mm

Along axis hardpoint: (range) +/- 10 mm

Resolution: $\approx 1 \mu\text{m}$

Linearity: $\approx 1\%$


Velocity: $< 30 \mu\text{m/s}$

Control bandwidth: $< 1 \text{ Hz}$

After the M1 mirror alignment the hardpoints do not have to change their length for any reason and the motor must switch off. In order to minimize the friction and to avoid and stick-slip effect, as usually we have with a traditional trapezoidal thread screw with the following data:

- Type: Rollvis RVR 250/63.2.R (Studio TecnicoTomellery Italy)
- Thread length: 130 mm
- Pitch: 2 mm
- Precision: $12 \mu\text{m}$
- Axial travel: 12 mm
- Number of rollers: 12
- Dynamic load: 114.3 kN
- Static load: 207.1 kN
- Axial Stiffness: $1.5 \times 10^6 \text{ N/mm}$
- Factory preload: 1250 N

The roller screw is driven by step motor ($1.8^\circ/\text{step}$) and a gearheads with 50:1 reduction ratio, a further reduction is realized by two gears 2:1. The total reduction step motor/roller screw is the 100:1. With these performances the maximum axial resolution achievable, considering avoiding any backlash in gears, is then $0.1 \mu\text{m}$ and to satisfy the $30 \mu\text{m/s}$ required for the axial velocity 90 RPM on the rotor are needed. Further, the static torque of the motor is 0.85 Nm and the dynamic is 0.15 Nm, corresponding to axial forces 1 600 kN and 470 kN: these values are oversize for loads

	<p>SPMT</p> <p>SPMT Conceptual Design Pre PDR</p>	<p>Code: TRP/TELE/001-R</p> <p>Issue: 1.C</p> <p>Date: 24/06/2014</p> <p>Page: 56 of 152</p>
---	--	--

on the hardpoint and a limiting device is then required. To protect overloads that could damage the mirror, each actuator has a break away mechanism to protect the system (see Figure 5-28).

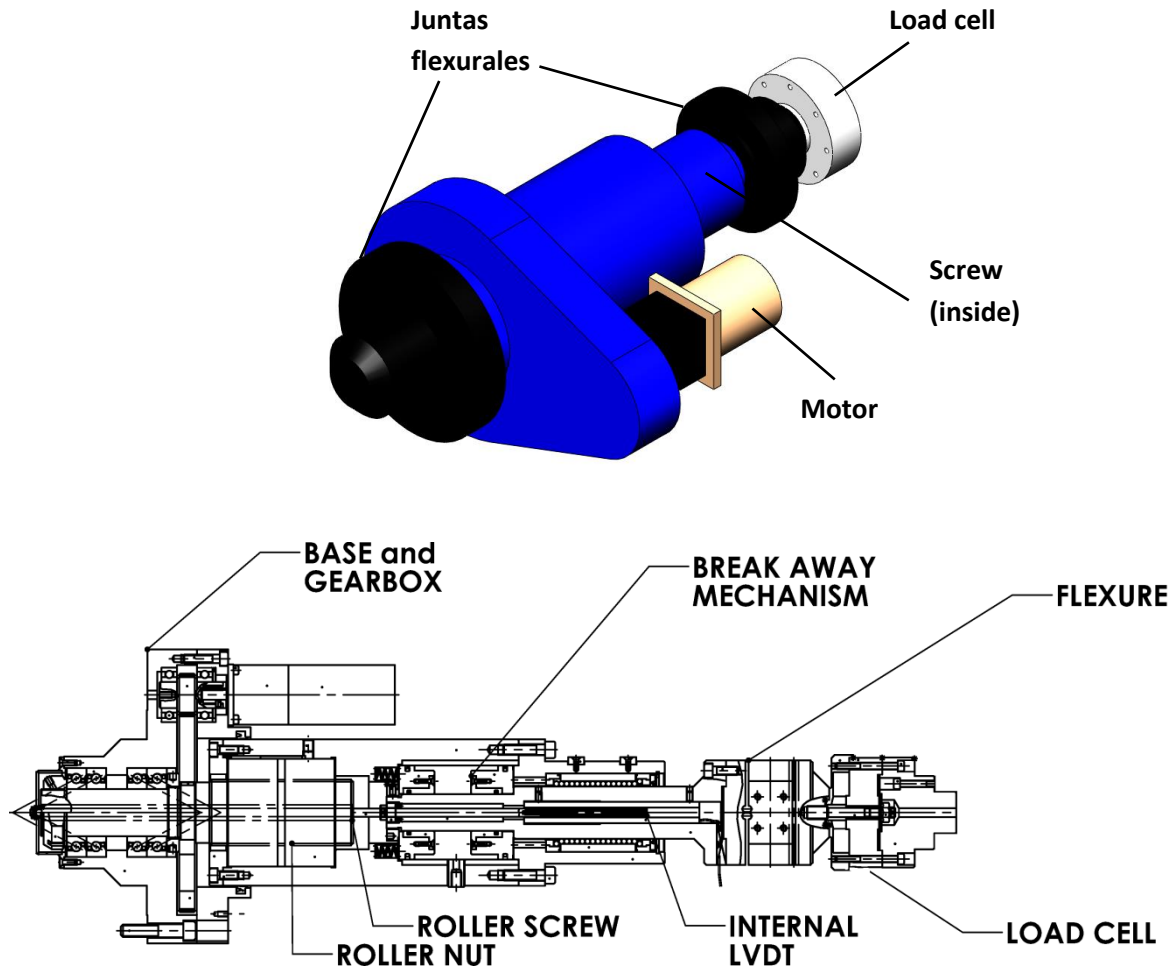



Figure 5-28 Hardpoint Actuator

Each actuator has attached to one end a flexural joints and a load cell at one end (see Figure 5-28). The load cell has the following specifications:

- Load capacity: 1000 lb (4450 N)
- Non- linearity (max): 0.05% F.S.
- Hysteresis (max): 0.05% F.S.

	<p>SPMT</p> <p>SPMT Conceptual Design Pre PDR</p>	<p>Code: TRP/TELE/001-R</p> <p>Issue: 1.C</p> <p>Date: 24/06/2014</p> <p>Page: 57 of 152</p>
---	--	--

- Non-Repeatability (max): 0.02% F.S.
- Deflection capacity: 0.005" (12.7 μm)
- Temperature (usable): -54°C to 93°C (-65°F to 200°F)
- Temperature effect on zero (max): 0.001% F.S./°F
- Temperature effect output (max): 0.002% reading/°F

As mentioned before, the hardpoint has a breakaway mechanism that extends or contracts when a specified load is reached. This is required for glass safety because the stress in the glass must be kept small (0.7MPa). The break-away mechanism is a pneumatically activated system that fixes the location of the shaft that exits the mirror side of the hardpoint body relative to the hardpoint body at loads below about 300 lbs, but allows extension or contraction at higher loads. There are two pistons having equal net area of 84.6 cm² sliding on the shaft. Pneumatic pressure is introduced between the two pistons driving piston 1 to the seat on the shaft, and piston 2 to the adjustable stop at the left end of the shaft in Figure 6.8. The net force on each piston with a pneumatic pressure of 0.26 MPa is 1431 N. The end stop is adjusted to leave a minimal gap and no interference. The springs push on piston 2 driving the shaft to the right until piston 1 contacts the main housing cap seat. Compressive breakaway occurs when the force between piston 1 and the seat on the main housing (not the shaft) drops to zero. This force is:

$$F_{1h} = F_{spring} - F_{comp}$$

Where: F_{1h} is the force between piston 1 and the main housing, F_{spring} is the force of the springs pushing on piston 2 and F_{comp} is the compressive force (a positive number).

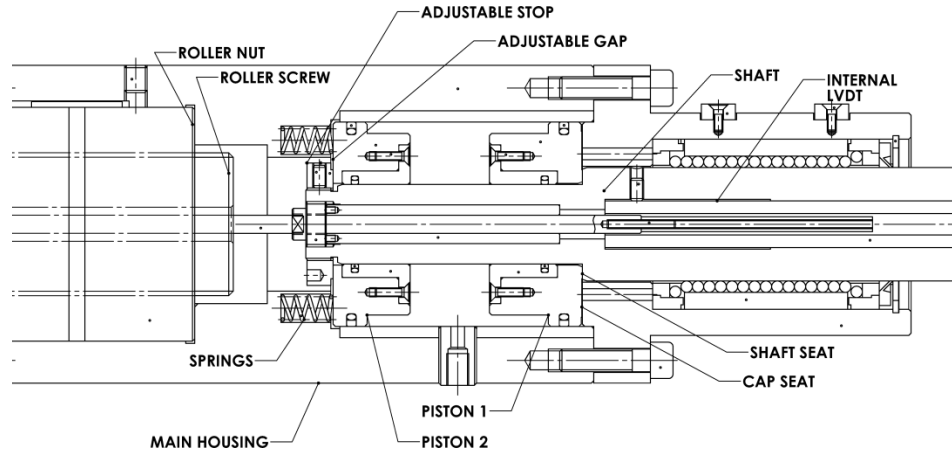



Figure 5-29 Break away mechanism

After compressive breakaway, the shaft moves through the minimal gap clearance between piston 2 and the main housing. Once piston 2 contacts the housing, the shaft is again constrained axially until the compressive load increases to the pneumatic pressure times the effective area of piston 2 at which point the shaft slides through piston 2 until piston 1 contacts piston 2 or the shaft contacts the main housing. Which contact occurs depends on the motorized axial extension of the hardpoint since the breakaway shaft may contact the stationary end of the roller screw shaft when the main housing has been contracted. If the clearance between piston 2 and the main housing is negative, the shaft will have axial play equal to the amount of interference. This condition is not allowed. Tension breakaway occurs when the force between piston 1 and the shaft seat drops to zero. This force is:

$$F_{1s} = PA - F_{spring} - F_{tension}$$

Where: F_{1s} is the force between piston 1 and the shaft, PA is the pressure force on piston 2 and $F_{tension}$ is the compressive force (a positive number). If the shaft continues to extend after a tension breakaway the spring force relaxes away to nothing after a few mm of travel leaving a net tensile load equal to PA .

The rotations and translations of the mirror have complex changes relationship to changes in the hardpoint lengths. To calculate these changes in hardpoint lengths, necessary to the control system, the lower attachment of the hardpoints is considered fixed to the cell plane and the upper attachment to the mirror plane to be moveable. The motion of the upper attachments

	SPMT SPMT Conceptual Design Pre PDR	Code: TRP/TELE/001-R Issue: 1.C Date: 24/06/2014 Page: 59 of 152
---	---	---

points is given by applying rotations and translations about the mirror vertex. With the “z” axis upward to the face of the mirror, the coordinate of the upper attachment is given by:

$$\begin{bmatrix} x' \\ y' \\ z' \end{bmatrix} = [E(\Delta\phi, \Delta\theta, \Delta\psi)] \begin{bmatrix} x \\ y \\ z \end{bmatrix} - \begin{bmatrix} \Delta X \\ \Delta Y \\ \Delta Z \end{bmatrix}$$

Where:

x, y, z : starting coordinates of the attachment point.

$\Delta X, \Delta Y, \Delta Z$: mirror translations

$[E(\Delta\phi, \Delta\theta, \Delta\psi)]$: Euler rotation matrix given by:

$$[E(\Delta\phi, \Delta\theta, \Delta\psi)] = \begin{bmatrix} \cos\theta\cos\phi & \cos\theta\sin\phi & -\sin\theta \\ \sin\psi\sin\theta\cos\phi - \cos\psi\sin\theta & \sin\psi\sin\theta\sin\phi + \cos\psi\cos\theta & \cos\theta\sin\psi \\ \cos\psi\sin\theta\cos\phi + \sin\psi\sin\theta & \cos\psi\sin\theta\sin\phi - \sin\psi\cos\theta & \cos\theta\cos\psi \end{bmatrix}$$

Where:

ϕ : rotation about “z” axis (yaw)

θ : is about the intermediate “y” (pitch)

ψ : is about the final “x” axis (bank or roll)


Positive angles are given by the right-hand rule.

5.2.3 Pneumatic suspension system

To support the whole mass of the mirror to prevent stress concentrations, a set of pneumatic actuators is provided. The actuators are connected to a load spreaders glued to the telescope mirror on the positions indicated on the Figure 5-30. There are double actuators (70) and single actuators (30) for a total of 170 pneumatic actuators. Figure 5-31 shows a section view of the loadspreaders supporting the mirror and the Figure 5-32 shows the different kind of loadspreaders and actuators.

The loadspreaders configuration is:

- 4 elements with four supports (pucks) in rectangular configuration
- 66 elements with three supports in a long triangle configuration
- 2 elements with three supports in a short triangle configuration
- 16 elements with two supports in a double configuration
- 12 single supports

	<p style="text-align: center;">SPMT</p> <p style="text-align: center;">SPMT Conceptual Design Pre PDR</p>	<p>Code: TRP/TELE/001-R</p> <p>Issue: 1.C</p> <p>Date: 24/06/2014</p> <p>Page: 60 of 152</p>
---	--	--

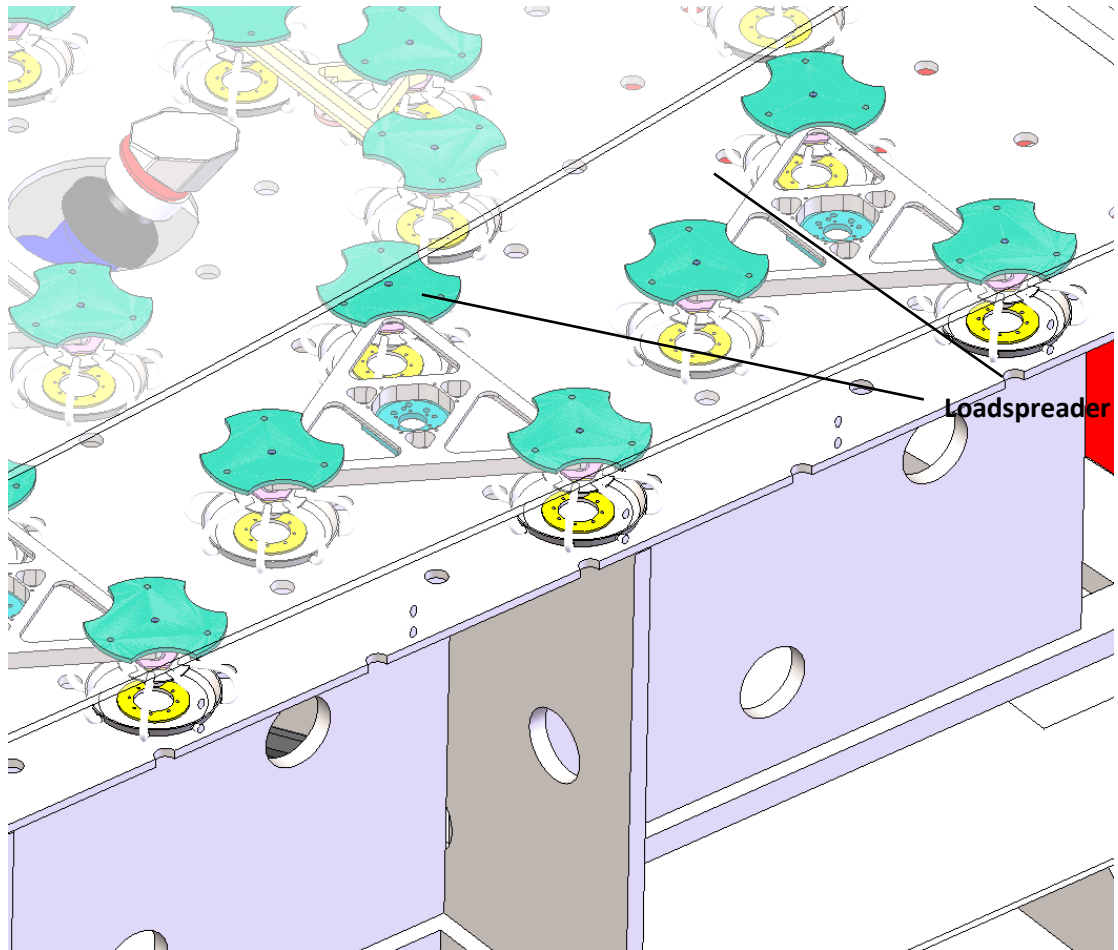



Figure 5-30 Loadspreaders

	<p style="text-align: center;">SPMT</p> <p style="text-align: center;">SPMT Conceptual Design Pre PDR</p>	<p>Code: TRP/TELE/001-R</p> <p>Issue: 1.C</p> <p>Date: 24/06/2014</p> <p>Page: 61 of 152</p>
---	--	--

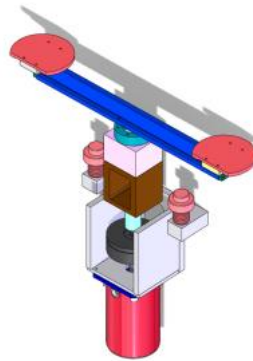
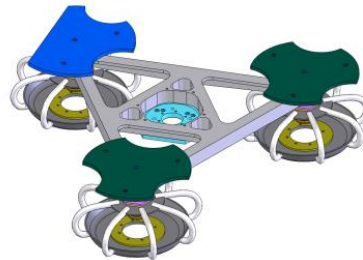
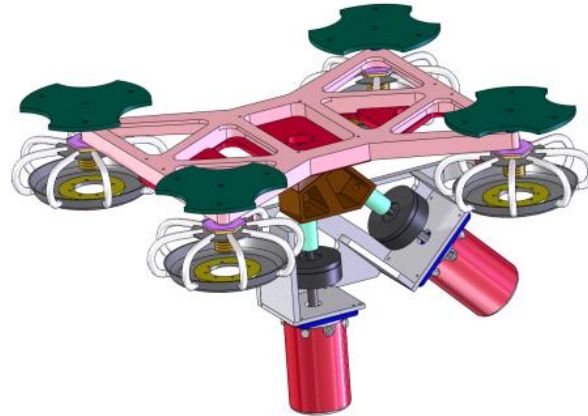



Figure 5-31 Loadspreaders configuration (four, three and double) and actuators

	<p style="text-align: center;">SPMT</p> <p style="text-align: center;">SPMT Conceptual Design Pre PDR</p>	<p>Code: TRP/TELE/001-R</p> <p>Issue: 1.C</p> <p>Date: 24/06/2014</p> <p>Page: 62 of 152</p>
---	--	--

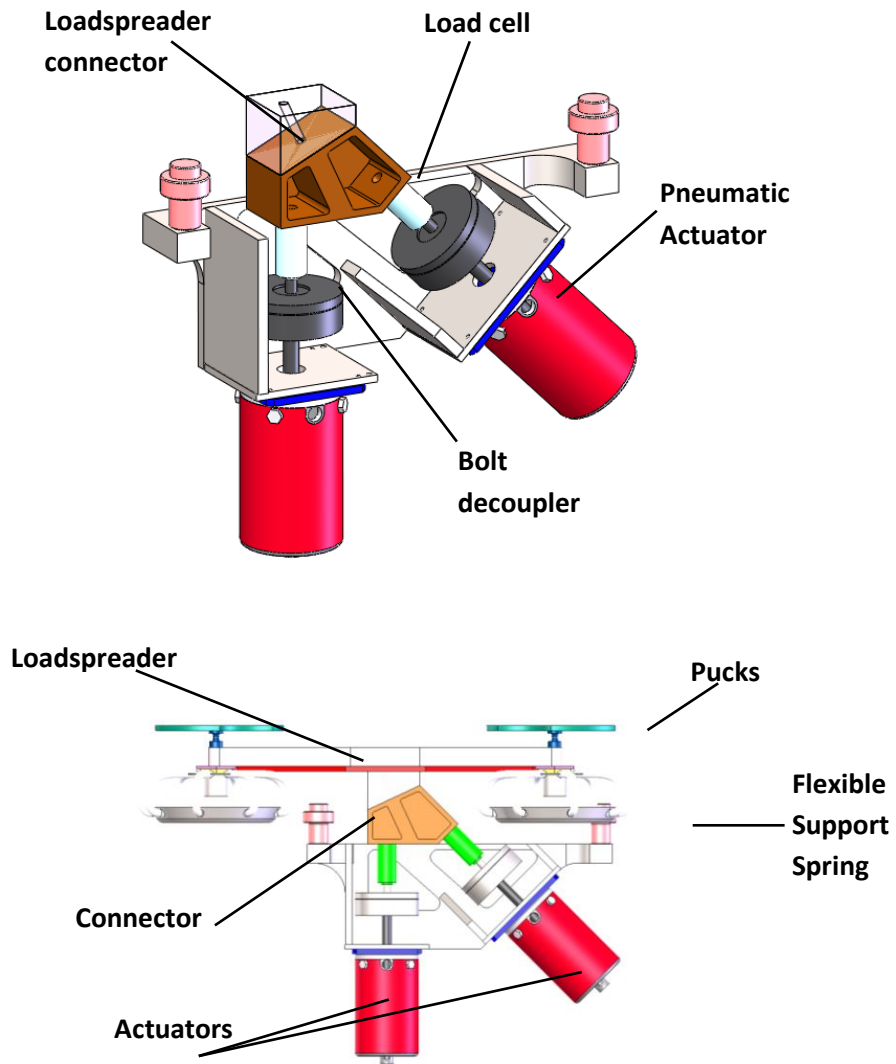



Figure 5-32 Suspension double actuator

Each actuator **Figure 5-32** is composed by:

- Load cell (INTERFACE)

	<p>SPMT</p> <p>SPMT Conceptual Design Pre PDR</p>	<p>Code: TRP/TELE/001-R</p> <p>Issue: 1.C</p> <p>Date: 24/06/2014</p> <p>Page: 63 of 152</p>
---	--	--

- Actuator, diaphragm pneumatic cylinder (CONTROLAIR, Inc. DE-6-L-XX-UM Mod 128)
- Pressure transducers (CONTROLAIR Inc. Type 500X, 0-10 VDC)
- Dual-single actuator card
- Actuator bolt decoupler Figure 5-33

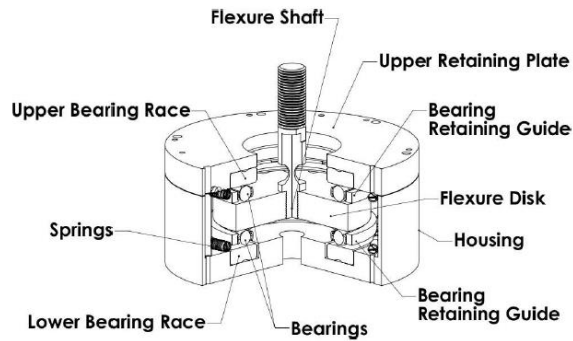


Figure 5-33 Actuator bolt decoupler

When the telescope is not in use or for the aluminizing process, the air supply to actuators can be suspended, with the telescope always in the zenith positions. Then a set of flexible spring supports hold the mirror. Figure 5-34 shows the mounting position of the supports and the configuration.

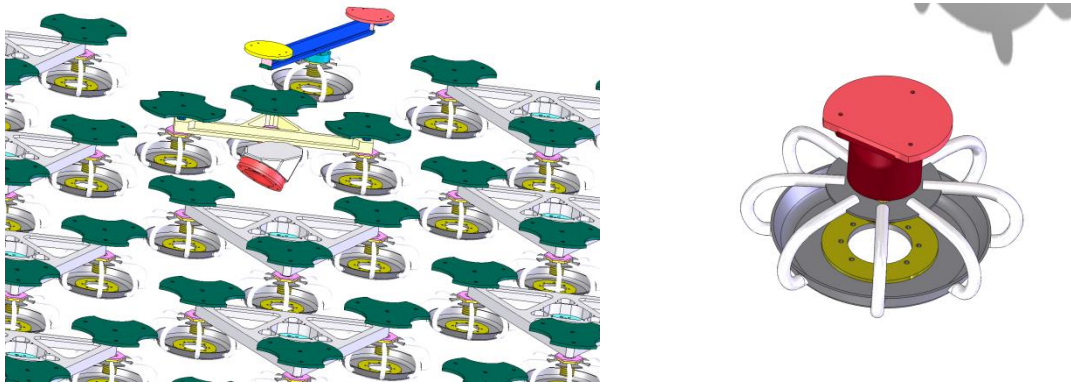



Figure 5-34 Flexible spring supports

	<p>SPMT</p> <p>SPMT Conceptual Design Pre PDR</p>	<p>Code: TRP/TELE/001-R</p> <p>Issue: 1.C</p> <p>Date: 24/06/2014</p> <p>Page: 64 of 152</p>
---	--	--

The static support was recommended the people of the MMT, for their experience in the manufacturing and implementation of the honeycomb mirrors on telescopes. On the base of this information and experiences the method of calculation for the supports can be resumed as follows.

The weight of the mirror is 8249 kg (18185 lbs), assuming for the preliminary conceptual axial and radial stiffness of the supports of 280 N/mm (1600 lb/in) (this data will be experimentally measured during the definitive design phase).

During the normal operation 170 pneumatic actuators hold the mirror each actuator controlled by a servo pneumatic valve. If the pressure fails, takes 0.5 seconds to the system from normal operation pressure to zero. In a one-dimensional analysis the static support assumes that the pressure falls off as a cosine function with a frequency ω equal to π rads/sec.

In the phase one is when the pneumatic actuators are turned off, if the mirror is holder by the actuators 7 mm above the static supports at a distance less than 7 mm the mirror began to be engaged to the support and assuming that takes 0.205 seconds, the equation form motion for these 0.205 seconds is:

$$y''(t) = g (\cos\omega t - 1)$$


The phase two describes the motion of the mirror from the instant that the static supports are engaged until the air pressure in the pneumatic cylinders reaches zero. This means after $t=0.205$ the mirror will have dropped 7 mm and begins to engage the static support. The velocity at the beginning of this phase is -0.111 m/s.

The one-dimensional natural frequency η of 170 supports, each with a stiffness of 1600 lb and a mirror weight of 18185 lbs mirror is:

$$\eta = \sqrt{\frac{k}{m}} = \sqrt{\frac{170 \times 1600 \times 384}{18185}} = 75 \frac{rad}{sec} = 11.9 Hz$$

The equation of motion from $t=0.205$ until the air pressure in pneumatic cylinders drops to zero at $t=0.5$ is:

$$y''(t) = g(\cos \omega t - 1) - \eta^2 \times y(t)$$

	<p>SPMT</p> <p>SPMT Conceptual Design Pre PDR</p>	<p>Code: TRP/TELE/001-R</p> <p>Issue: 1.C</p> <p>Date: 24/06/2014</p> <p>Page: 65 of 152</p>
---	--	--

The phase three describes the mirror motion after the air in the pneumatic cylinders is depleted then after $t=0.5$, the air in the pneumatic cylinder is depleted and the entire weight of the mirror is supported by the static support. The equation of motion simplifies to:

$$y''(t) = -(\eta^2 \times y(t)) - g$$

Using the maximum deflection of the support of 3.2 mm, the maximum deceleration equals 9.7 m/s^2 or 0.99 g.

The static deflection of the support under the mirror weight can be calculates from the natural frequency:

$$y(static) = \frac{g}{\eta^2} = \frac{9810}{(75)^2} = 1.74 \text{ mm}$$

This means that with 170 supports with an axial and lateral stiffness per support of 1600 lb the mirror compress the supports 1.74 mm when the pressure is turned off.

On the Figure 5-35 and Figure 5-36, the conceptual pneumatic and control diagrams for actuators are shown.

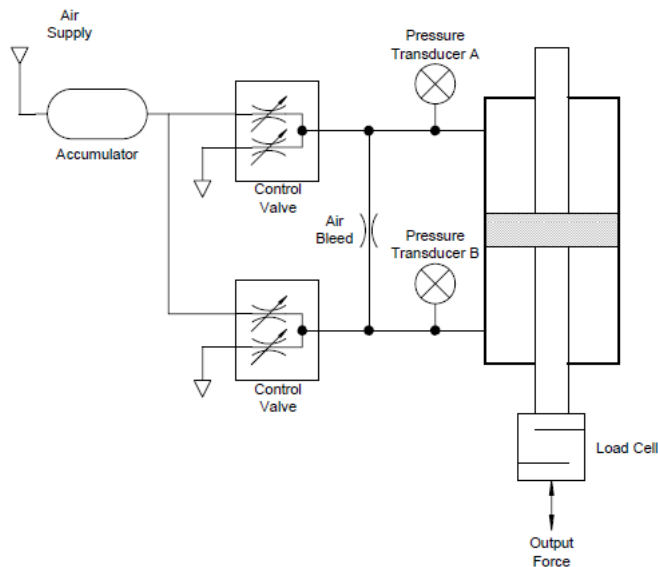


Figure 5-35 Actuators pneumatic diagram

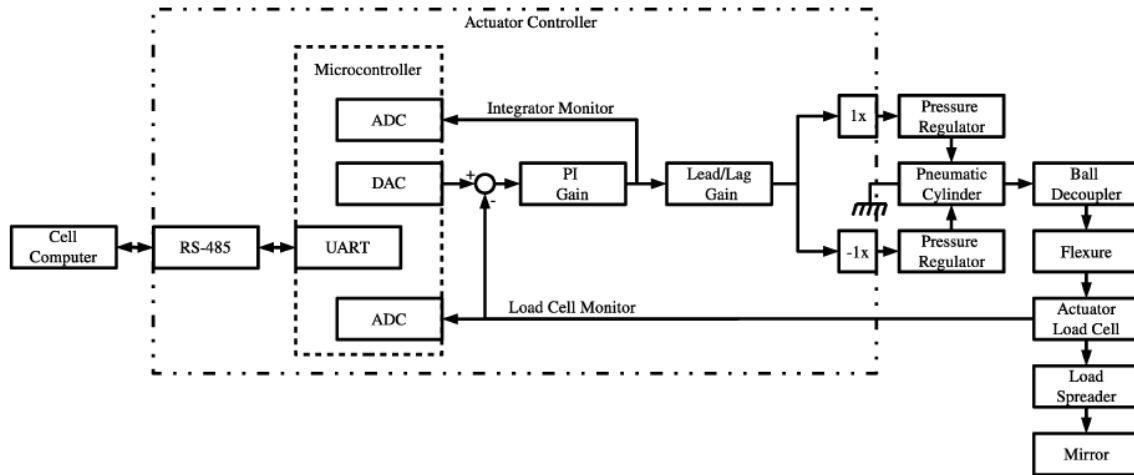


Figure 5-36 Actuators control diagram

5.2.4 Primary mirror thermal system

The mirror thermal system, consist in a set of 56 independent air injection system. The air is taken from the outside of the mirror cell and is thermalized with cold air via a glycol cold plate or with a hot air via a pair of resistors installed in a hot plate. Both plates attached to a centrifugal axial fan that injects the air to the mirror via a flexible air duct. Figure 5-37 shows the thermalizing system mounted on the mirror cell.

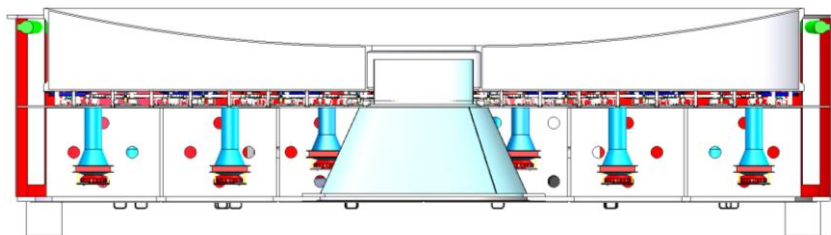



Figure 5-37 Primary mirror thermal system

	<p style="text-align: center;">SPMT</p> <p style="text-align: center;">SPMT Conceptual Design Pre PDR</p>	<p>Code: TRP/TELE/001-R</p> <p>Issue: 1.C</p> <p>Date: 24/06/2014</p> <p>Page: 67 of 152</p>
---	--	--

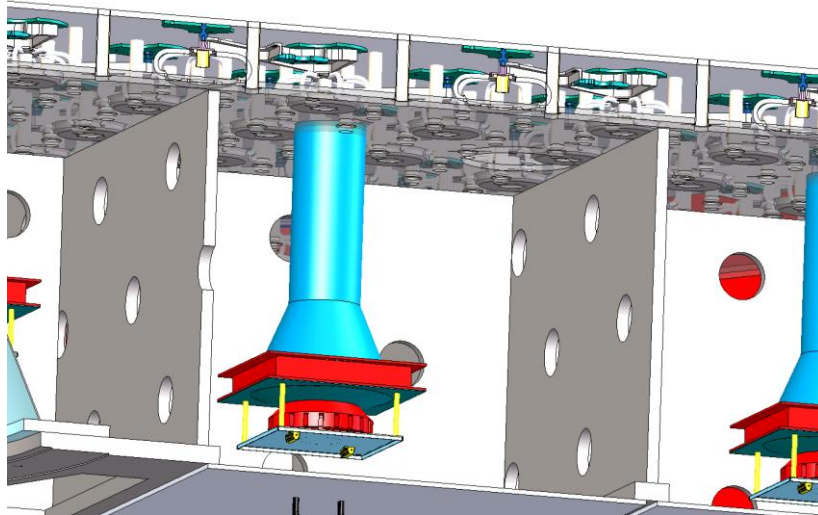


Figure 5-38 Primary mirror thermal system

Each of the 56 temperature systems can be managed as an independent subsystem for maintenance, Figure 5-39 shows a subsystem with the components. Each subsystem has an estimated power demand of 17.3 KW at a transient load and 12.2 KW at a steady state load.

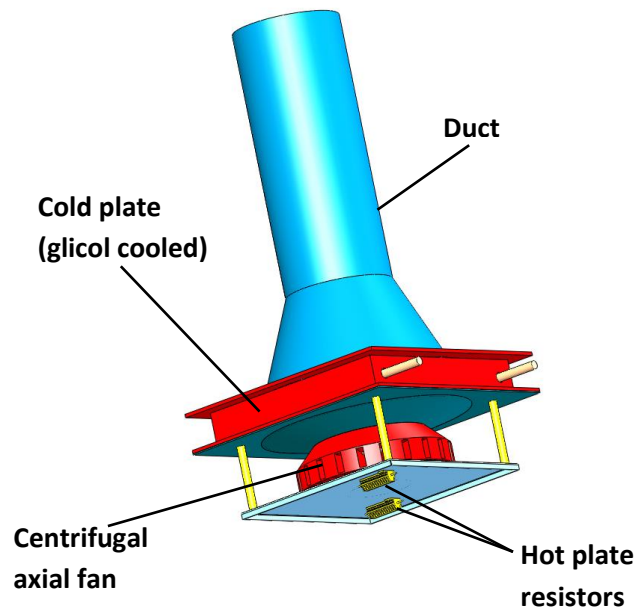



Figure 5-39 Primary mirror thermal system

	<p>SPMT</p> <p>SPMT Conceptual Design Pre PDR</p>	<p>Code: TRP/TELE/001-R</p> <p>Issue: 1.C</p> <p>Date: 24/06/2014</p> <p>Page: 68 of 152</p>
---	--	--

As parts of the thermal system are include nozzles for the interchange of air between the two chambers of the primary cell. These nozzles are in an arragment given by the manufacturers of the mirror and are shown in the following figure.


5.2.5 Thermocouple mirror temperature measurement

The temperate measurement can be taken for the honeycomb mirror with a Type E thermocouple chromium-constantan (like the MMT and Magellan teams) where the individual wires are converted to copper. The absolute temperature for the isothermal junction block IJB is measured as a single point with a solid state AD590 sensor all attached to the mirror backplate ventilation ducts (see Figure 5-40).



Figure 5-40 Thermocouple installation example

The final location of the measurement temperature will be defined on the definitive design phase, Figure 5-41 shows and example of the thermocouples location on the MMT.

	<p>SPMT</p> <p>SPMT Conceptual Design Pre PDR</p>	<p>Code: TRP/TELE/001-R</p> <p>Issue: 1.C</p> <p>Date: 24/06/2014</p> <p>Page: 69 of 152</p>
---	--	--

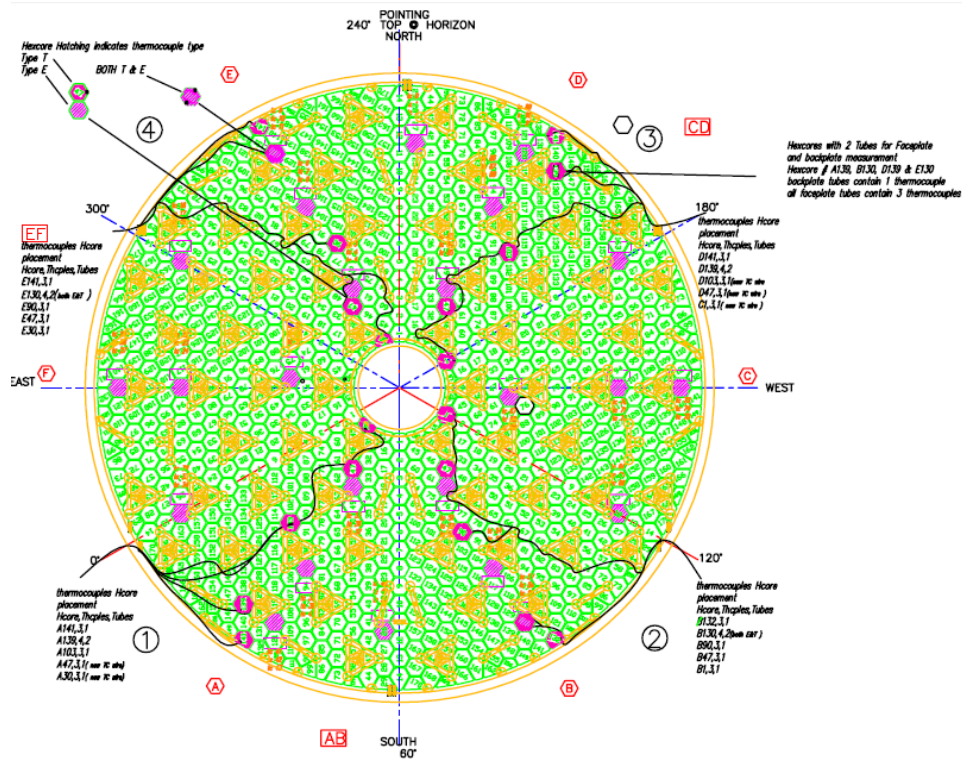



Figure 5-41 Thermocouple location example

5.3 Telescope structure

The telescope structure is mostly manufactured of structural steel AISI A36, with a first modal frequency above 2.3 Hz: The estimated stiffness for drive mount in the axial direction is around 6.7×10^6 N/mm and in the radial of 0.93×10^7 N/mm.

The total mass of the telescope including mount is 172 Tons and the telescope structure is 77 109 kg.

Figure 5-42, shows a section view and a lateral view of the telescope structure and mount.

	<p>SPMT</p> <p>SPMT Conceptual Design Pre PDR</p>	<p>Code: TRP/TELE/001-R</p> <p>Issue: 1.C</p> <p>Date: 24/06/2014</p> <p>Page: 70 of 152</p>
---	--	--

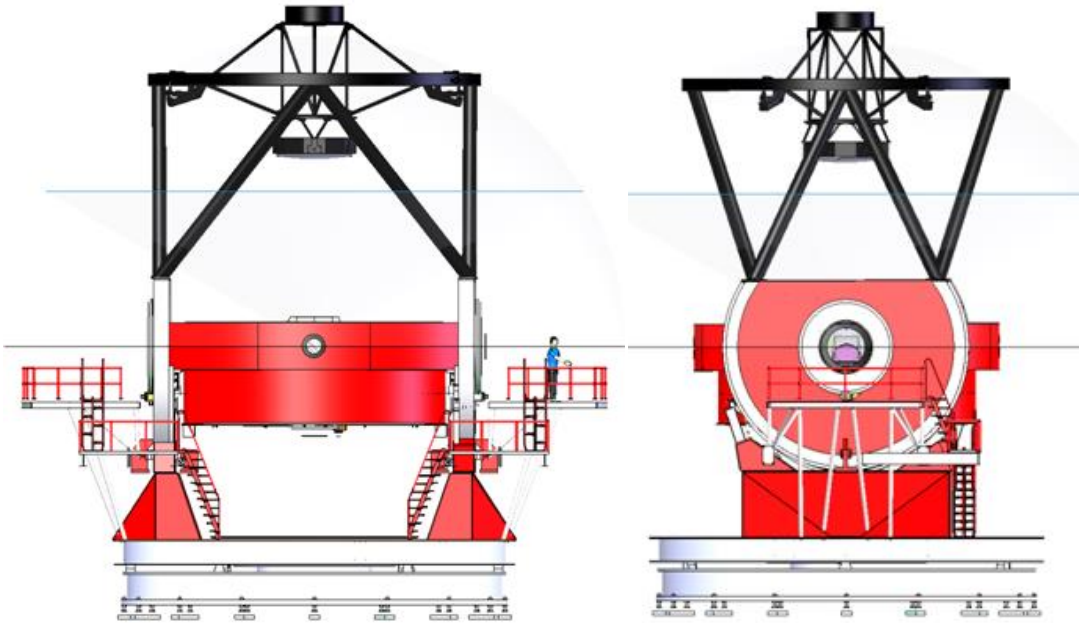


Figure 5-42 SPMT structure

5.4 Telescope counterweights

To balance the telescope during the elevation, a set of counterweights controlled by the elevation control system will be installed. Figure 5-43 show the vertical and the horizontal counterweights system, the vertical are located inside the elevation track rings and the horizontal at both sides of the primary mirror cell attached to the elevation ring.

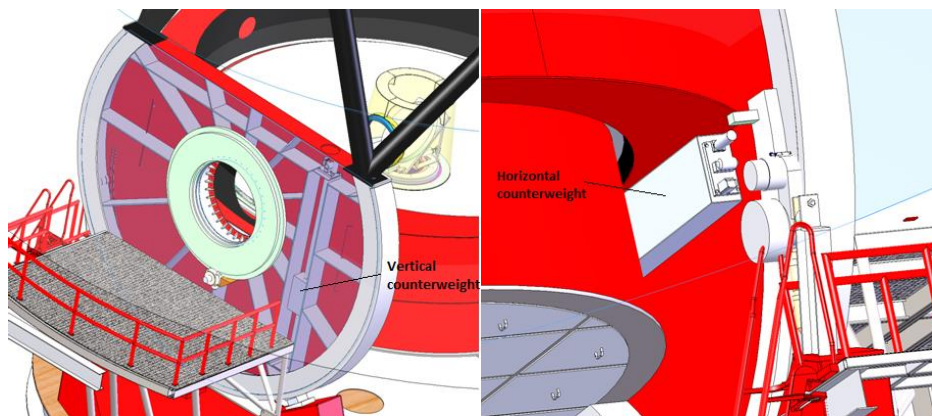



Figure 5-43 Vertical and horizontal counterweights

	SPMT SPMT Conceptual Design Pre PDR	Code: TRP/TELE/001-R Issue: 1.C Date: 24/06/2014 Page: 71 of 152
---	---	---

5.5 Secondary Mirror

The secondary mirror will be mounted on a cell with all the actuators necessary for active optics, this cell is on a basket-like structure suspended, 2 different configurations are proposed depending on the f secondary mirror configuration; a four vane end, tensioned spider from the top-end ring of the telescope for f/11 for Cassegrain focus. An Hexapod configuration (without vane end), as MMT telescope secondary mirror configuration, is proposed for f/5 Cassegrain and f/5 Nasmyth.

5.5.1 Vane system

The secondary mirror support is a cross spider structure (see Figure 5-44). This kind of structure has three advantages, stiff and stable, small aperture blockage; and easy to manufacture and assemble. For the structure, the natural frequency is:

$$f = \frac{1}{\pi} \sqrt{[(4EI/L) + (12EIr^2/L^3)]/J}$$

Where

E= Young modulus

I= moment of inertia of the spider structure beams

L= length of the spider beams

J=moment of inertia of the secondary unit

r= radius of the secondary unit

The spider stiffness reduces as the aperture size increases. To maintain a good frequency the spider must be pre-stressed using a vane system. The resonance frequency of a pre-stressed vane structure is:


$$f = f_0 \sqrt{(1 + P)/P_{Euler}}$$

$$P_{Euler} = \pi^2 EI/L^2$$

Where

f_0 : Frequency without preload

P: preload

	<p>SPMT</p> <p>SPMT Conceptual Design Pre PDR</p>	<p>Code: TRP/TELE/001-R</p> <p>Issue: 1.C</p> <p>Date: 24/06/2014</p> <p>Page: 72 of 152</p>
---	--	--

P_{Euler} : Euler critical load of the spider beam

I : moment of inertia of the beam

L : Length of the spider




Figure 5-44 Secondary spider

5.5.1.1 Description

The cage of the secondary mirror is supported by four vanes, each vane attached on the top end ring (see Figure 5-46). Each “vane end”, where a vane connects to the top end ring, is composed of a pair of levers connected to each other; the vanes and the top end ring are pivots (see Figure 5-45 Vane end detail). Rotation of one of the levers about its pivot results in a predominately axial motion; the other lever mostly controls radial motion, though there is some interplay. The levers are driven by stepper motors connected to screw drives. There are a total of eight motors, two at each vane end; one for axial motion and one for radial motion. Each lever is also connected to a linear encoder, so there are also eight encoders, four axial and four radial. Finally, there are eight load cells that measure the tension on each axial and radial lever. Together, these systems allow the secondary mirror to be positioned down to a micrometer. In addition, the Vane End program also must control all instrument rotators.

5.5.1.2 Mechanisms of the vanes

Each vane set consists of an upper and lower vane which intersect at a point, defined here as the “vane end node”. The purpose of the vane end actuators is to position each vane end node with

	<p>SPMT</p> <p>SPMT Conceptual Design Pre PDR</p>	<p>Code: TRP/TELE/001-R</p> <p>Issue: 1.C</p> <p>Date: 24/06/2014</p> <p>Page: 73 of 152</p>
---	--	--

sufficient accuracy to define the six degrees of freedom for the secondary mirror. Alignment tolerances for which the system is designed are 3 arcsec tilt, 0.762 mm lateral (radial position), and 0.0762 mm focus (axial position). At the same time the actuators must establish and maintain a 10,000 lb preload in each vane set. This will assure that the lowest local resonant frequency in the secondary end is above 8 Hz.

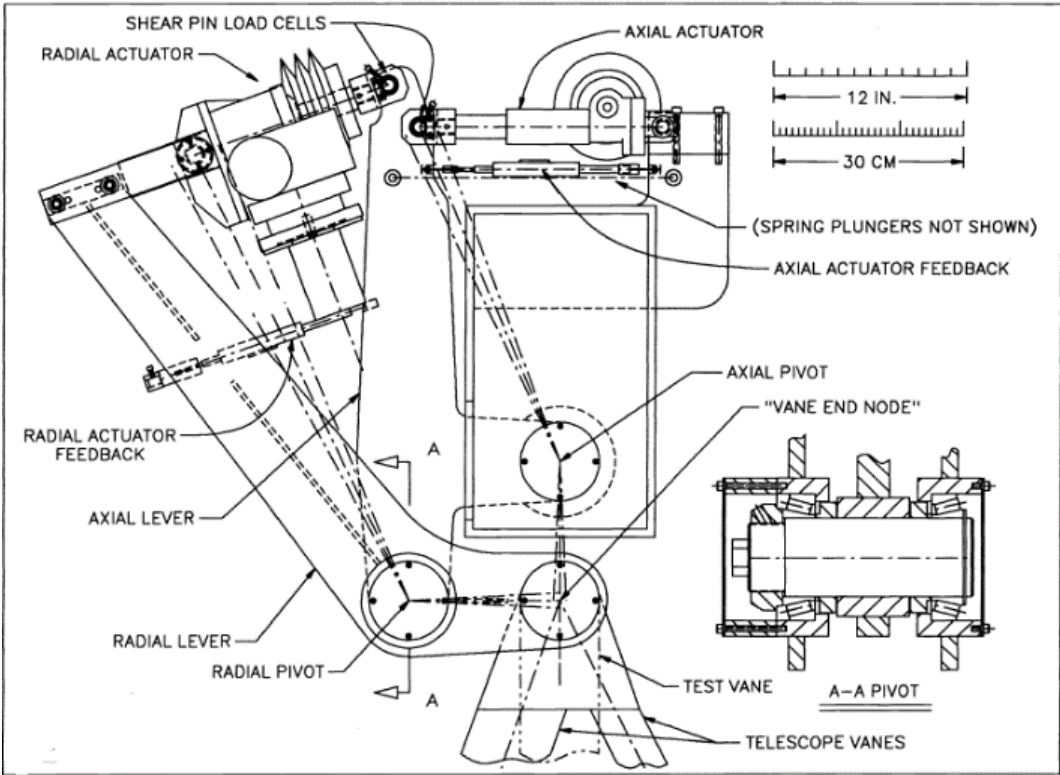



Figure 5-45 Vane end detail

	<p>SPMT</p> <p>SPMT Conceptual Design Pre PDR</p>	<p>Code: TRP/TELE/001-R</p> <p>Issue: 1.C</p> <p>Date: 24/06/2014</p> <p>Page: 74 of 152</p>
---	--	--


A system of levers was chosen to position the vane end node as shown in Figure 5-46. The radial lever is pivotally mounted to the end of the axial lever so that when the radial actuator alone moves, the vane end node moves with radial motion. The axial lever is pivotally mounted to the support structure (the secondary circular end ring) so that when the axial actuator alone moves, the two-lever assembly moves so that the vane end node moves axially. The two motions will be computer controlled to compensate for the slightly accurate paths. The use of levers, as compared to a two axis linear system, has the following advantages in this application:

- The force of each actuator is amplified due to the mechanical advantage of the levers. This decreases the force, and increases the stroke, required from each actuator. The commercially available actuators are therefore smaller in this short-stroke application.
- The positioning error of each actuator is de-amplified due to the motion of the levers.
- The effective friction of the system is reduced. Although two bearings rotate for either independent motion, the bearing radius is much smaller than half the arc radius of the motion of the vane end node.
- The system is compact in the area inside the circular end ring, where space is at a premium.

Each assembly requires three main pivots for the levers and two small pivots for each actuator. Timken precision class no" tapered roller bearings were finally selected for their relatively high load capacity, ease of preload, acceptable precision and relatively low cost. Each bearing has a dynamic radial load rating of 2585.47 kg (5700 lbs) for 3000 hours at 500 rpm L_{10} and can withstand a static radial load of 15195.34 kg (500 lbs)/bearing and experience only very slight brinelling of the rolling surfaces.

Although friction on the small pivots would not contribute substantially to positioning error at the vane end nodes, it could cause considerable error in the load feedback devices. Therefore, rolling element bearings were used for the small actuator pivots. Needle bearings were selected for their low cost and ease of mounting. They were used at the ends opposite the load cells as well as in the load cell devices.

With the lever geometry shown in figure 6.23, the axial actuator requires a capacity of about 453.59 kg (1000 lbs), the radial of about 1814.36 kg (4000 lbs).

	<p>SPMT</p> <p>SPMT Conceptual Design Pre PDR</p>	<p>Code: TRP/TELE/001-R</p> <p>Issue: 1.C</p> <p>Date: 24/06/2014</p> <p>Page: 75 of 152</p>
---	--	--

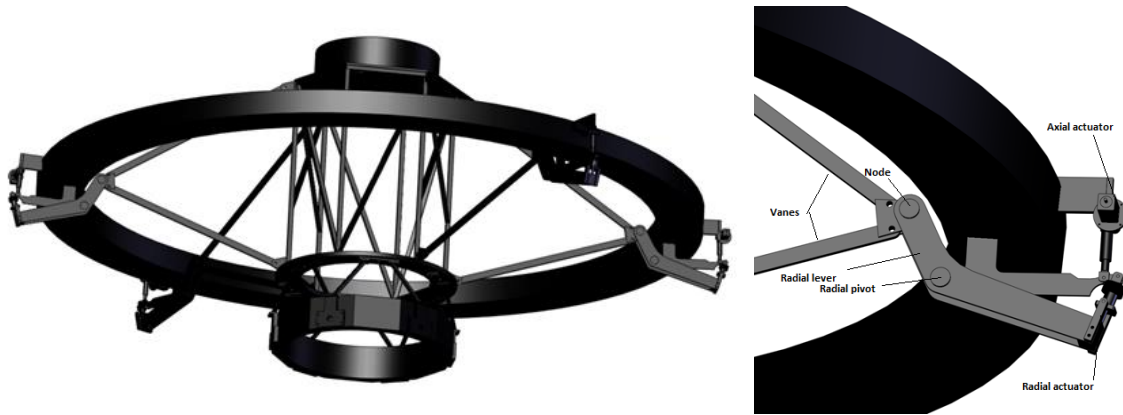



Figure 5-46 Vane end configuration

The actuators are a machine screw type with the encoder on the motor or screw. That is, that a linear encoder would be mounted in parallel with the actuator so that we could truly control the length of the actuator at or near the level of the encoder resolution.

The axial actuator is a rotating nut, translating screw unit. The Duff-Norton Model M-2465-2-1 consists of a 25.4 mm (1") diameter, 6.35 mm (1/4") pitch single lead acme screw driven by a 20:1 worm, defining an overall ratio of 80 turns of the worm (and therefore motor) per inch of stroke. The unit will include a NEMA 56C flange to which we mount a Mycom UPS52-5913(B) 5-phase stepping motor. At 500 (full) steps/revolution, the motor provides a theoretical resolution of 6.6 $\mu\text{m}/\text{step}$ at the vane end node, or 16 $\mu\text{m}/\text{step}$ at the actuator.

The screw is enclosed by a tube with a wiper-scraper seal to keep dust out and grease lubrication in. It includes a threaded end on the moving tube to which we mount a special clevis with load-sensing pin. The opposite end includes mounting provisions for a similar special clevis. The unit includes a limit switch assembly which is used to limit both ends of travel.

The actuator has a load rating of 907.18474 kg (2000 lbs) limited by the worm and nut. In this application the 6.1 Nm (54 lb-in) peak torque rating of the motor will be limited to about 2.25 Nm (20 lb-in) by a current limitation in the control system. The calculated maximum output force we require from the actuator is about 453.59 kg (1000 lbs), which would require about 1.58 Nm (14 lb-in) input torque. The actual current will be determined using the shear pin load cells for force feedback during calibration of the telescope control system. The actuator manufacturer states that due to internal friction the required input torque can vary by something like 15% to 40% over the life of the actuator.

	<p>SPMT</p> <p>SPMT Conceptual Design Pre PDR</p>	<p>Code: TRP/TELE/001-R</p> <p>Issue: 1.C</p> <p>Date: 24/06/2014</p> <p>Page: 76 of 152</p>
---	--	--


The radial actuator is also a rotating nut, translating screw unit. The Duff-Norton Model LTM-9705-4-B-C consists of a 38.1 mm (1 1/2") diameter, 9.525 mm (3/8") pitch single lead acme screw driven by a 6: 1 worm plus a 12: 1 input gearbox. This defines an overall ratio of 192 turns of the motor per inch of stroke. The unit also includes a NEMA 56C flange to which we mount the Mycom UPS52-5913(B) 5-phase stepping motor. At 500 (full) steps/revolution, the motor provides a theoretical resolution of 2 $\mu\text{m}/\text{step}$ at the vane end node, or 6.5 $\mu\text{m}/\text{step}$ at the actuator. The screw is enclosed by a flexible bellows-type boot. The screw includes a threaded end to which we mount a special load-pin clevis identical to that used for the axial actuator. We have adapted the base-mounting of the body of the actuator to turn unions using a special turn union plate. This unit also includes a limit switch assembly which is used to limit both ends of travel.

This actuator has a structural rating as a jack of 5 tons but is de-rated to 2267.96 kg (5000 lbs) due to the input gearbox. The 6.10 Nm (54 lb-in) parallel peak torque rating for the motor will be limited to about 3.6 Nm (32 lb-in) by a current limitation in the control system. This will limit the force from the actuator to a level slightly above the 1769 kg (3900 lb) maximum force which we require. The actual current will be determined using the shear pin load cells for force feedback during calibration of the telescope control system, and again the required input torque can vary by something like 15% to 40% over the life of the actuator.

The axial actuator requires external preloading to accommodate load reversal at low altitude angles. The load reversal (compression to tension at lowering altitude angles) would otherwise cause a sudden and uncontrollable focus and tilt motion of the secondary due to clearance on the clevis bearings and acme threads.

Two spring plunger assemblies straddling each axial actuator have been included to assure that the actuator is in compression for all secondary assemblies and at all altitude angles. Each plunger houses two Century D51 die springs or equivalent preloaded to about 113.39 kg (250 lbs) per plunger in the minimally compressed condition. The maximum force in each plunger is about 149.68 kg (330 lbs) at maximum compression. The plungers are used to house the springs (so that they are contained should one ever structurally fail) and to provide a convenient means of preloading.

Two modes of operation will be used for the vane end actuator system. The focus and collimation will occasionally be reset under closed loop control of both actuators. That is, the secondary will be realigned with the primary using sensors which are in the focal plane. While tracking or slewing between those resets, the actuators will be under open loop control to compensate for gravity and thermal effects. That is, the computer will monitor the telescope altitude angle and structure

	<p>SPMT</p> <p>SPMT Conceptual Design Pre PDR</p>	<p>Code: TRP/TELE/001-R</p> <p>Issue: 1.C</p> <p>Date: 24/06/2014</p> <p>Page: 77 of 152</p>
---	--	--


temperature, determine the expected relative motion of the secondary with respect to the primary and continuously calculate the desired actuator positions and rates necessary to keep the secondary focused and collimated. The actuators will be controlled as dictated by computer calculation using only their local feedback devices (encoders).

Two encoders Mitutoyo 542-325 linear (glass) scales, with 1 μm resolution, have been tentatively chosen. The axial unit is mounted very close to the axial actuator. As located it will provide maximum control resolution and adequate stroke (50.8 mm stroke). The radial unit is mounted about midway between the actuator and its pivot, where 58.5 mm of stroke is required. The lost accuracy is not a problem here since the radial precision required is much less demanding (30 μm at the vane end node). Both encoders are flexure mounted with piano wire flexures mounted to sleeves at each end of the unit and at the structure. The flexures must have relatively low off-axis stiffness so as not to cause binding of the encoder plunger. However, axial stiffness of the flexures is not particularly critical, so this should be achievable.

Shear pin type load cells were selected as the simplest and least expensive means of monitoring the actuator forces. The load pins are retained to the central support lug by a cap screw against a slotted flat on the outside diameter of the pin. Needle bearings mounted in the mating special clevis accommodate the small rotation angles established by the pivot motions. The error due to the friction torque from the needle bearings was estimated to be less than 1%. This mounting (as opposed to having the bearing in the central lug) makes for reduced looseness under the slight torsional loading created by the acme screw/nut friction (the supporting levers and structure must react these small torques). In theory, only two load cells are necessary, one axial and one radial. However, two load cells will be used in each subsystem for redundancy (for comparison with each other, should either fail).

5.6 Tertiary Mirror

In order to deflect the light to the Nasmyth location, a flat diagonal tertiary mirror is required. Figure 5-2 shows the SPMT tertiary mirror. The specific characteristics and detailed design will be defined on the definitive design phase.

	<p>SPMT</p> <p>SPMT Conceptual Design Pre PDR</p>	<p>Code: TRP/TELE/001-R</p> <p>Issue: 1.C</p> <p>Date: 24/06/2014</p> <p>Page: 78 of 152</p>
---	--	--

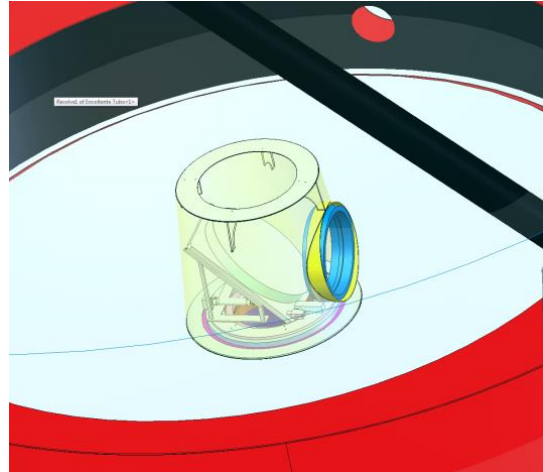
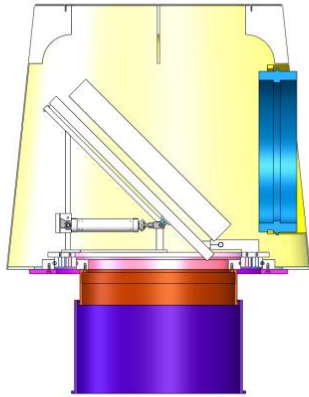


Figure 5-47 Tertiary mirror

5.7 Telescope Building

Telescope building will be designed by M3 Engineering. The following images represent the details of the SPMT building requirements. The definitive design will contemplate the final design.

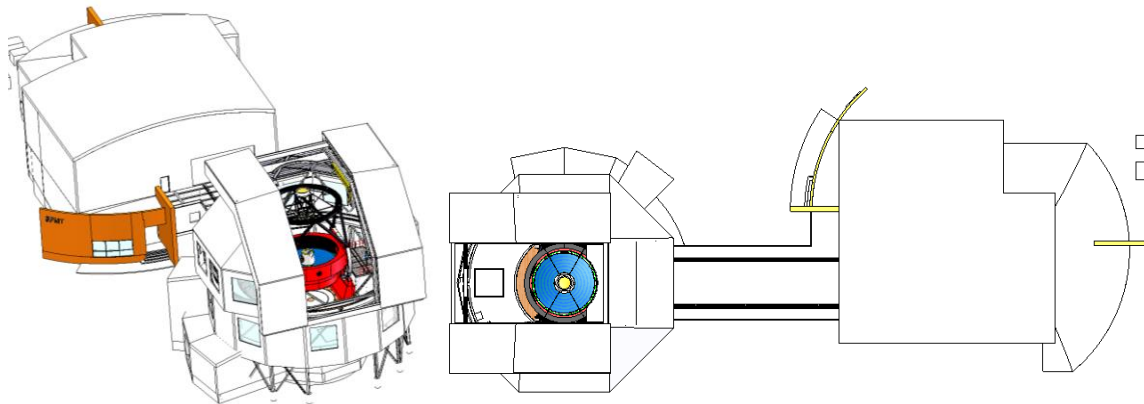


Figure 5-48 SPMT building (telescope enclosure and services building) aerial view.

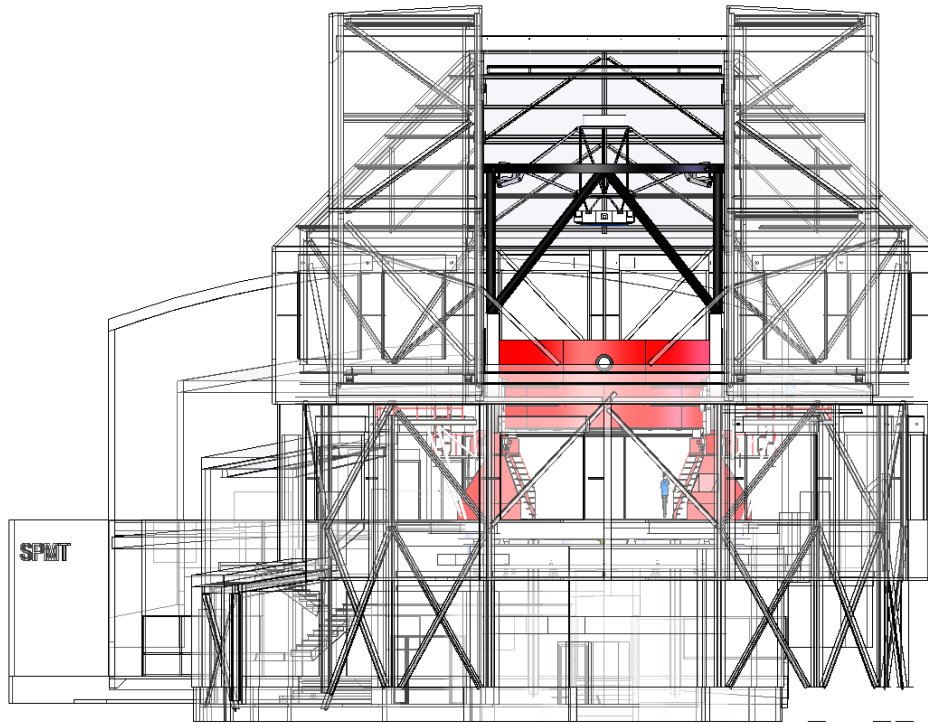


Figure 5-49 Telescope enclosure

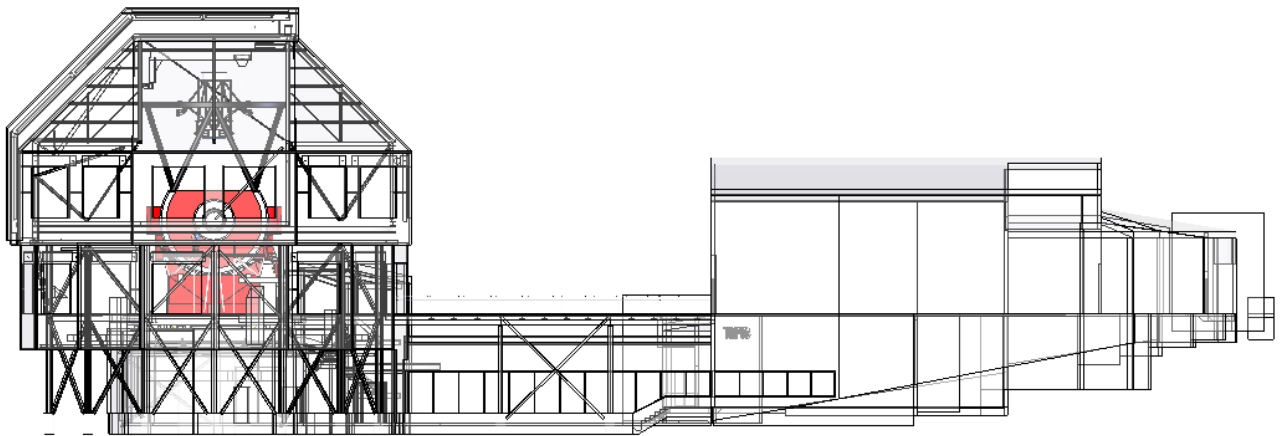



Figure 5-50 Cross section of the telescope enclosur

	<p>SPMT</p> <p>SPMT Conceptual Design Pre PDR</p>	<p>Code: TRP/TELE/001-R</p> <p>Issue: 1.C</p> <p>Date: 24/06/2014</p> <p>Page: 80 of 152</p>
---	--	--

5.8 F/5 INSTRUMENTS

For the SPMT design is considered a battery of F/5 instruments to start operations

The first possible instruments for SMPT are: Hectospec, Hectochelle, Binospec, MMIRS, and Megacam, all for f/5 secondary mirror. In the future for the SPMT concept also another f like f/9, or f/11 will be considered.

5.8.1 Hectochelle and Hectospec

Hectospec (see Figure 5-51) is a moderate resolution multi-object spectrograph the instrument receives the light from the f/5 focus into a multifiber positioner attached to the MMT Cassegrain rotator (see Figure 5-52). The instrument consist in a positioner robot (see Figure 5-53) inside the multifiber positioner a fiber duct (300 fibers of 25 m long) inside a cable wrap (see Figure 5-54) to transfer the light from the positioner to the spectrograph and the spectrograph itself mounted on a big optical bench (see Figure 5-55) inside a room on the MMT building. Hectochelle is the other spectrograph with similar installation requirements of Hectospec.

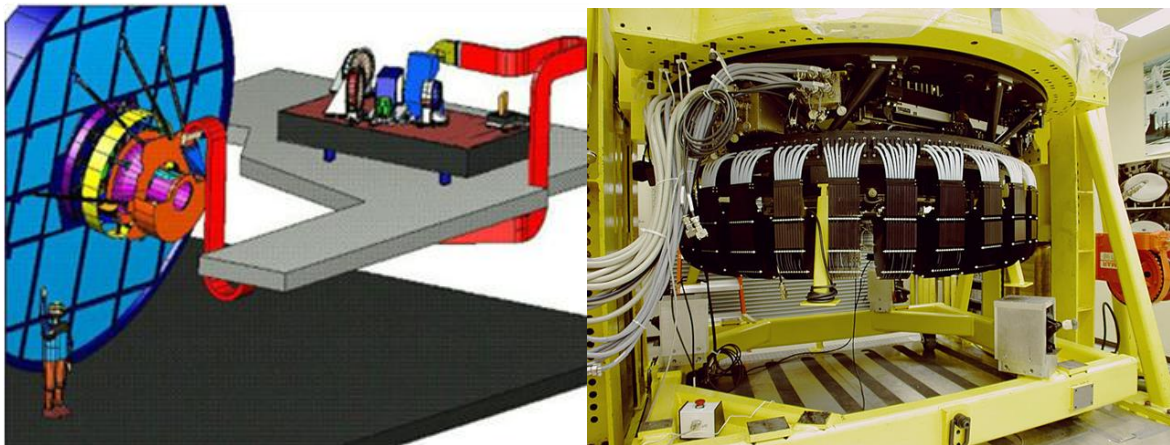


Figure 5-51 Hectospec concept



Figure 5-52 Hectospec positioner on the MMT Cassegrain rotator

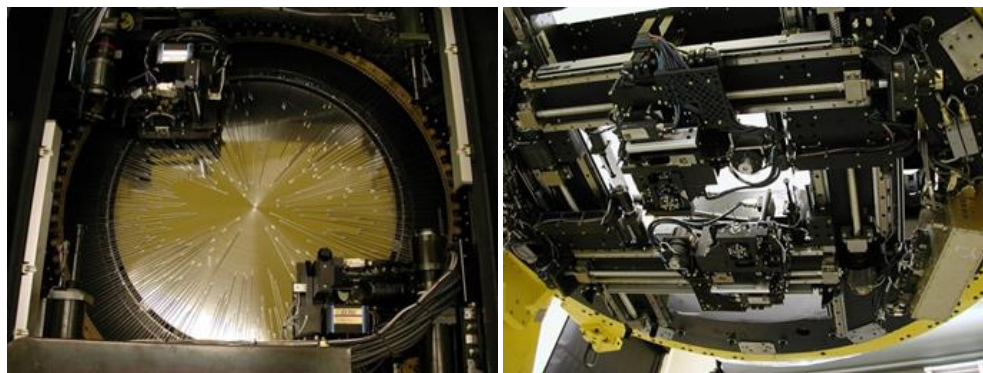


Figure 5-53 Hectospec multifiber robot positioner




	<p>SPMT</p> <p>SPMT Conceptual Design Pre PDR</p>	<p>Code: TRP/TELE/001-R</p> <p>Issue: 1.C</p> <p>Date: 24/06/2014</p> <p>Page: 82 of 152</p>
---	--	--

Figure 5-54 Hectospec multifiber cable wrap to spectrograph room

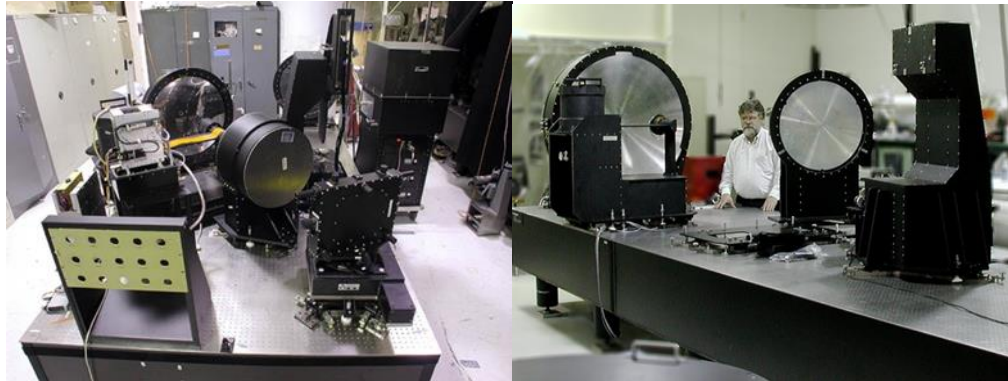



Figure 5-55 Hectospec (left) and Hectochelle (right) optical benches

Like Hectospec, Hectochelle also is a fiber-fed, bench mounted Hectochelle spectrograph that operates at the post-conversion MMT. Hectochelle is designed to operate with the MMT in its F/5, wide field mode. In this mode, a triplet wide field corrector and atmospheric dispersion compensator delivers a 1° field of view between zenith and two air masses (60°). The robot positioner (Figure 5-53) and fiber system can be operated both with Hectochelle and Hectospec a moderate dispersion spectrograph designed primarily for galactic red shift surveys and studies of large scale structure. The robot positioner places all 300 fiber buttons for observation in 5 min with an accuracy of 25 μ m or better. The fiber system consists of turning prisms at the input end, a 26 m fiber run and a fiber feed at the spectrograph end. The fiber diameter is 250 μ m, or 1.500 at the MMT F/5 plate scale.

5.8.1.1 Hectospec and Hectochelle mounting considerations on the SPMT

The design mounting considerations for Hectospec and Hectochelle are:

- Both instruments are designed to operate on the Cassegrain focus and the light is transferred to the instrument via a 25 m long cable wrap, in the case of the MMT there's no problem in this configuration due the rotation of the MMT building. In the case of SPMT if the telescope rotates independent to the building like traditional telescopes (Magellan for example), is too complex to mount the instrument on the Cassegrain focus, unless that the optical bench where located under the telescope for this it is necessary to

	SPMT	Code: TRP/TELE/001-R
	SPMT Conceptual Design Pre PDR	Issue: 1.C Date: 24/06/2014 Page: 83 of 152

have more height on the cassegrain focus to allocate the instrument and the protection cabin with Air Conditioned system. Another option is to mount the optical bench on the Nasmyth platforms of the SPMT with the cabin, and maintain the instrument on the cassegrain rotator. This second option also has several technical problems to solve during the elevation movement of the telescope. This technical problems and options will be developed during the concept design.


- Another problem to solve is the focal distance of the instrument; this must be maintained despite the changes implemented on the SPMT to obtain a telescope with Cassegrain and Nasmyth rotators included. The solution will be analyzed during the concept design.
- Independently to the final solution, the vibration induction due to the instrument location over the instrument optical bench must be analyzed.

5.8.2 **MMIRS**

The MMT and Magellan infrared spectrograph (MMIRS) is a cryogenic multislit spectrograph that operates from 0.9 to 2.4 microns. It will be deployed at the f/5 foci of the MMT and Magellan 6.5m telescopes. Using a fully refractive design, MMIRS offers R=1200-3000 spectral resolution with a spatial resolution of 0.2 arcsec per pixel on a 2kx2k Hawaii-2 array (2048x2048 pixel array). It offers a 7_x7_ imaging field of view and a 4_x7_ field of view for multi-object spectroscopy. MMIRS is the first detector infrared camera developed by wide field Smithsonian.


One of the major goals for MMIRS is developing a physical understanding of high redshift galaxies.

MMIRS	
Parameter	Value
Configurations	Imaging, long slit, multislit
Operating Bands	Y, J, H, K, HK, JH, zJ
Field of View	6.9 x 6.9 arcmin
Detector	Hawaii-2 HgCdTe

	SPMT	Code: TRP/TELE/001-R
	SPMT Conceptual Design Pre PDR	Issue: 1.C Date: 24/06/2014 Page: 84 of 152

Detector Format	2048 pix, square
Read noise	16 e-
Dark Current	0.06 e-/pixel_sec
Data Acquisition	Double correlated or Up-the-ramp
Resolution	1200-3000
Grism Available	J, H, HK
Slit Mask Field	4.0 x 6.9 arcmin
Long Slit Widths	0.2, 0.4, 0.6, 0.8, 1.0, 1.2, 2.4 arcsec
Long Slit Length	7 arcmin
Cooling	LN2
Guide	2 Instrument Mounted CCDS

Table 5-2 Parameters and values of the instruments MMRIS

	<p>SPMT</p> <p>SPMT Conceptual Design Pre PDR</p>	<p>Code: TRP/TELE/001-R</p> <p>Issue: 1.C</p> <p>Date: 24/06/2014</p> <p>Page: 85 of 152</p>
---	--	--

5.8.2.1 MMIRS overview

The slit mask chamber is a vacuum vessel at the top of the instrument sealed at the top by the first corrector lens and at the bottom by a gate valve. The slit mask chamber and all of its contents can be disconnected from the bulkhead that forms the top of the main instrument chamber. The slit mask chamber contains the corrector optics, the Dekker wheel for aperture selection, the slit mask wheel, a dewar assembly, and the guider pick off mirror. The gate valve, located between the slit mask wheel and the first collimator lens, isolates the optics and detector during slit mask exchange. The gate valve is mounted to the top bulkhead of the main instrument chamber.


The toroidal slit mask LN2 reservoir is supported by an insulating G-10 ring from the bottom flange of the slit mask chamber. The top of the slit mask LN2 reservoir serves as the mounting plate for the slit and Dekker wheels and the guider pick off mirrors. To the sides are two windows that pass the guider light outside the cryostat. The cold baffle that blocks thermal emission from the warm gate valve is mounted to the central wall of the slit mask chamber LN2 reservoir.

The main chamber, sealed at the top by the gate valve, contains the collimator optics, Lyot stop, filter and disperser wheels, camera optics, and detector assembly. A second G-10 ring mounted on the inside of the main chamber bulkhead supports the D-shaped LN2 reservoir in the camera section. The face of this reservoir is the main optical bench supporting the collimator and camera optics, disperser and filter wheels, and the detector assembly. All major aluminum cryogenic components in MMIRS were stress relieved by cooling from room temperature to 77K at several steps during the machining process.

MMIRS contains ten mechanisms: a calibration fold mirror slide, two guider assemblies, a Dekker wheel, a slit mask wheel, a gate valve (and its baffle), two filter wheels, a disperser wheel, and a detector focus assembly. All of the internal mechanisms are driven by 200 step revolution-1 Phytron VSS-52 vacuum rated stepper motors with 0.35 N-m of holding torque. The external guider mechanisms are driven by normal duty Phytron ZSS-52 stepper motors with 0.45 N-m of torque.

Effective thermal design of MMIRS requires balancing competing factors:

1. To minimize dark current the detector should be as cold as possible
2. To avoid damage the optics and detector cannot be cooled or warmed too rapidly
3. The slit masks need to be warmed and cooled as rapidly as possible to allow convenient daytime exchange and
4. The system should be as simple as possible

	<p>SPMT</p> <p>SPMT Conceptual Design Pre PDR</p>	<p>Code: TRP/TELE/001-R</p> <p>Issue: 1.C</p> <p>Date: 24/06/2014</p> <p>Page: 86 of 152</p>
---	--	--

Our approach was to build MMIRS around two liquid nitrogen dewars which are coupled as tightly as possible to the spectrograph components. We control the detector and optics warmup and cool down rates by regulating heater power or the flow of LN2.

Radiation shields surround the cold spectrograph components. The radiation shields are 1.26mm thick aluminum 1100 sheet metal supported with G-10 standoffs for thermal isolation from the warm and cold surfaces. A single layer of aluminized Mylar covers both sides of the G-10 rings, the radiation shields and much of the LN2 tank surfaces. Electrical connections pass through connectors mounted on the thermal shield flange. The flange connectors allow easy shield removal and provide a light-tight shield penetration. Multiple sensors in each chamber provide temperature information.

A section view of instrument is shown on the next figure.

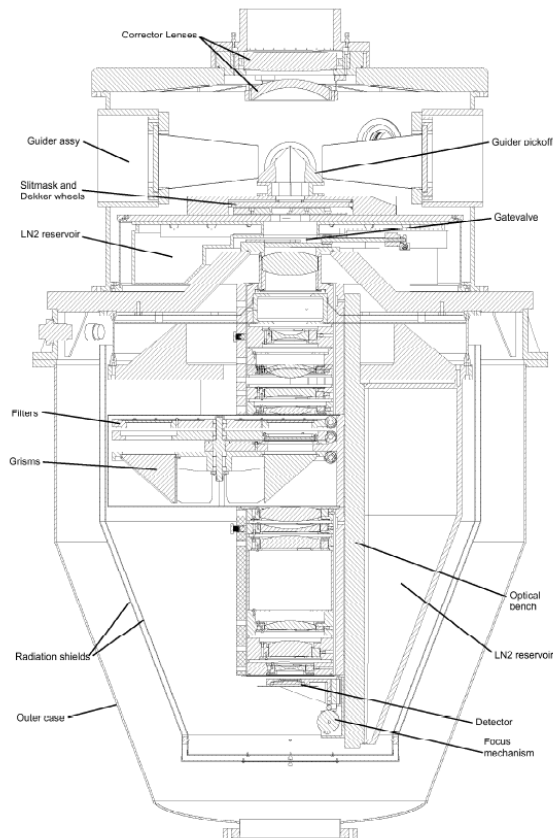



Figure 5-56 MMIRS parts

	<p>SPMT</p> <p>SPMT Conceptual Design Pre PDR</p>	<p>Code: TRP/TELE/001-R</p> <p>Issue: 1.C</p> <p>Date: 24/06/2014</p> <p>Page: 87 of 152</p>
---	--	--

Below is a table with the weights of the instrument and the tools to transport and use.

Components	Weight
MMIRS Instrument (operational)	4500 libras
MMIRS Instrument and handling Cart	5300 libras
MMIRS Instrument and Magellan lift stand	5870 libras
MMIRS Instrument and CIR as installed on telescope	5750 libras

Table 5-3 MMIRS mass

5.8.2.2 3D Model

For this stage of the project was prepared a 3D model with the information collected. The Figure 5-57 and Figure 5-57 show the model generated of this instrument and the general dimensions.



SPMT

SPMT Conceptual Design Pre PDR

Code: TRP/TELE/001-R

Issue: 1.C

Date: 24/06/2014

Page: 88 of 152

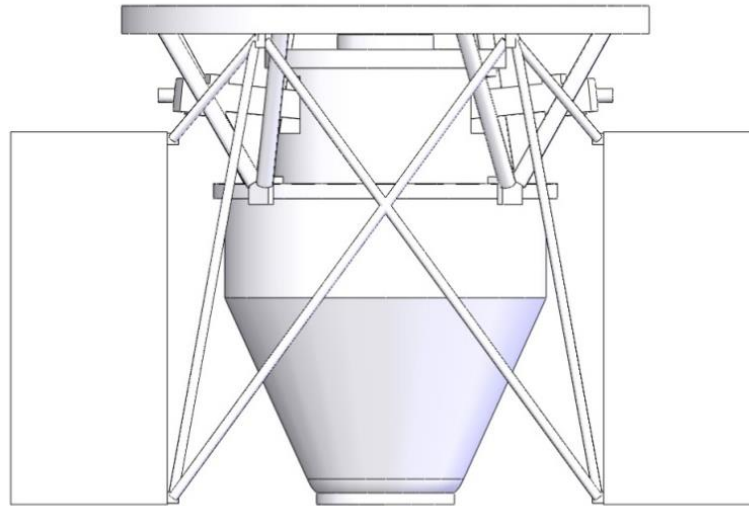



Figure 5-57 MMIRS 3D model

	<p>SPMT</p> <p>SPMT Conceptual Design Pre PDR</p>	<p>Code: TRP/TELE/001-R</p> <p>Issue: 1.C</p> <p>Date: 24/06/2014</p> <p>Page: 89 of 152</p>
---	--	--

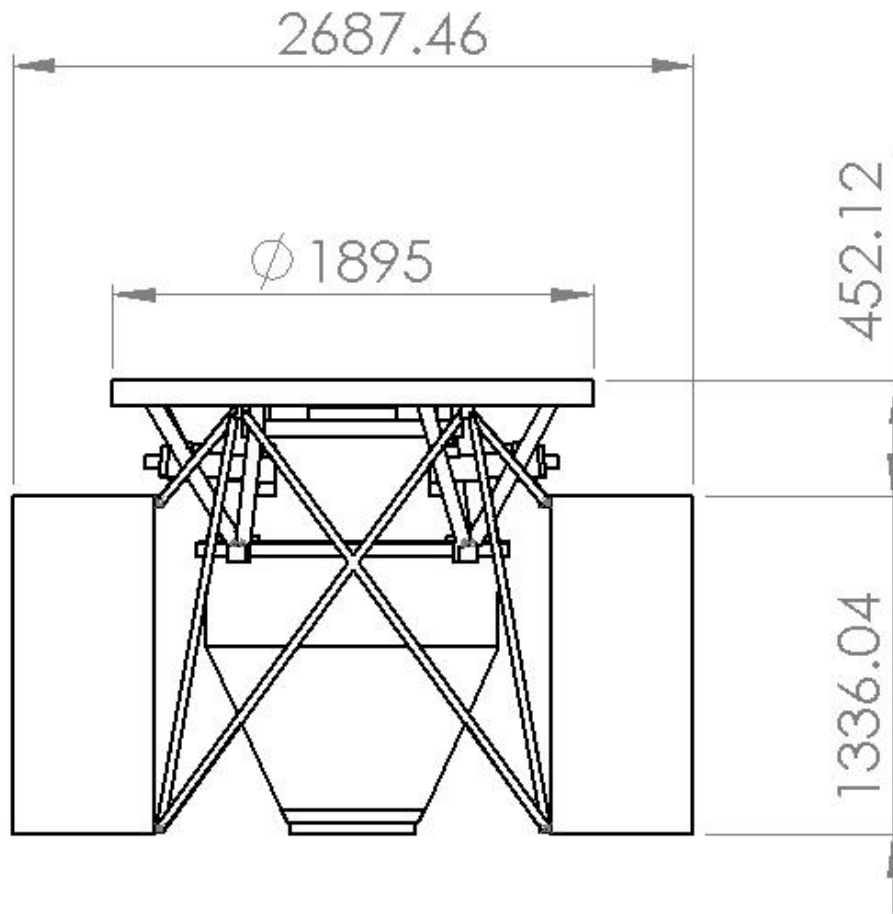



Figure 5-58 MMIRS general dimensions

According with de geometry and the mass properties of the components was obtained the center of mass of the model. The center of mass is located 849mm below the instrument mounting flange in Y direction (Figure 5-59)

	<p style="text-align: center;">SPMT</p> <p style="text-align: center;">SPMT Conceptual Design Pre PDR</p>	<p>Code: TRP/TELE/001-R</p> <p>Issue: 1.C</p> <p>Date: 24/06/2014</p> <p>Page: 90 of 152</p>
---	--	--

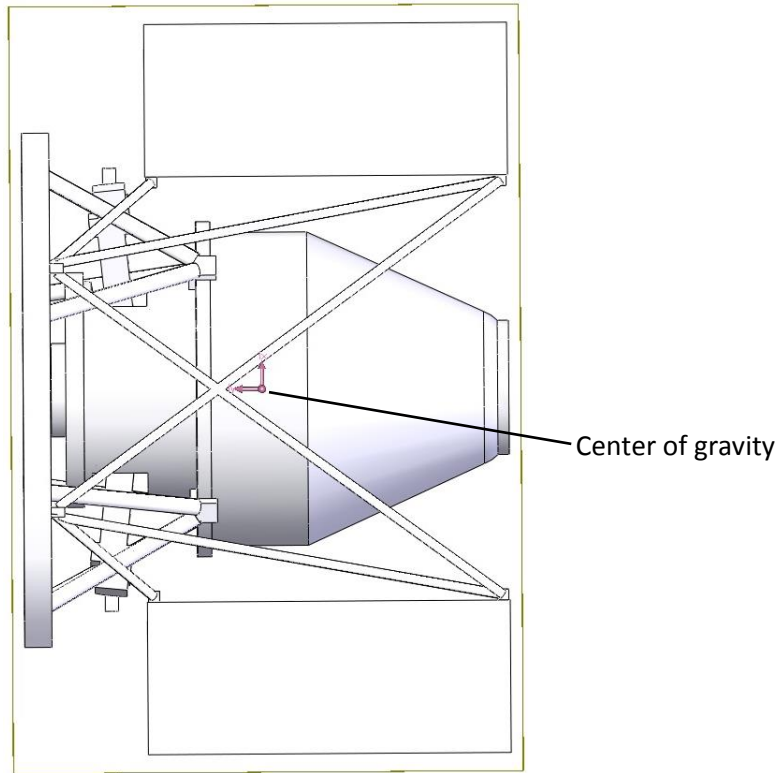



Figure 5-59 MMIRS center of mass

The model of the instrument MMIRS was placed in the bottom of the telescope. The Figure 5-60 shows an image of the model.

	<p>SPMT</p> <p>SPMT Conceptual Design Pre PDR</p>	<p>Code: TRP/TELE/001-R</p> <p>Issue: 1.C</p> <p>Date: 24/06/2014</p> <p>Page: 91 of 152</p>
---	--	--

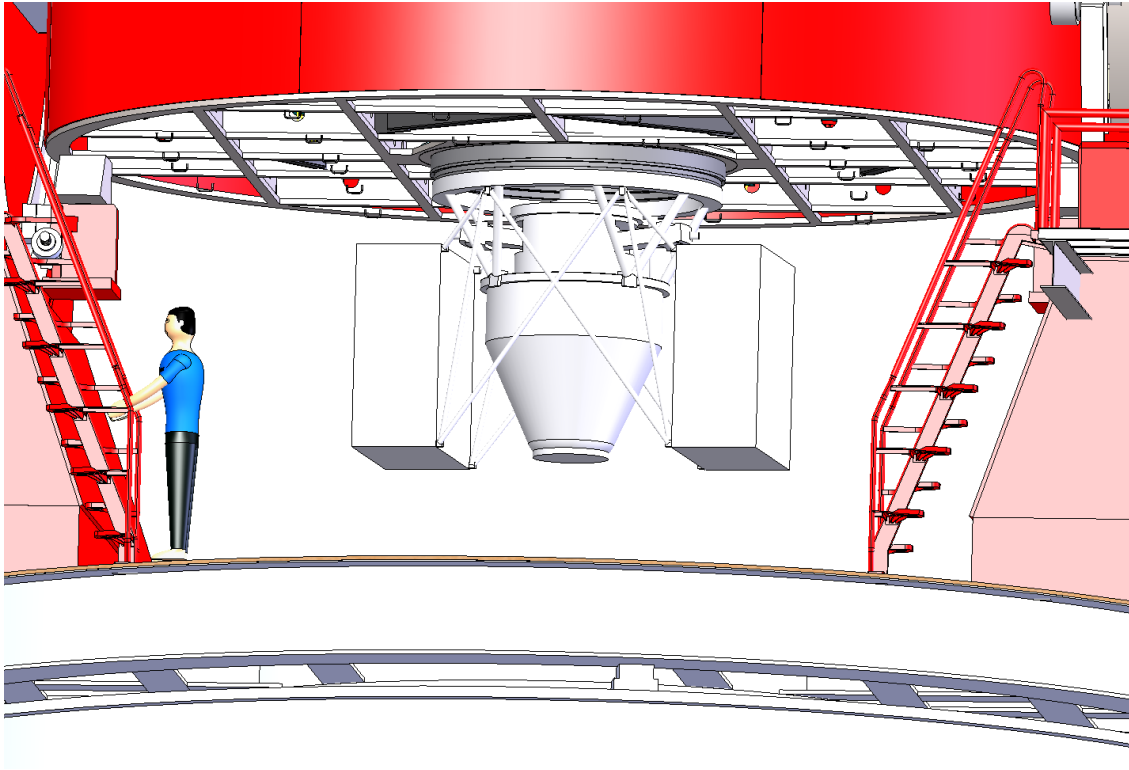



Figure 5-60 MMIRS in the Telescope


5.8.3 Megacam

Megacam is a panoramic, square format CCD mosaic imager, 0.4° on a side. It is instrumented with a full set of Sloan filters. MMIRS is a multislit NIR spectrograph that operates in Y through K band and has long slit and imaging capability as well. Megacam requires a wide field refractive corrector and a Topbox to support shutter and filter selection functions, as well as to perform wavefront on previous designs for MMT.

	SPMT	Code: TRP/TELE/001-R
		Issue: 1.C
	SPMT Conceptual Design Pre PDR	Date: 24/06/2014
		Page: 92 of 152

Megacam	
Parameter	Value
Field of View	25 x 25 arcmin
Plates Scale	0.169 mm/arcsec
Available Filters	Sloan u' , g' , r' , i' and z'
Pixel Scale	0.08 arcsec/pixel, unbinned
Focal Plane Format	18k x 18k pixels
Pixel size	13.5 μ / 0.05 arcsec
Number of CCDs	36 (4 x 9 mosaic)
CCD Format	2048 x 4608 pixels
CCD Type	E2V CCD42-90, Thinned
Quantum Efficiency	55% @ 3500 \AA 82% @ 5000 \AA 30% @ 9000 \AA
Shutter Type	Focal Plane
Cooling	LN2
Guide	2 In-Dewar CCDs

Table 5-4 Parameters and values of Megacam

	<p>SPMT</p> <p>SPMT Conceptual Design Pre PDR</p>	<p>Code: TRP/TELE/001-R</p> <p>Issue: 1.C</p> <p>Date: 24/06/2014</p> <p>Page: 93 of 152</p>
---	--	--

The wavefront sensor had to be integrated into the shutter/filter wheel “Topbox”. This had two technical impacts:

1. Only on-axis wavefront sensing was possible.
2. The wavefront sensor blocked the telescope beam to the focal plane so continuous wavefront sensing. Megacam required a completely new wavefront sensing design.


As we have previously mentioned, the Topbox, which is used in conjunction with Megacam, provides, shutter, filter handling and wavefront sensing functions. The shutter is a dual blade, focal plane design that permits a “scanning slit” mode for extremely short, accurate, uniform exposures. There are two filter wheels, each of which has five slots, to permit simultaneous mounting of all five Sloan filters, with room for extra filters if they are needed. The filters are square, 300 mm on a side and were fabricated by Sagem REOSC.

The Topbox/Megacam system can be rotated on trunnions in this fixture about the horizontal axis to provide good access to all areas of the instrumentation for maintenance and inspection.

The mirror is statically supported by an array of rolling diaphragm (Bellofram) pneumatic lifters connected by short steel cables to one-inch diameter steel pucks glued to the mirror with 3M 2216 2-part epoxy.

The array of pneumatic lifters is divided into four zones, three axial and one lateral, allowing us to hold the mirror with minimal force against four hard point references. Load cells monitor the reference point forces. The air pressure in each zone is adjusted with a pair of small poppet valves, one high pressure inlet and one exhaust, that are controlled by software that actively minimizes the force on the reference points reported by the load cells. The mirror is protected against excessive force on the reference points (for example, when the support system is turned off) by a bi-directional pneumatic cylinder breakaway system.

The mirror is thus precisely positioned in its cell without disturbing its figure. The mirror cell is attached to the bottom of the Magellan secondary support cage, which handles the mechanics of focus and active optics collimation.

	<p>SPMT</p> <p>SPMT Conceptual Design Pre PDR</p>	<p>Code: TRP/TELE/001-R</p> <p>Issue: 1.C</p> <p>Date: 24/06/2014</p> <p>Page: 94 of 152</p>
---	--	--

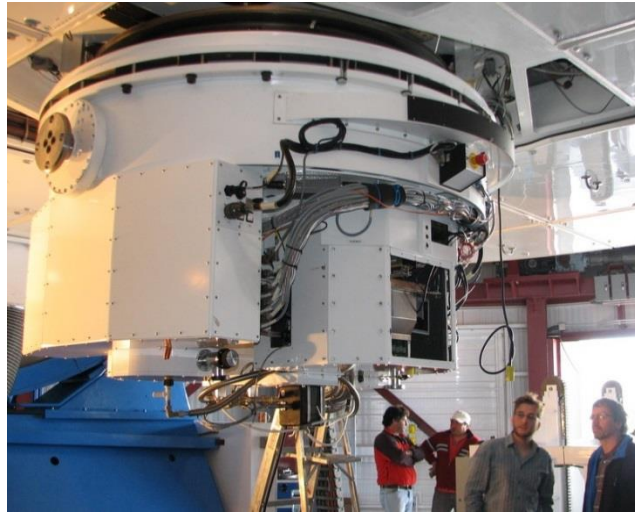


Figure 5-61 Megacam and telescope

The MMT Megacam is a mosaic camera with 36 2048x4608 pixel CCDs, covering a 25'x25' field of view and mounted at the f/5 Cassegrain focus of the 6.5m MMT. Megacam diagram is shown in the Figure 5-62

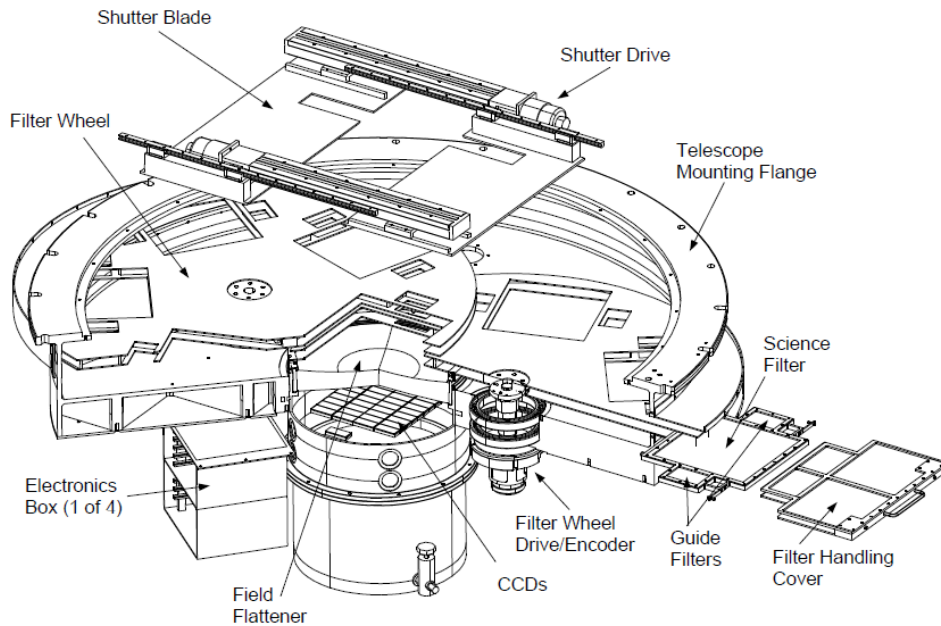



Figure 5-62 Megacam drawing


	<p>SPMT</p> <p>SPMT Conceptual Design Pre PDR</p>	<p>Code: TRP/TELE/001-R</p> <p>Issue: 1.C</p> <p>Date: 24/06/2014</p> <p>Page: 95 of 152</p>
---	--	--

One of the challenges in building a large CCD mosaic is getting all the detectors in-focus simultaneously when they are cold. The CCD42-90 package is ideally suited for this purpose. The CCD is epoxied to an Invar block. To the bottom of this block are attached 3 precision shims, lapped by the manufacturer so that they define a plane 14 mm from the CCD surface. We then were left with the task of providing a flat surface to bolt them to. We chose to mount them to a 6 mm thick Invar plate, suspended around the edge by six Titanium flexures from a warm support ring. These flexures provide the necessary thermal isolation. The tilt and axial position of the cold plate was set by adjusting the location of the warm ring with a set of spring loaded screws. Once the location was set, precision spacers were machined and bolted into place. The mounted plate was measured to be flat to $\sim 10\mu\text{m}$ P-V before any CCDs were installed. (We note that our original design used a Molybdenum plate, which provides a factor of several better thermal conductivity. However, this plate arrived from the vendor broken in two pieces, so we chose to replace it with the less brittle material.)

To verify the focal plane flatness we relied on focus measurements on the sky. Our current measurements indicate that there is roughly $100\mu\text{m}$ PV of deviation from the best focus across the plate. This is larger than expected, but has a completely negligible effect on the image quality. An image taken in 0.4 arcsec seeing shows essentially no variation in FWHM across the entire Megacam field. There are no discontinuities from one CCD to the next, showing that the CCD packages were manufactured well.

The thermal design, the cooling path from the CCDs goes through the CCD42-90 package's precision shims to the Invar mounting plate. Copper straps connect the Invar plate to a set of four cold copper bars. These copper bars are connected to two IRLabs ND-14 dewars mounted on opposite sides of the central dewar. The copper straps were trimmed once after the initial cool down and the CCDs vary in temperature from -130C to -115C across the focal plane. A more uniform distribution could have been obtained with further iterations of trimming. The temperature of the CCDs can be stabilized using a set of heater resistors mounted on the back side of the Invar plate. The heaters are all wired in a single zone.

The total LN2 consumption of the Megacam is 40 W or 20 liter/day. The ND-14 dewars are filled from the bottom and thus contain a tube that extends up inside the tank to prevent the liquid from running back out. We have chosen to make this tube extend 60% the height of the tank. This means we can fill the tank only 60% full, but don't have to worry about dumping out large quantities of LN2 when the telescope tips over. The hold time in this configuration is roughly 36 hours. The thermal load is dominated by radiation coupling from the dewar window to the CCDs. Several features minimize other sources of thermal loading. We have gold plated the Invar plate

	<p>SPMT</p> <p>SPMT Conceptual Design Pre PDR</p>	<p>Code: TRP/TELE/001-R</p> <p>Issue: 1.C</p> <p>Date: 24/06/2014</p> <p>Page: 96 of 152</p>
---	--	--


and copper straps and bars. The flex circuits connecting to the CCDs have two ground layers to provide electrical isolation between the AC and DC signals. Instead of a solid plane, these layers are laid out in a serpentine path to minimize the thermal conductivity. Titanium was chosen for the flexures because of its high stiffness and low thermal conductivity. The flexures contribute only 5W of the 40W load. Finally, we put radiation shields between the flex circuits and the Invar cold plate.

The camera housing, or “topbox”, is a 2m diameter, 0.3m deep steel structure that contains the shutter and filters wheels, and provides a rigid interface between the CCD Dewar and the telescope.

The shutter consists of two aluminum plates mounted on pairs of THK rails. Notches are cut in the shutter blades so that light reaches the guide chips when the shutter is closed. It is also possible to close the shutter completely so that no light hits the guide chips. The exposure is taken by opening one blade and ended by closing the other blade. This ensures an even exposure time over the full focal plane. A shutter blade traverses the focal the focal plane in less than 5 sec; however, shorter exposures can be achieved by having the closing blade follow the leading blade closely, effectively scanning a slit across the focal plane. This style of shutter is used in the Big Throughput Camera. The shutter is driven from one edge with a DC servo motor and a lead-screw with a rotary encoder. The blade is attached to the other rail with a flexure to allow for differential expansion between the steel structure and the aluminum shutter blade without binding.

The housing contains two overlapping filter wheels, each with five slots, normally one of these slots will be left blank in each filter Wheel, allowing a choice of eight filters at any given time. The filter wheels are driven from their centers with a DC-servo motor, harmonic drive gear reduction, and a rotary encoder, which provides a lateral repeatability of 10µm at the radius of the filters. This high repeatability allows us the potion to use segmented filters without incurring flat-fielding errors due to misregistration of the filters. Each filter wheels is composed of two Steel facesheets separated by a web of reinforcements. Filters are mounted in a steel frame that is inserted between the two facesheets of the filter wheel from access ports on each side of the housing.

Actually Megacam is in operation on the Magellan Clay telescope (see Figure 5-63).

	<p>SPMT</p> <p>SPMT Conceptual Design Pre PDR</p>	<p>Code: TRP/TELE/001-R</p> <p>Issue: 1.C</p> <p>Date: 24/06/2014</p> <p>Page: 97 of 152</p>
---	--	--

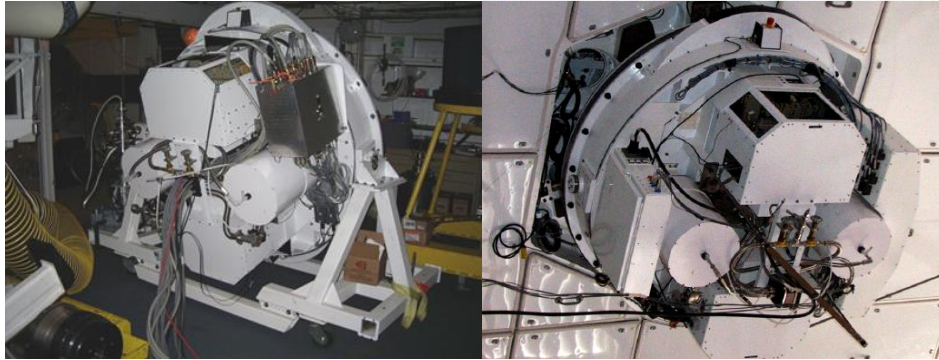


Figure 5-63 Megacam on Magellan Clay

5.8.3.1 Megacam mounting considerations on the SPMT

There are not available detailed mounting size and envelope data of Megacam, during the development of the conceptual design of the SMPT we will consider the available information. At this moment the use of Megacam on the SPMT is only a probability.

5.8.4 Binospec


Binospec is a wide-field, multi-object optical spectrograph to be used at the f/5 focus of the converted 6.5 m Multiple Mirror Telescope. Binospec has been designed to aggressively pursue wide-field surveys using moderate dispersion optical spectroscopy.

5.8.4.1 Instrument Overview

5.8.4.1.1 Support Structure

Binospec's structure is comprised of four major components (see Figure 5-64):

- 1) An instrument mounting flange,
- 2) An A-frame truss that connects the instrument to the mounting flange,
- 3) An optical bench that supports most of Binospec's components, and
- 4) A focal plane bench that supports the slit mask assembly, the guiders, and the periscope fold mirrors.

	<p>SPMT</p> <p>SPMT Conceptual Design Pre PDR</p>	<p>Code: TRP/TELE/001-R</p> <p>Issue: 1.C</p> <p>Date: 24/06/2014</p> <p>Page: 98 of 152</p>
---	--	--

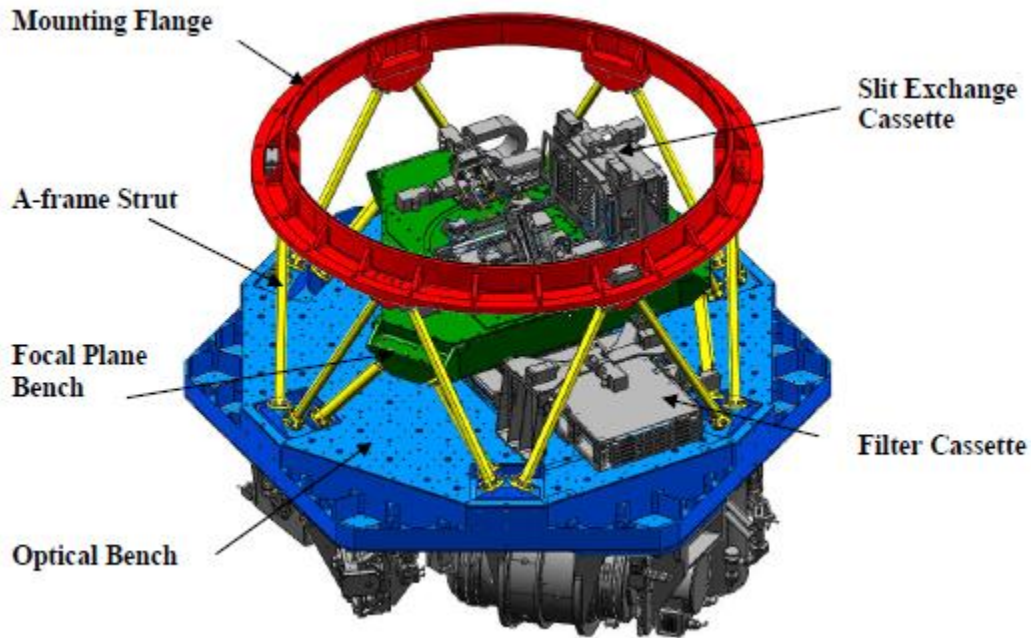



Figure 5-64 Binospec structure with covers removed

The mounting flange is made from 400 series stainless steel for thermal expansion compatibility with the carbon steel telescope rotator flange, while eliminating the potential for corrosion. The outer A-frame truss members are made from 300 series stainless steel for its low thermal conductivity, to minimize conduction between the mounting flange and the optical bench. The inner truss and support benches are made from aluminum to meet the optical element spacing characteristics assumed in the athermalization of the optical design as well as to minimize the overall weight of the instrument.

The optical bench is a closed-back honeycomb structure, approximately 90 inches in diameter and 8 inches thick to minimize the relative motion between each optical assembly, all of the lenses, gratings, and science cameras mount directly to the bottom of the optical bench as shown in Figure 5-64. The focal plane bench is attached to the top of the optical bench with three A-frame truss members. The focal plane bench supports the slit mask mechanism, the guiders, the wave front sensor, the acquisition camera, and the periscope fold mirrors.

	<p>SPMT</p> <p>SPMT Conceptual Design Pre PDR</p>	<p>Code: TRP/TELE/001-R</p> <p>Issue: 1.C</p> <p>Date: 24/06/2014</p> <p>Page: 99 of 152</p>
---	--	--

5.8.4.1.2 Calibration System

A retractable calibration screen and calibration light source is mounted directly above Binospec on the telescope rotator assembly (see Figure 5-65) to provide periodic wavelength calibration of the detector before or after an observation without repointing the telescope or closing the dome. The calibration system consists of a set of wavelength standard and continuum lamps in an integrating sphere with fold mirrors that illuminate a Spectralon-coated diffuse reflective screen. This subsystem also derotates the power cables, Ethernet cable, pneumatic air lines and coolant lines. The cables and lines will be routed through the primary mirror cell and enter the flexible e-chain through a hole in the central cone. During installation, the electrical, coolant and air connections will be made at the telescope cone end and where the cables enter through the top of Binospec.

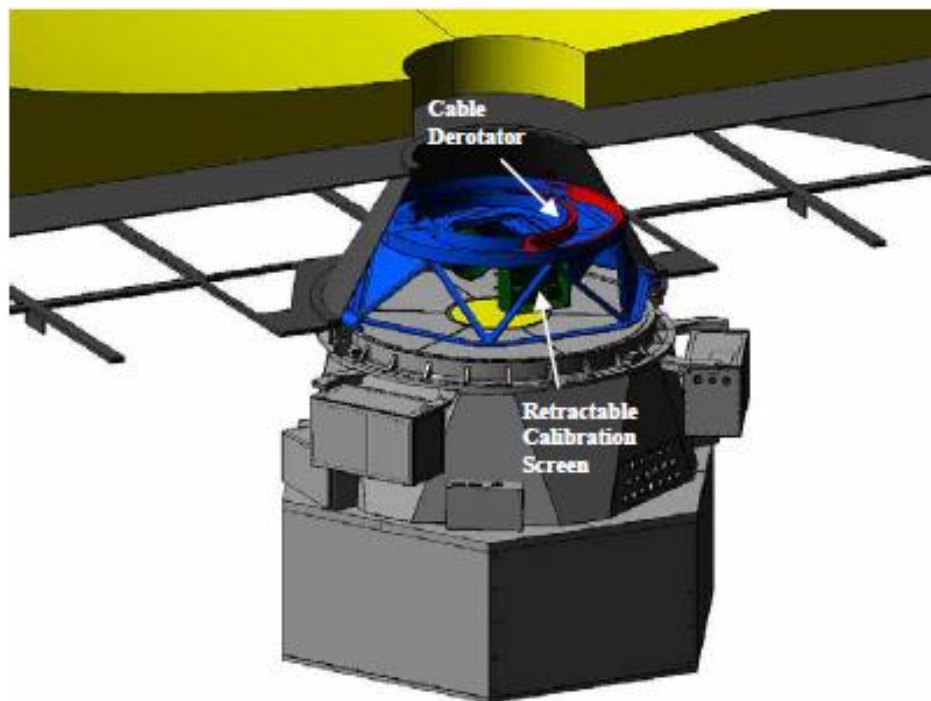



Figure 5-65 Binospec along with the retractable calibration screen/cable derotator mounted on the MMT rotator bearing.

	<p>SPMT</p> <p>SPMT Conceptual Design Pre PDR</p>	<p>Code: TRP/TELE/001-R</p> <p>Issue: 1.C</p> <p>Date: 24/06/2014</p> <p>Page: 100 of 152</p>
---	--	---

5.8.4.1.3 Calibration / Derotator Assembly

The calibration/derotator subassembly serves two purposes:

(1) It provides an external platform, thermally isolated from the Binospec optics, for the calibration system. The calibration system light is injected into an integrating sphere, and the light leaving the integrating is baffled and sent to a rear projection screen that illuminates the slit mask focal plane. The rear projection screen can be shuttled into and out of the optical path as commanded.

(2) The calibration/derotator assembly also derotates the service umbilicals for the instrument that pass through a service port in the inner cone of the MMT primary mirror cell.

These service umbilicals include:

- System main electrical power
- Fiber-optic communication
- Pneumatic supply and exhaust
- Coolant supply and exhaust

This assembly mounts to the same mounting ears on the instrument rotator bearing that support the f/5 Wave Front Sensor that is used with Hectospec/Hectochelle and Megacam. The assembly is similar in size to the existing Wave Front Sensor but is one third the weight at about 185 lbs. Its mounting position relative to Binospec is shown in Figure 5-66 and Figure 5-67

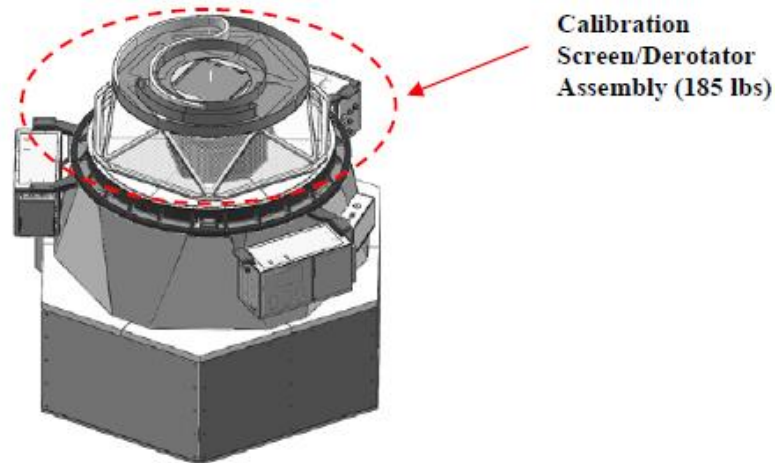



Figure 5-66 Calibration screen/derotator in relation to Binospec.

	<p style="text-align: center;">SPMT</p> <p style="text-align: center;">SPMT Conceptual Design Pre PDR</p>	<p>Code: TRP/TELE/001-R</p> <p>Issue: 1.C</p> <p>Date: 24/06/2014</p> <p>Page: 101 of 152</p>
---	--	---

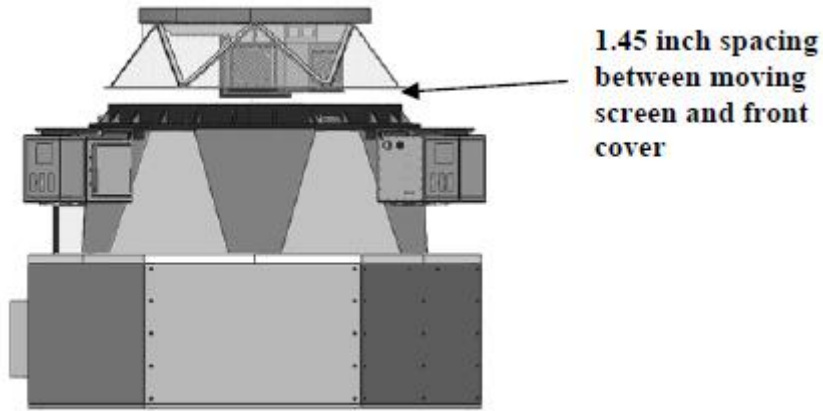


Figure 5-67 Calibration screen/derotator in relation to Binospec (side view)

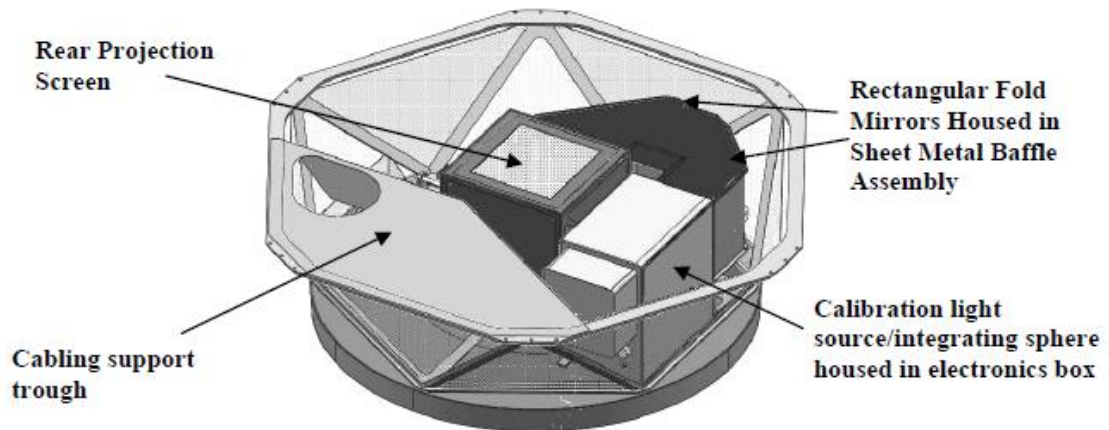



Figure 5-68 Inverted calibration screen / derotator assembly with screen deployed.

	<p>SPMT</p> <p>SPMT Conceptual Design Pre PDR</p>	<p>Code: TRP/TELE/001-R</p> <p>Issue: 1.C</p> <p>Date: 24/06/2014</p> <p>Page: 102 of 152</p>
---	--	---

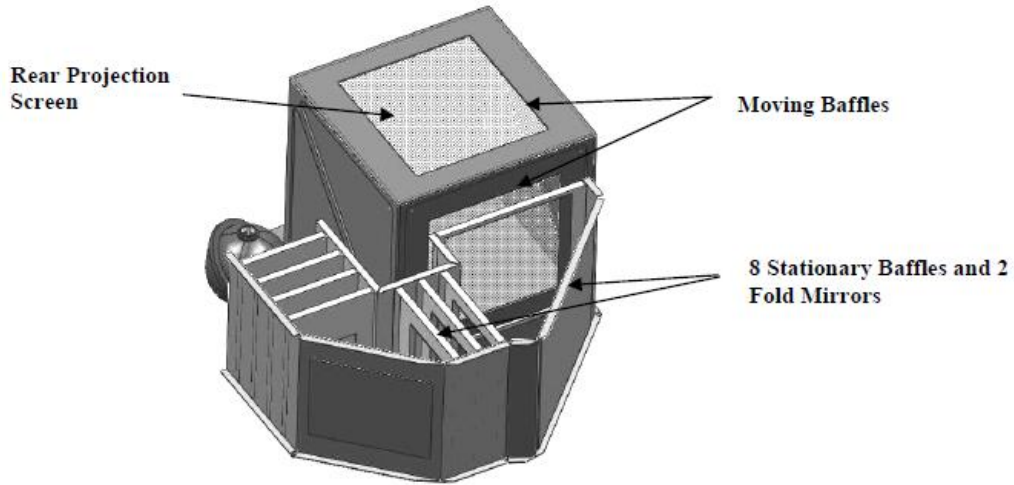


Figure 5-69 Baffle Assembly – Baffles exposed

A baffle system, is shown in Figure 5-69, of sheet metal construction conforms to the prescription generated by Deborah Woods on August 1, 2007.

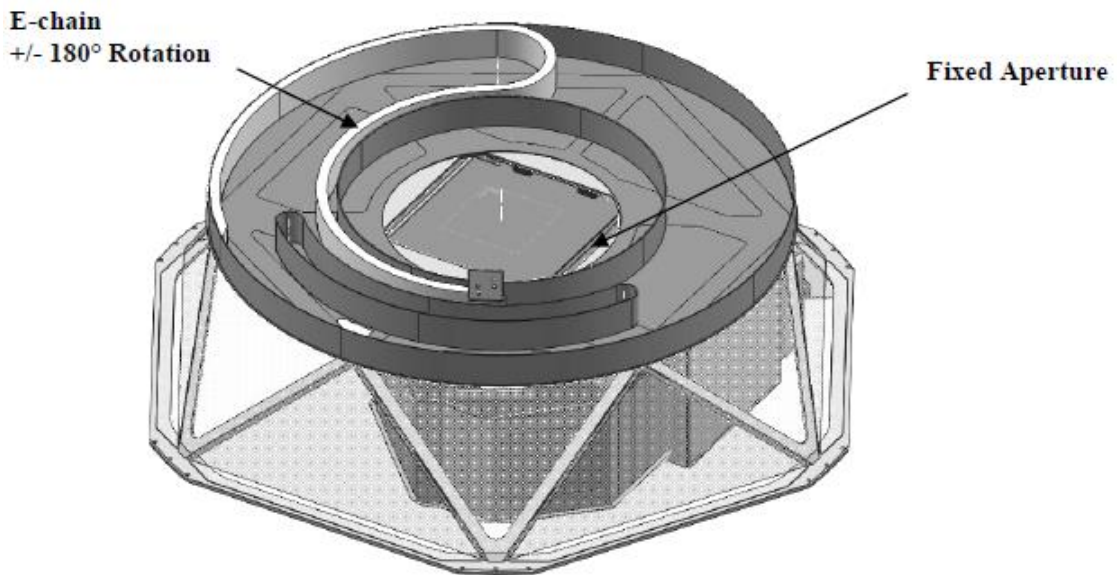



Figure 5-70 View of zenith-pointed calibration screen showing cable derotator.

	<p>SPMT</p> <p>SPMT Conceptual Design Pre PDR</p>	<p>Code: TRP/TELE/001-R</p> <p>Issue: 1.C</p> <p>Date: 24/06/2014</p> <p>Page: 103 of 152</p>
---	--	---

Screen Moved out of
Optical Path – 16.5 inches
of travel required

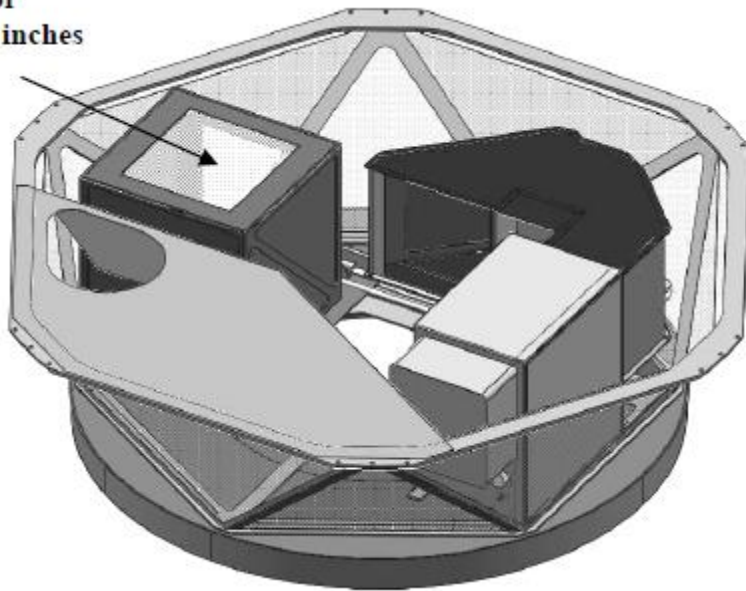


Figure 5-71 Inverted calibration screen /derotator assembly with screen retracted.

Figure 5-70 shows an overhead view of the Calibration Screen/Derotator assembly. The cable derotator is based on the successful f/5 Wave Front Sensor design. The energy chain interfaces to connection points in the MMT Cassegrain cone. This configuration will provide a minimum of +/- 180° of rotation. The f/5 Wave Front Sensor achieves approximately +/- 200° of rotation, and we should be able to duplicate this without issue. Figure 5-71 shows the screen retracted for observation.

5.8.4.2 Telescope Envelope and instrument Mass Constraints

The MMT accepts only Cassegrain instruments mounted to a 72 inch rotator bearing. Critical clearances are shown in Figure 5-72 and Figure 5-73. The horizontal span between the two telescope drive arcs on either side of the instrument volume is 175 inches.

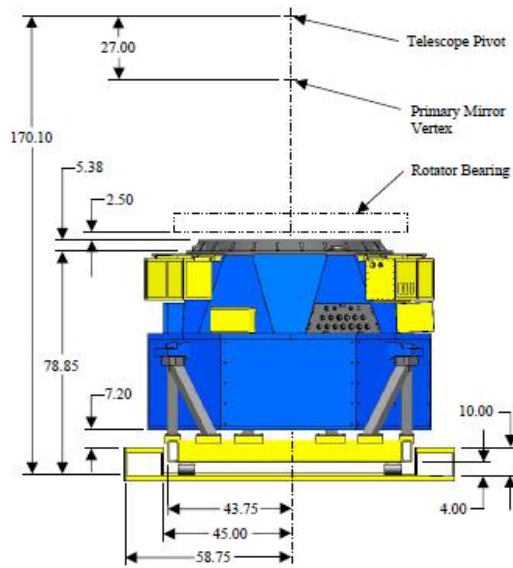


Figure 5-72 Critical dimensions for mounting Binospic

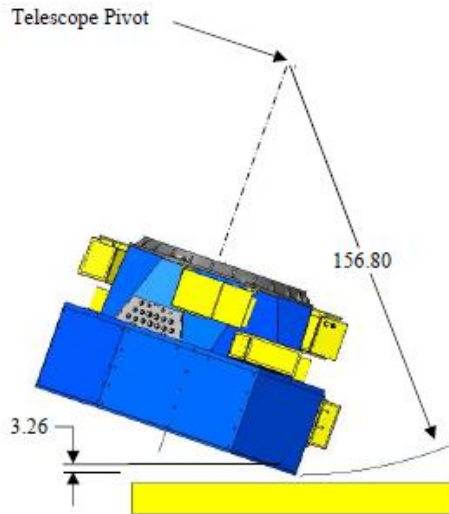



Figure 5-73 Side view of Binospic on the MMT showing allowed swing clearance

	SPMT	Code: TRP/TELE/001-R
		Issue: 1.C
	SPMT Conceptual Design Pre PDR	Date: 24/06/2014
		Page: 105 of 152

Binospec weights is around of 6000 lbs with a center of gravity 30.0 inches below the instrument mounting flange, yielding a maximum overturning moment of 15000 ft-lbs. Reducing the Binospec weight would require accepting larger gravitational flexure.

Simpson Gumpertz and Heger (SG&H) analyzed the MMT telescope for the Binospec loads, which are larger than with current instruments. Their results show that there is no significant optical or structural degradation of the MMT optical support structure or instrument rotator resulting from the increased Binospec weight.

The full SG&H report is in a memo by Frank Kan dated April 12, 2006. Summarize the SG&H results in Table 5-5.


Load Case	ΔZ shift	ΔY shift	ΘX Rotation
Gravity Zenith Pointing	-.0049 in.		13.9 μrad^1
Gravity Horizon Pointing		-.0029 in.	-49.0 μrad^2

Table 5-5 Displacements and rotations relative to the optical axis (Z=-70.67 in)

Note:

1. This tilt results in a ± 0.0002 in. defocus at the edge of the full 24 in. dia. focal surface.
2. This tilt results in a ± 0.0006 in. defocus at the edge of the full 24 in. dia. focal surface.

The maximum stress levels in the instrument rotator and OSS near the rotator are low: 1.3 ksi and 2.5 ksi respectively. SG&H consulted with Avon Bearing to evaluate the rotator bearing with the Binospec loads. Avon Bearing show the increased weight is not a problem for the rotator bearing. The minimum safety factor on the static loading is 6.5 and the minimum safety factor on theoretical stress limit is 12.4. The theoretical life of the rotator bearing run at 4 rpm continuously with the Binospec loads applied is 235,700 hours. There appears to be no significant optical or structural degradation of the MMT OSS or the instrument rotator resulting from the increased Binospec loads. However, additional counterweights must be added to balance the MMT with Binospec mounted.

	SPMT	Code: TRP/TELE/001-R
	SPMT Conceptual Design Pre PDR	Issue: 1.C
		Date: 24/06/2014
		Page: 106 of 152

5.8.4.3 Interface Connections

In order to simplify the mounting and dismounting of Binospec on the MMT, was adopting the strategy that the only wiring and plumbing connections between the instrument and the outside world are power, ethernet, compressed air and coolant.

5.8.4.3.1 Cable Connection to the Telescope

Figure 5-74 shows the relation of the calibration/derotator assembly and the primary mirror cell, as well as the cable attachment points.

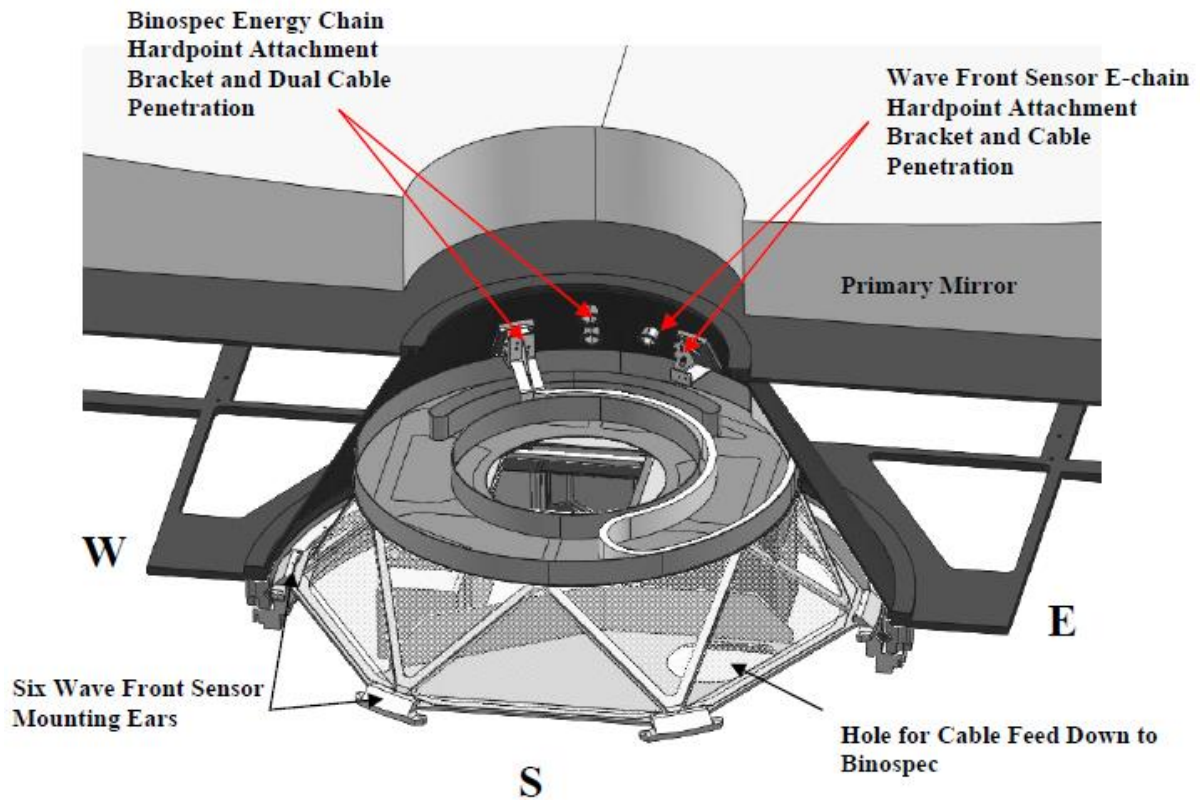



Figure 5-74 Calibration / derotator assembly mounted into primary mirror cell

	<p>SPMT</p> <p>SPMT Conceptual Design Pre PDR</p>	<p>Code: TRP/TELE/001-R</p> <p>Issue: 1.C</p> <p>Date: 24/06/2014</p> <p>Page: 107 of 152</p>
---	--	---

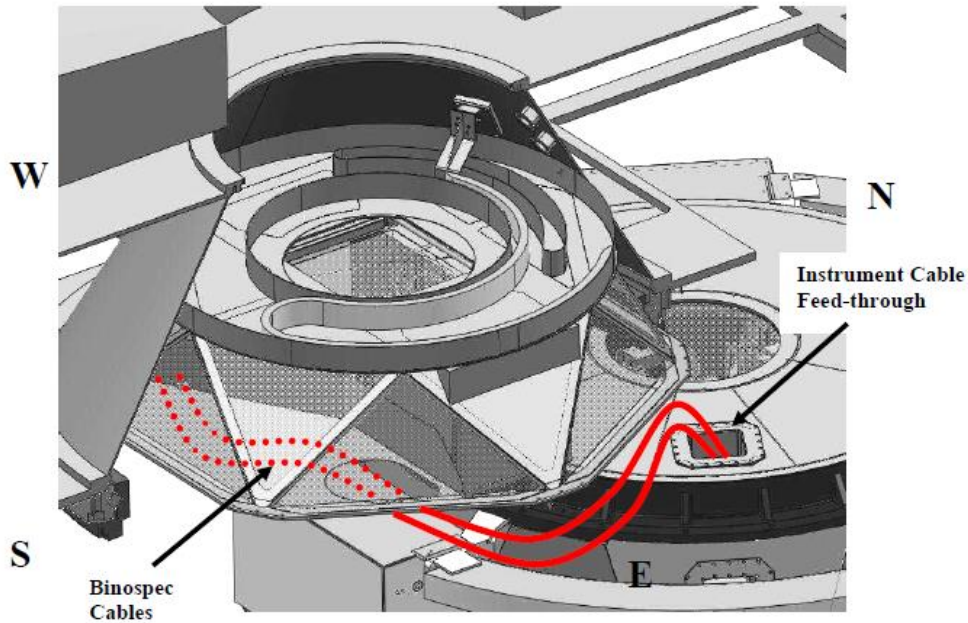



Figure 5-75 Binospec offset from IR bearing during installation

Installation of the calibration screen and connection of cabling to the telescope and through to the instrument will proceed as follows:

1. Prior to calibration screen installation:
 - a. Ensure that the backlit screen is in the retracted position Figure 5-70 This allows a technician to look and reach up through the opening to connect the e-chain and all umbilical connections.
 - b. Ensure all Binospec cables are tucked neatly up into the cabling support trough.
2. Raise the calibration screen into position (noting the correct orientation with respect to telescope north) mating it to the wave front sensor mounting ears.
3. Install 18 mounting bolts.
4. Stand up in the clear aperture of the calibration screen and do the following:
 - a. Connect the e-chain to the designated telescope hardpoint.
 - b. Make power, communications, air and coolant connections.

	<p>SPMT</p> <p>SPMT Conceptual Design Pre PDR</p>	<p>Code: TRP/TELE/001-R</p> <p>Issue: 1.C</p> <p>Date: 24/06/2014</p> <p>Page: 108 of 152</p>
---	--	---

5. Begin moving Binospec into position below the IR bearing. Stop once the instrument cable feed- through is just within the perimeter of the IR bearing.
6. Feed all umbilical connections from the calibration screen cable support trough the instrument cable feed through Figure 5-75.
7. Continue moving Binospec into position underneath the IR bearing.
8. Pull all umbilical connections through the instrument cable feed through.
9. Raise Binospec to mate the mounting flange with the IR bearing and install all instrument mounting hardware.
10. Connect all umbilical connections to Binospec.

5.8.4.4 Binospec mounting considerations on the SPMT

The mounting design considerations of Binospec on SPMT were described on the previous paragraph, during the conceptual design additional considerations will be evaluated.

6. TELESCOPE FINITE ELEMENT MODEL (FEM)

6.1 Structural and modal analysis report of spmt telescope


6.1.1.1 Analisis objective.

The objective in the modal and structural FEM is to analyze the state of stress, stiffness and strain at SPMT to comply with the conditions of material strength and expected deflections without neglecting the telescope optics.

6.1.1.2 Analisis description.

SPMT telescope was modeled using SolidWorks[®], the model was simplified and prepared to optimize computing resources in software ANSYS, where working conditions were simulated for analysis.

This report shows the procedure carried out for the computational analysis of SPMT telescope; Figure 6-1 likewise applicable to different design proposals to reduce the possibility of failure in its operation as excessive deflection or failure of the materials mentioned.

	<p>SPMT</p> <p>SPMT Conceptual Design Pre PDR</p>	<p>Code: TRP/TELE/001-R</p> <p>Issue: 1.C</p> <p>Date: 24/06/2014</p> <p>Page: 109 of 152</p>
---	--	---

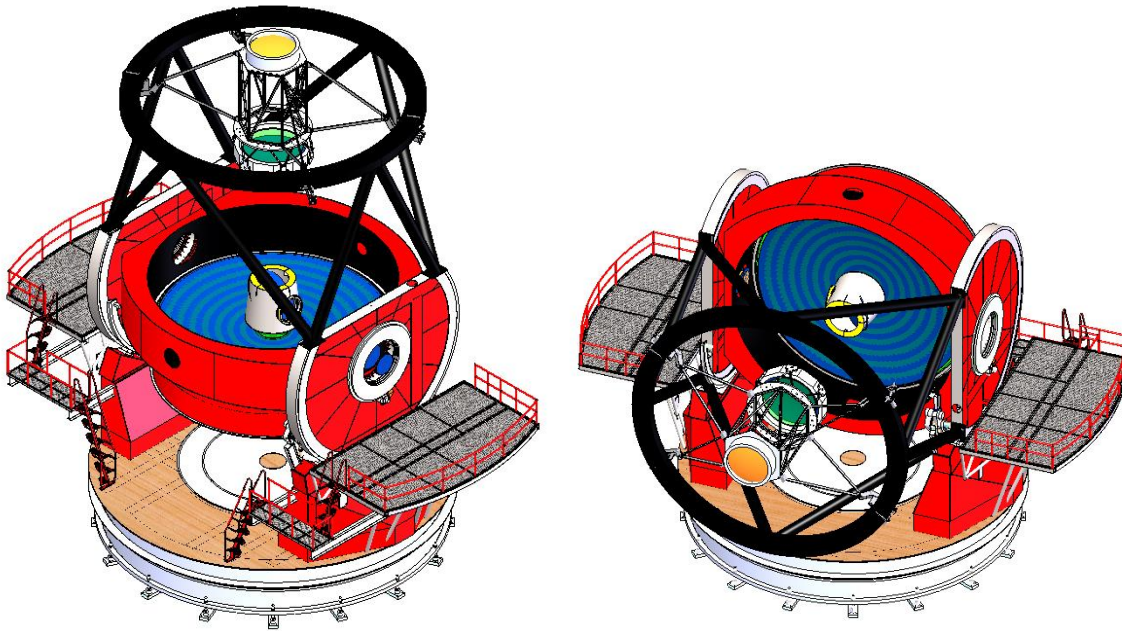


Figure 6-1 *Left isometric view of SPMT Telescope Zenith position. Right. Isometric view of SPMT Telescope at horizon position.*

6.1.1.3 Analysis procedure for SPMT

Telescope was modeled in surfaces so considerations and recommendations are made for the model was generated. First the initial analysis to see the state of stress and strain, and a modal analysis was performed so that, based on these results model of the telescope SPMT can be improved depending on optical considerations.

6.1.1.4 Model FEM description.


After model preparation using Solidworks[®], it was imported into ANSYS[®] APDL version 13 for analysis.

First we proceeded to perform static analysis of the structural model to determine the stress and strain level in the model due to gravity loads.

The considerations made for the model based on a conceptual design are presented.

Considerations:

Overall dimensions of the components of the telescope SPMT

	SPMT SPMT Conceptual Design Pre PDR	Code: TRP/TELE/001-R Issue: 1.C Date: 24/06/2014 Page: 110 of 152
---	---	--

a:

Assembly name: SPMT-TL-PM-100-000 Primary Mirror M1 Cell Structure

Dimensions: Diameter=6740.525mm height=1576.0625mm

Approx. weight: 15893.874 kg

Material: ASTM A36

b:

Assembly name: SPMT-TL-EL-101-000

Dimensions: Diameter=7025.4mm Height= 1580mm

Approx. weight: 8194.54 kg

Material: ASTM A36

c:

Assembly name: SPMT-TL-EL-102-000

Dimensions: Diameter ext=6295.35mm Diameter int=1351.74mm Width=402.65mm

Approx. weight: 13386.85 kg.


Material: ASTM A36

d:

Assembly name: SPMT-TL-TU-000-001 Telescope Tube Ring

Dimensions: Diameter max= 8572.50mm Diameter min=7480.30mm Width: 304.80mm

Approx. weight: 6129.35 kg.

	<p>SPMT</p> <p>SPMT Conceptual Design Pre PDR</p>	<p>Code: TRP/TELE/001-R</p> <p>Issue: 1.C</p> <p>Date: 24/06/2014</p> <p>Page: 111 of 152</p>
---	--	---

Material: ASTM A36

e:

Assembly name: SPMT-TL-TU-000-001 Telescope Tube Structure

For Telescope tube lines was used for only.

Dimensions: Diameter ext= 355.60mm Diameter Int= 336.55mm long: 5305.803mm y
6176.75mm

Approx. weight: 4207.63 kg.

Material: ASTM A36

f:

Assembly name: SPMT-TL-SS-100-000 Secondary Mirror Assembly

For spider lines was used for only.

Vanes (SPMT-TL-SS-103-003) Dimensions: 25.40mm x 79.20mm x 2559.20mm


Basket (SPMT-TL-SS-103-002) profile 2X2 in.

Dimensions: Diameter 240mm, length: 70mm

Approx. weight: 201.66kg.

Material: Aluminum 6061

Considerations: The total weight of the secondary mirror assembly is considering the mass of the three mirrors mounted at the same time on the basket.

	<p>SPMT</p> <p>SPMT Conceptual Design Pre PDR</p>	<p>Code: TRP/TELE/001-R</p> <p>Issue: 1.C</p> <p>Date: 24/06/2014</p> <p>Page: 112 of 152</p>
---	--	---

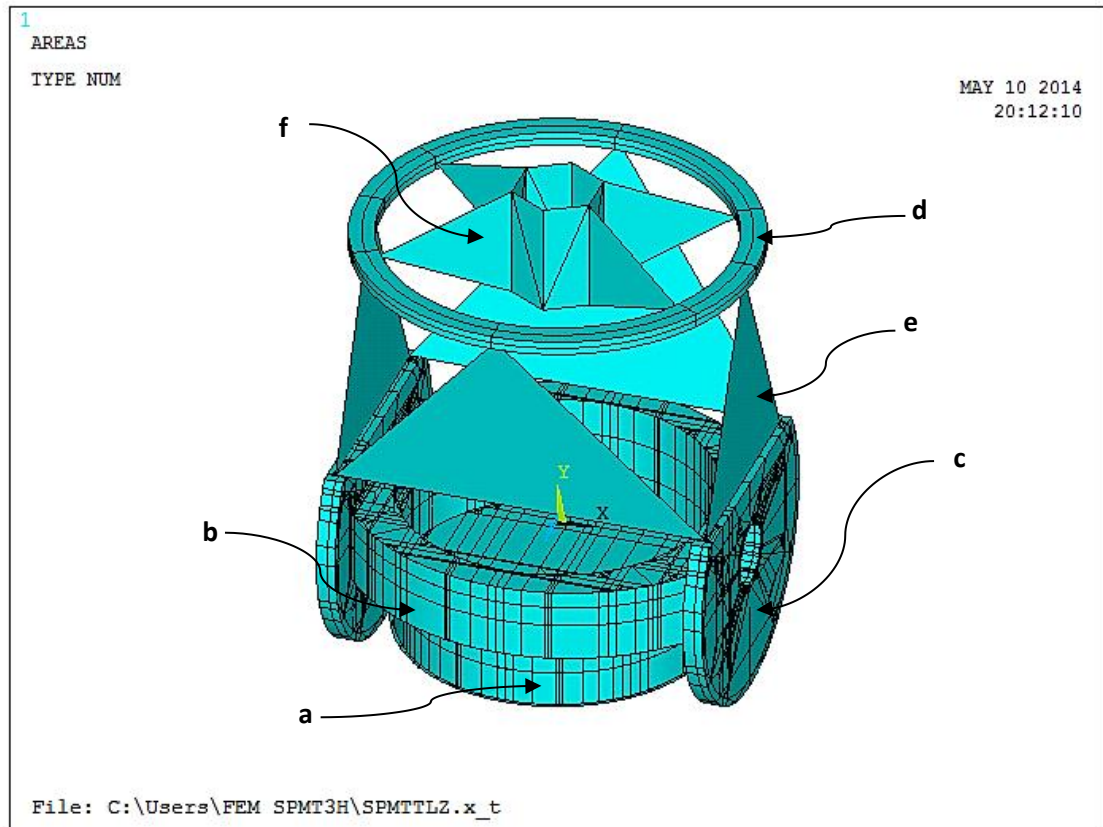



Figure 6-2 Model initial surfaces SPMT Telescope imported ANSYS ®.

Considered the mechanical properties of the material selected for the conceptual design, as shown in tables overall dimensions is a ASTM A36, which has a minimum yield strength of 250 Mpa and a limit to the breakdown of each of the components ultimate stress of 400-550 MPa and 6061, having a minimum yield strength of 255 MPa and a limit of rupture 290 Mpa according to MatWeb (2)

Meshing

For this analysis, three types for generating finite element mesh used a mapping model which is:

	<p>SPMT</p> <p>SPMT Conceptual Design Pre PDR</p>	<p>Code: TRP/TELE/001-R</p> <p>Issue: 1.C</p> <p>Date: 24/06/2014</p> <p>Page: 113 of 152</p>
---	--	---

6.1.1.4.1 BEAM4⁽¹⁾

BEAM4 is a uniaxial element with tension, compression, torsion, and bending capabilities. The element has six degrees of freedom at each node: translations in the nodal x, y, and z directions and rotations about the nodal x, y, and z axes. Stress stiffening and large deflection capabilities are included. A consistent tangent stiffness matrix option is available for use in large deflection (finite rotation) analyses.

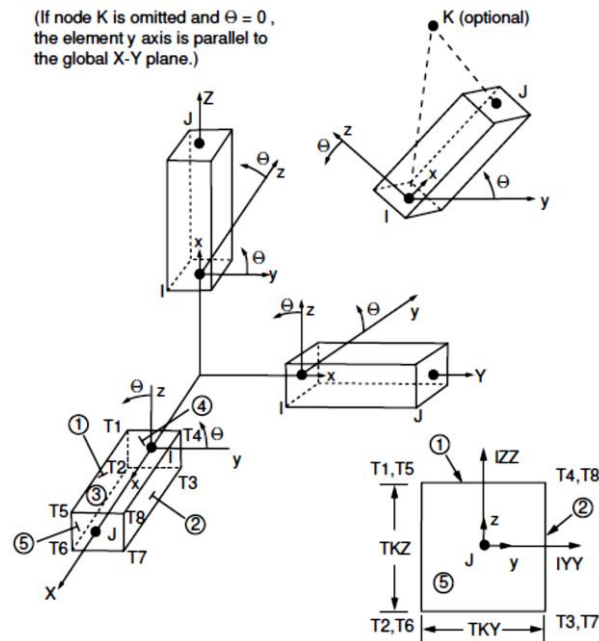



Figure 6-3 BEAM4 Geometry. ⁽¹⁾

6.1.1.4.2 SHELL93⁽¹⁾

SHELL93 is particularly well suited to model curved shells. The element has six degrees of freedom at each node: translations in the nodal x, y, and z directions and rotations about the nodal x, y, and z-axes. The deformation shapes are quadratic in both in-plane directions. The element has plasticity, stress stiffening, large deflection, and large strain capabilities.

	<p>SPMT</p> <p>SPMT Conceptual Design Pre PDR</p>	<p>Code: TRP/TELE/001-R</p> <p>Issue: 1.C</p> <p>Date: 24/06/2014</p> <p>Page: 114 of 152</p>
---	--	---

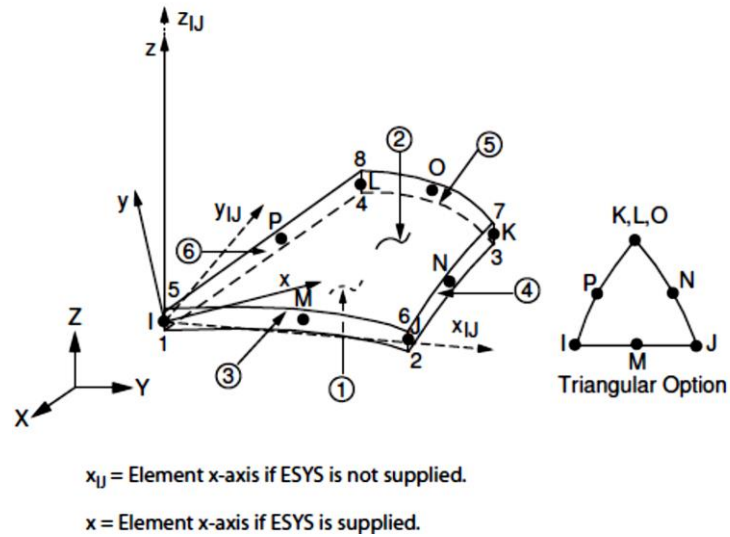


Figure 6-4 SHELL93 Geometry. ⁽¹⁾

6.1.1.4.3 MASS21 ⁽¹⁾

MASS21 is a point element having up to six degrees of freedom: translations in the nodal x, y, and z directions and rotations about the nodal x, y, and z axes. A different mass and rotary inertia may be assigned to each coordinate direction.

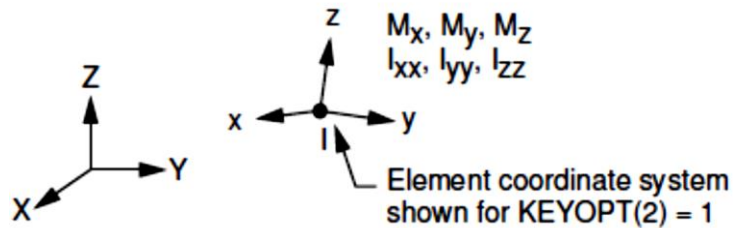



Figure 6-5 MASS21 Geometry. ⁽¹⁾

6.1.1.5 Boundary conditions zenith position:

Were restricted in all degrees of freedom the contact areas of the hydrostatic pads with lifting system, the MASS21 elements were used to simulate the mass of the primary mirror in his cell and the mass of the secondary mirror system (secondary mirror f / 5 with hexapod f/11 Gregorian) and the model with gravitational load (-9.81 m/s² in Y) strived to indicated by the red

	<p>SPMT</p> <p>SPMT Conceptual Design Pre PDR</p>	<p>Code: TRP/TELE/001-R</p> <p>Issue: 1.C</p> <p>Date: 24/06/2014</p> <p>Page: 115 of 152</p>
---	--	---

arrow in Figure 6-6 and Figure 6-7, to simulate the weight of the entire telescope find the conditions of stress and strain from the original design concept.

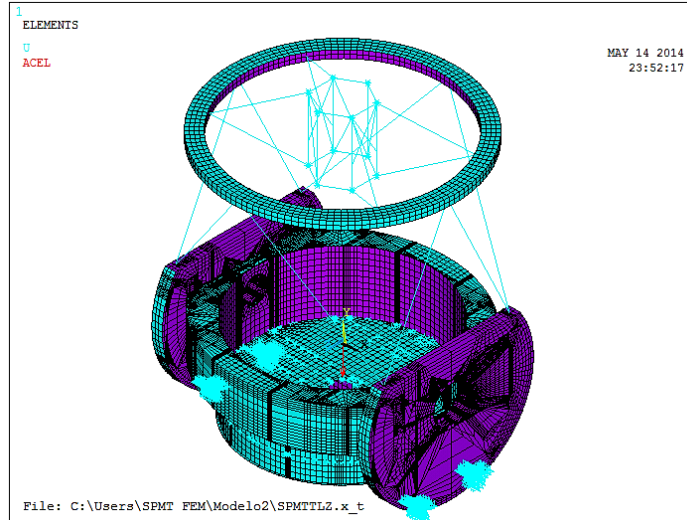


Figure 6-6 Meshing of surfaces model SPMT Telescope with loads and constraints.

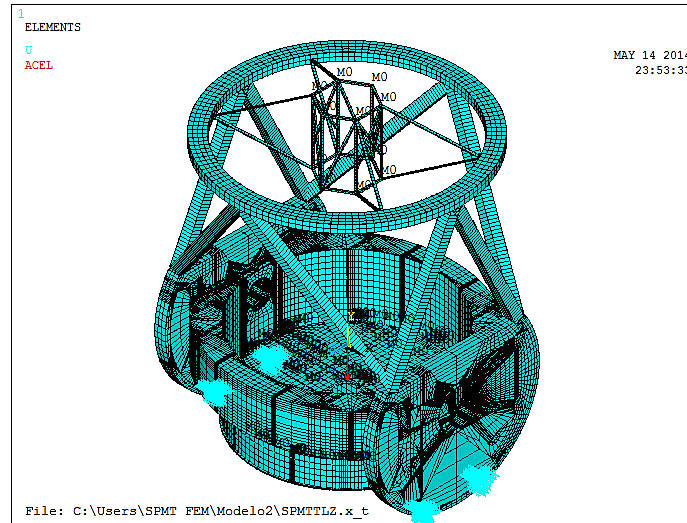



Figure 6-7 Meshing of model with cross sections elements BEAM4.

	<p>SPMT</p> <p>SPMT Conceptual Design Pre PDR</p>	<p>Code: TRP/TELE/001-R</p> <p>Issue: 1.C</p> <p>Date: 24/06/2014</p> <p>Page: 116 of 152</p>
---	--	---

Analysis with the conditions described above was performed and obtaining the results shown below:

Results

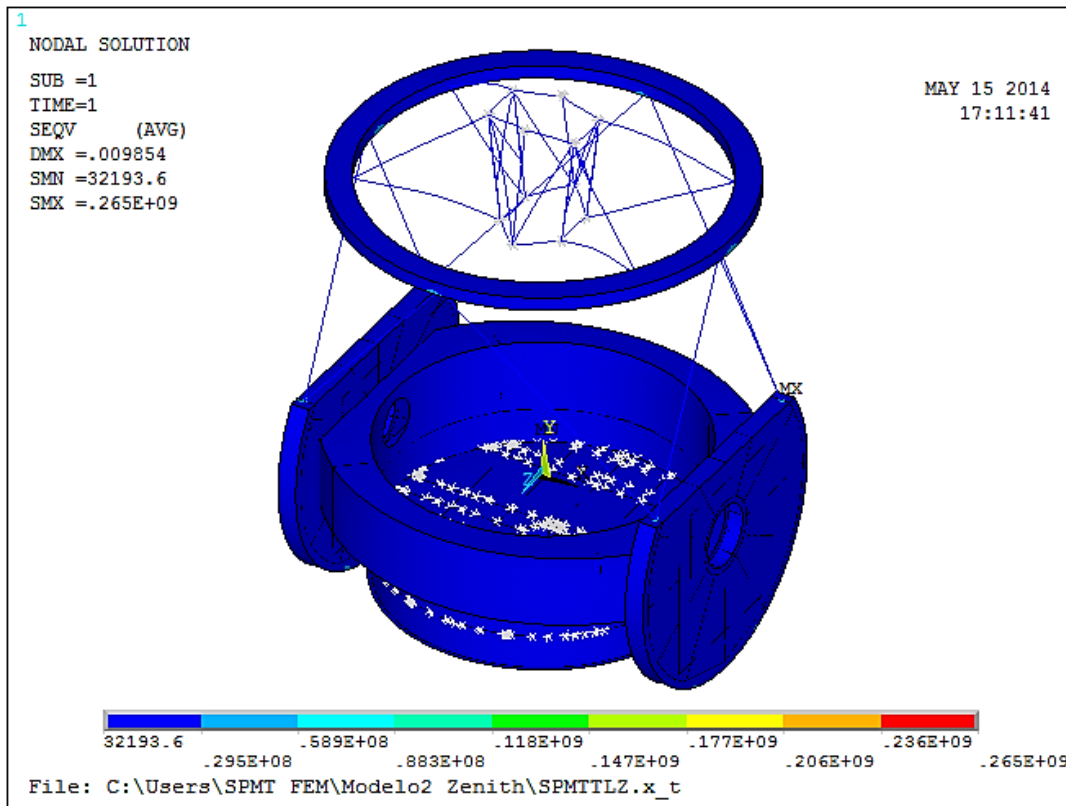


Figure 6-8 Stress in SPMT Telescope Model.

According to Figure 6-8, we can notice that the maximum stress value is in contact Telescope Tube and lifting system, indicated by the letter c in Figure 2, and this maximum stress value corresponds to 265 Mpa being highly concentrated at a point on the upper plate denoted as a shown in Figure 6-9 and Figure 6-10

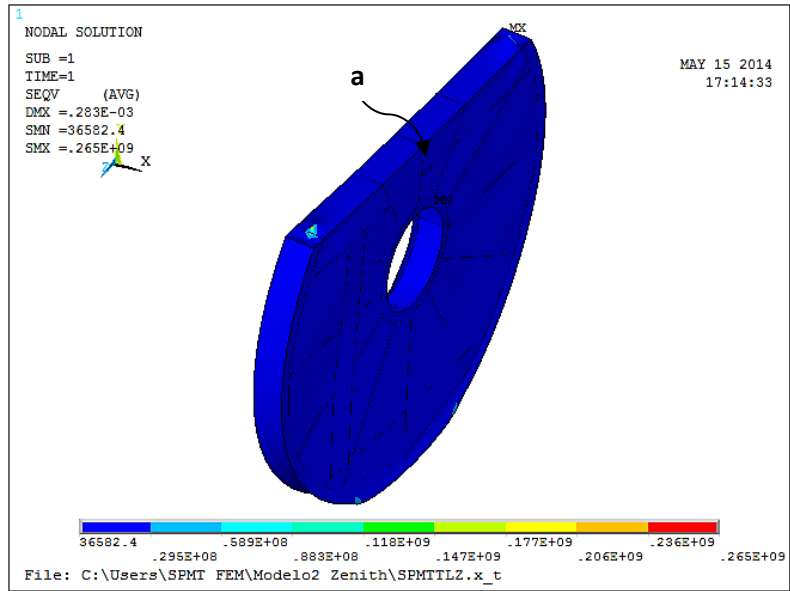


Figure 6-9 Stress in elevation system.

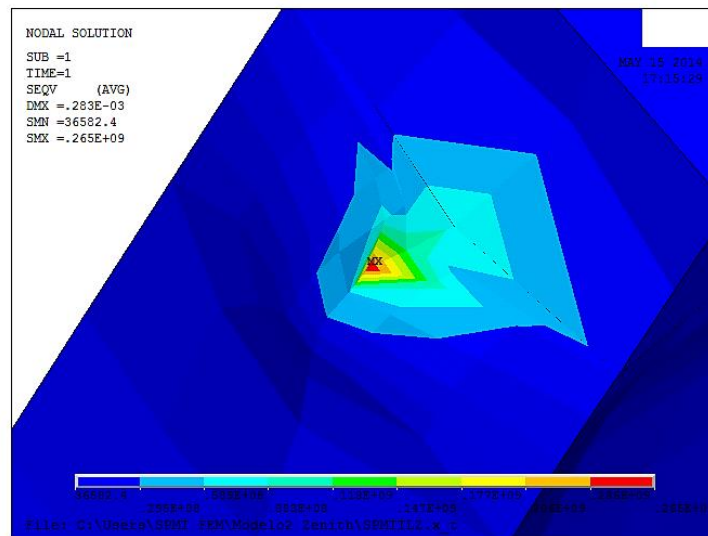



Figure 6-10 Approach to stress concentration zone in the elevation system.

	SPMT	Code: TRP/TELE/001-R
	SPMT Conceptual Design Pre PDR	Issue: 1.C
		Date: 24/06/2014
		Page: 118 of 152

Analyzing the pattern of stress distribution and magnitude of displacement in which the spider can reach 9,854 mm in the maximum (see Figure 6-11), we can review and correct thicknesses to optimize the stress distribution, and make better use of the time inertia and the areas of the components to make a safer design using less material.

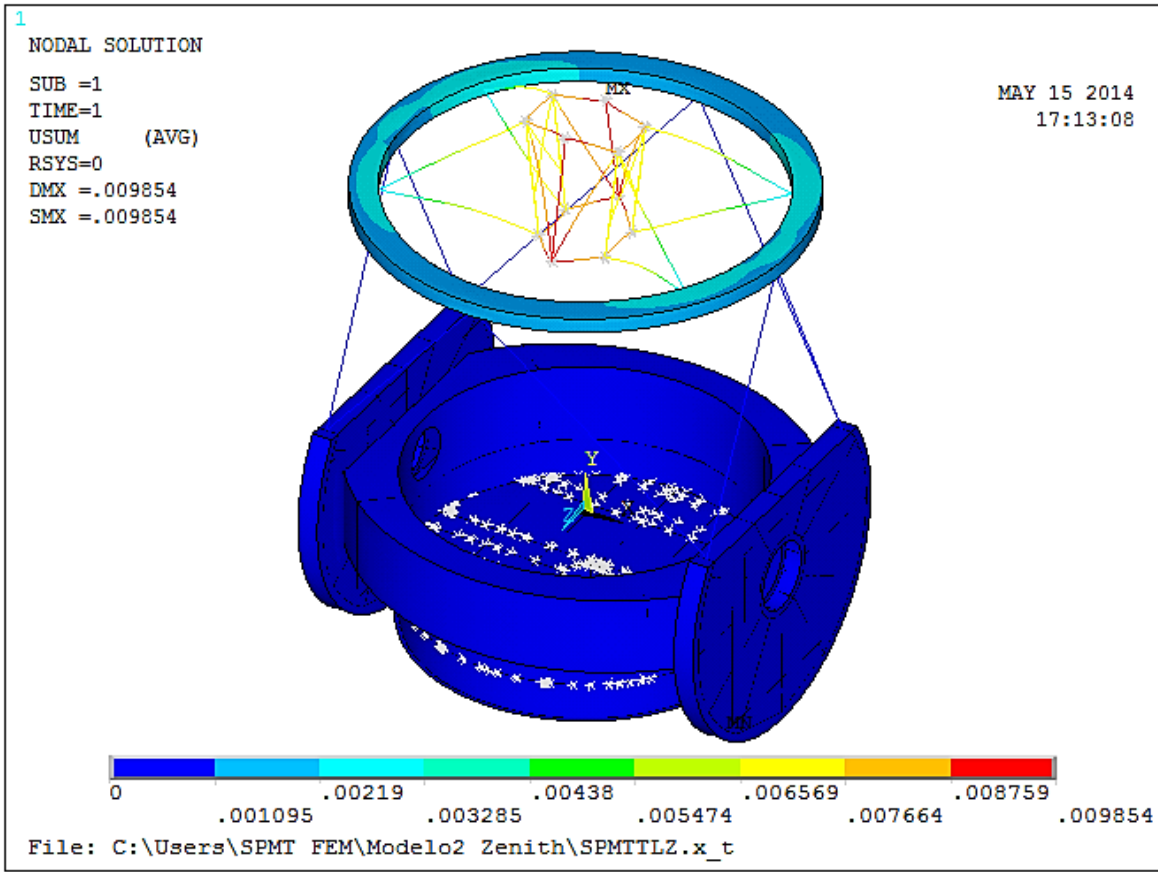



Figure 6-11 Displacement in SPMT Telescope model.

Observing Figure 6-12, we can notice that the maximum displacement of the spider is given in the upper joints that are on the far side to the fixing part there of to the upper ring end, due to the weight of the entire assembly of the structure of the secondary (hexapod, $f / 5$, $f / 1$) which is reflected in a shift of 9.854mm in the most critical part.

	<p>SPMT</p> <p>SPMT Conceptual Design Pre PDR</p>	<p>Code: TRP/TELE/001-R</p> <p>Issue: 1.C</p> <p>Date: 24/06/2014</p> <p>Page: 119 of 152</p>
---	--	---

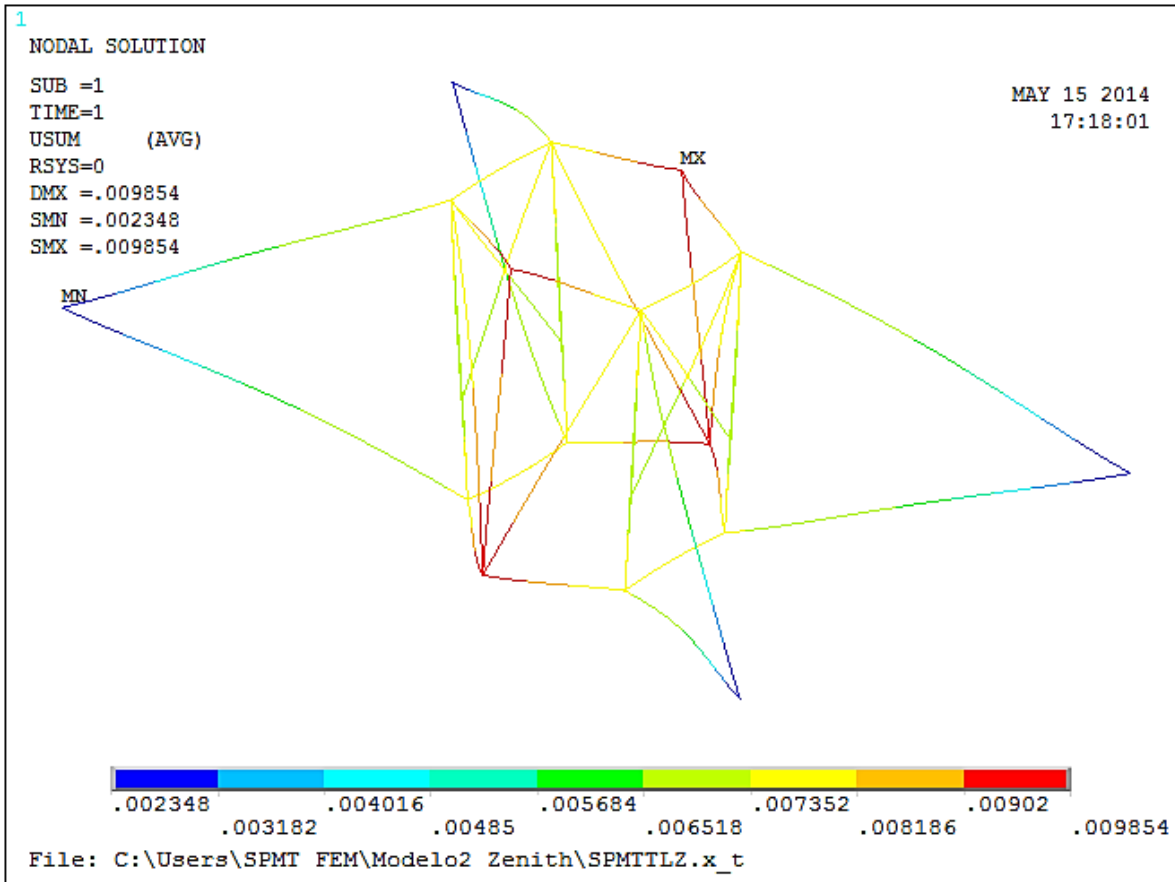



Figure 6-12 Displacements in the spider.

In Figure 6-13, the maximum stress in the primary mirror cell is 48.2 Mpa, comparing the stress ASTM A36 material is 250 Mpa, can see that is within the safe area of design with a load factor of 5.18, due to this very conservative load factor is possible to decrease the thickness of the plate to redistribute the load and on the component stress to improve performance and optimize the use of materials.

	<p>SPMT</p> <p>SPMT Conceptual Design Pre PDR</p>	<p>Code: TRP/TELE/001-R</p> <p>Issue: 1.C</p> <p>Date: 24/06/2014</p> <p>Page: 120 of 152</p>
---	--	---

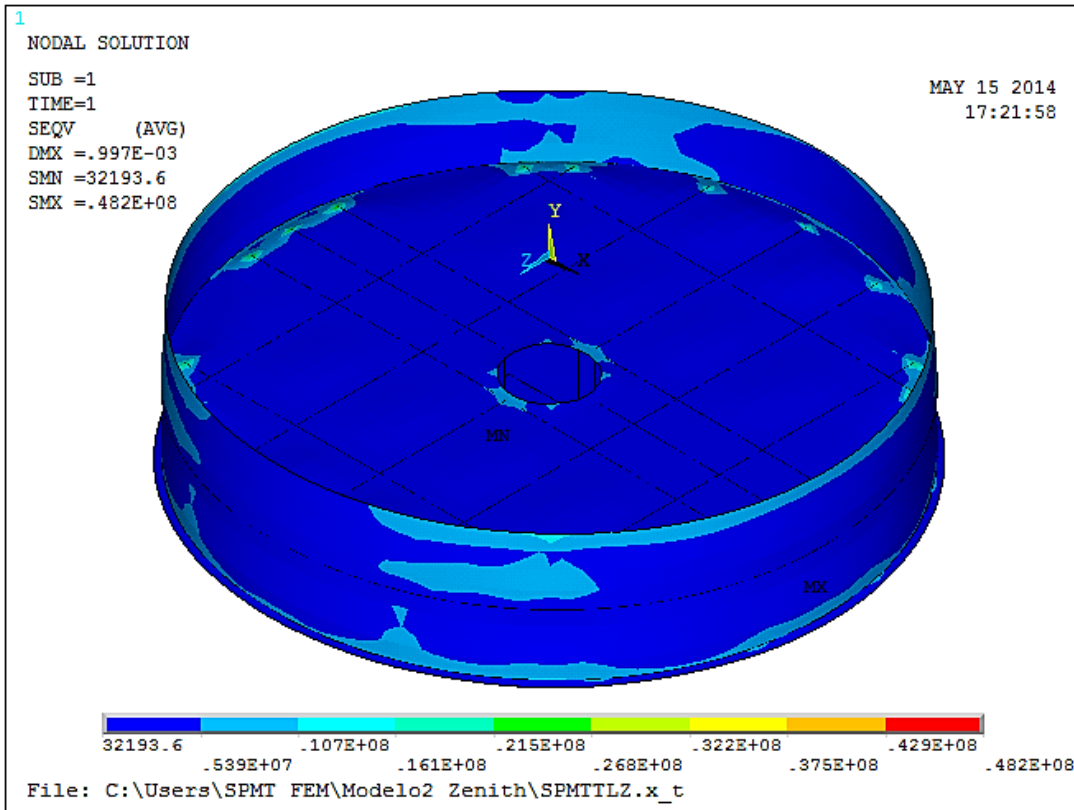



Figure 6-13 Stress in Primary mirror cell.

In Figure 6-14 , we can notice that the maximum displacement is at the plate where the primary mirror is placed due to buckling caused by the weight of the mirror, which is reflected in a shift of 0.997 mm in the most critical part.

	SPMT	Code: TRP/TELE/001-R
	SPMT Conceptual Design Pre PDR	Issue: 1.C Date: 24/06/2014 Page: 121 of 152

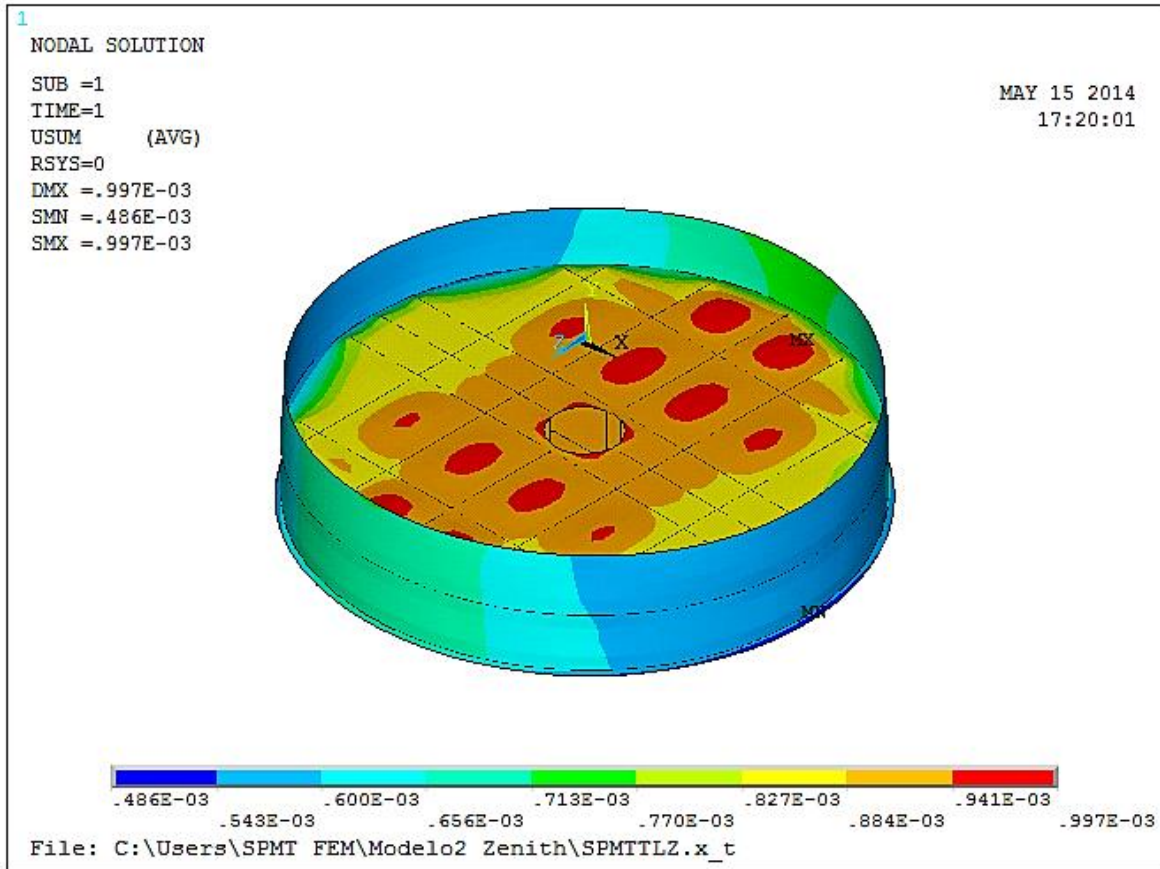


Figure 6-14 Displacements in Primary mirror cell.

6.1.1.6 Boundary conditions horizon position:

Were restricted in all degrees of freedom the contact areas of the hydrostatic pads with the lift system when the telescope were in the horizontal position the MASS21 elements were used to simulate the mass of the primary mirror in his cell and the mass the secondary mirror (secondary mirror $f / 5$ to $f/11$ Gregorian hexapod) system and the model with gravitational load (9.81 m/s^2 in the Z axis) indicated by the red arrow in Figure 15 and 16 endeavored to simulate the weight of the entire telescope to find the conditions of stress and strain from the original design concept.

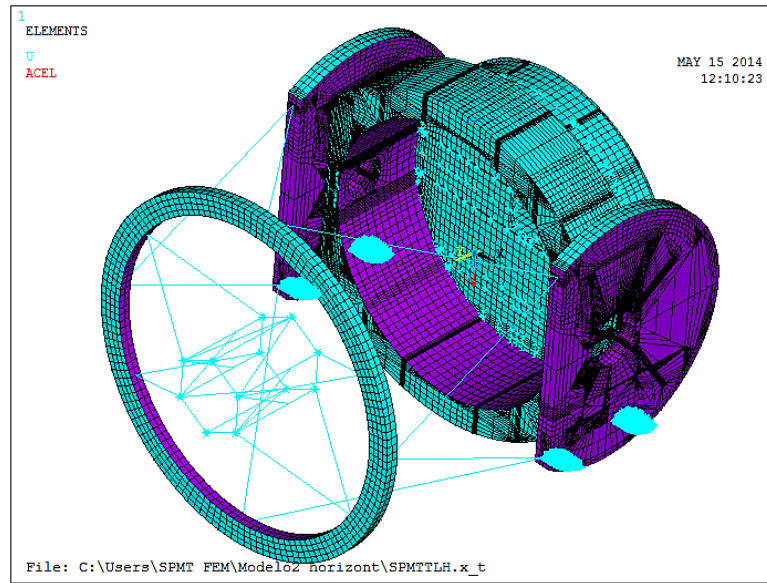


Figure 6-15 Meshing of surfaces model SPMT Telescope with loads and constraints.

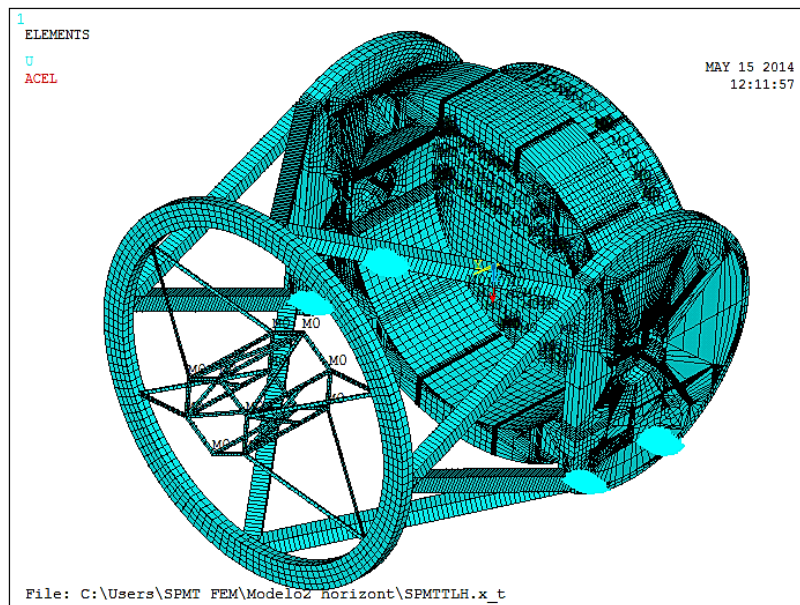



Figure 6-16 Meshing of model with cross sections elements BEAM4.

	<p>SPMT</p> <p>SPMT Conceptual Design Pre PDR</p>	<p>Code: TRP/TELE/001-R</p> <p>Issue: 1.C</p> <p>Date: 24/06/2014</p> <p>Page: 123 of 152</p>
---	--	---

The analysis conditions described above and the study was conducted position and obtaining the results shown below:

RESULTS

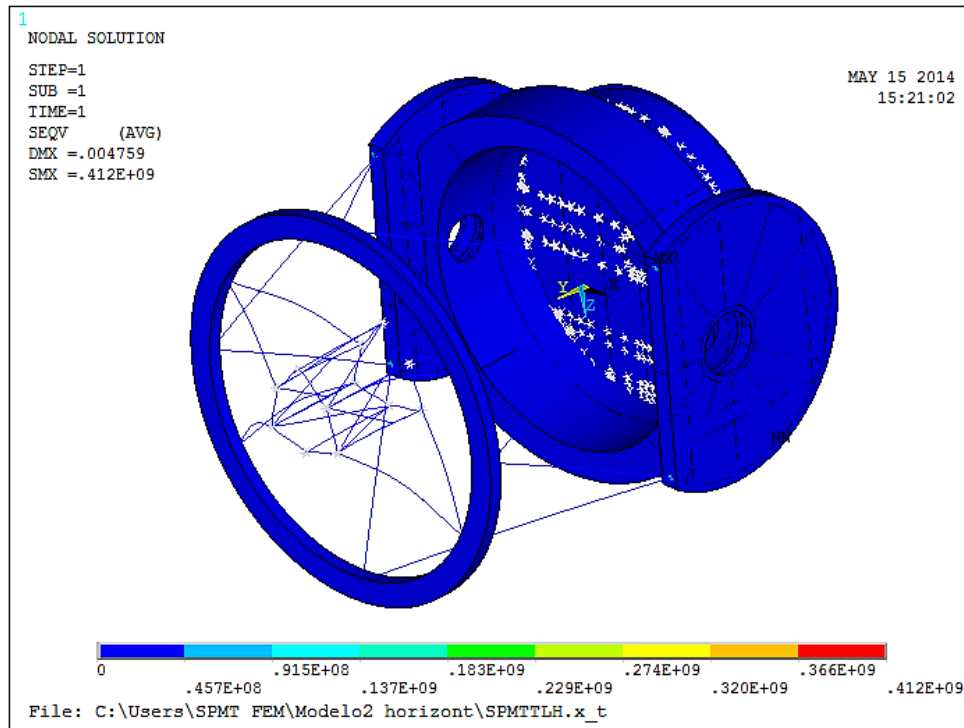


Figure 6-17 Stress in SPMT Telescope Model.

According to Figure 6-17 , the telescope pointing at this position, we can see that the maximum stress value is again in the intersection of the Telescope Tube and lifting system, indicated by the letter **c** in Figure 6-2, and the maximum value of stress corresponds to 412 MPa still very concentrated at a point where the top plate denoted as **A** (Figure 6-18 and Figure 6-19)

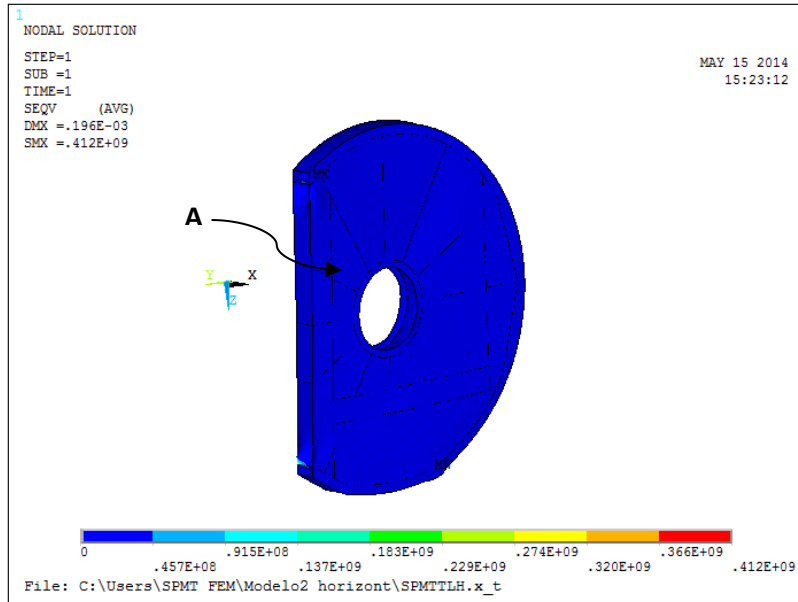


Figure 6-18 Stress in elevation system.

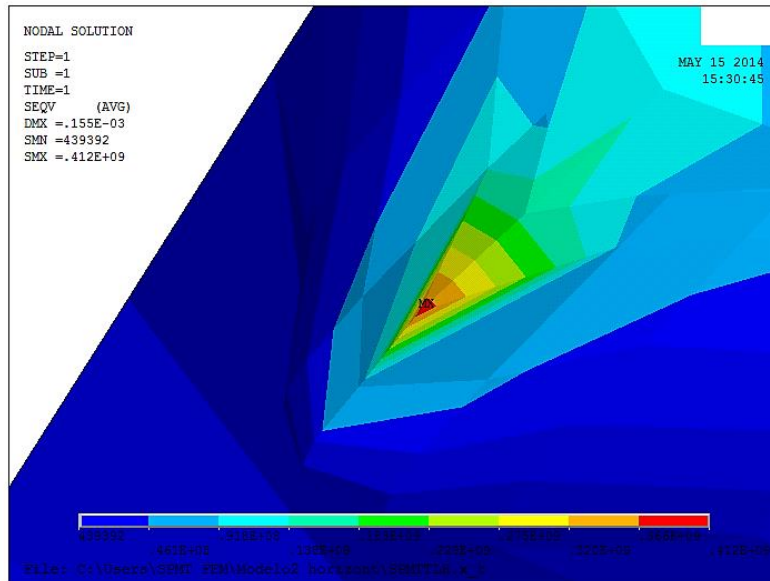



Figure 6-19 Approach to stress concentration zone in the elevation system.

	SPMT	Code: TRP/TELE/001-R
		Issue: 1.C
	SPMT Conceptual Design Pre PDR	Date: 24/06/2014
		Page: 125 of 152

Analyzing the pattern of stress distribution and magnitude of displacement which still appear in the spider and reach with the 4.759 mm in the maximum position (see Figure 6-20), we can review and optimize thicknesses to correct the stress distribution, and make better use of the moments of inertia and the areas of the components to make a safer design using less material.

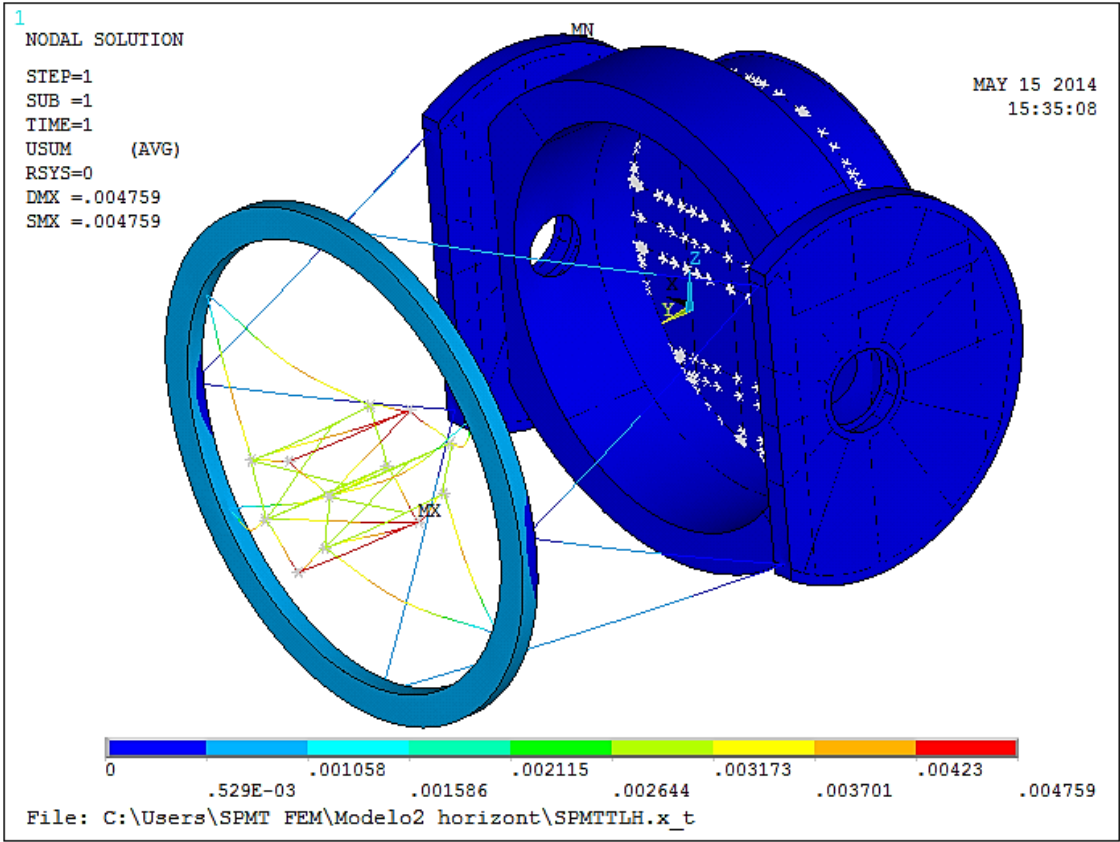



Figure 6-20 Displacements in SPMT Telescope model.

Looking at Figure 6-21, we can notice that the maximum displacement of the spider is given in one of the joints of the structure of the primary mirror that is farthest to the fixing portion of the structure to the top ring due to the weight of the entire assembly secondary structure (hexapod, $f/5$, $f/11$) which is reflected in a shift of 4.759mm in the most critical part.

	<p>SPMT</p> <p>SPMT Conceptual Design Pre PDR</p>	<p>Code: TRP/TELE/001-R</p> <p>Issue: 1.C</p> <p>Date: 24/06/2014</p> <p>Page: 126 of 152</p>
---	--	---

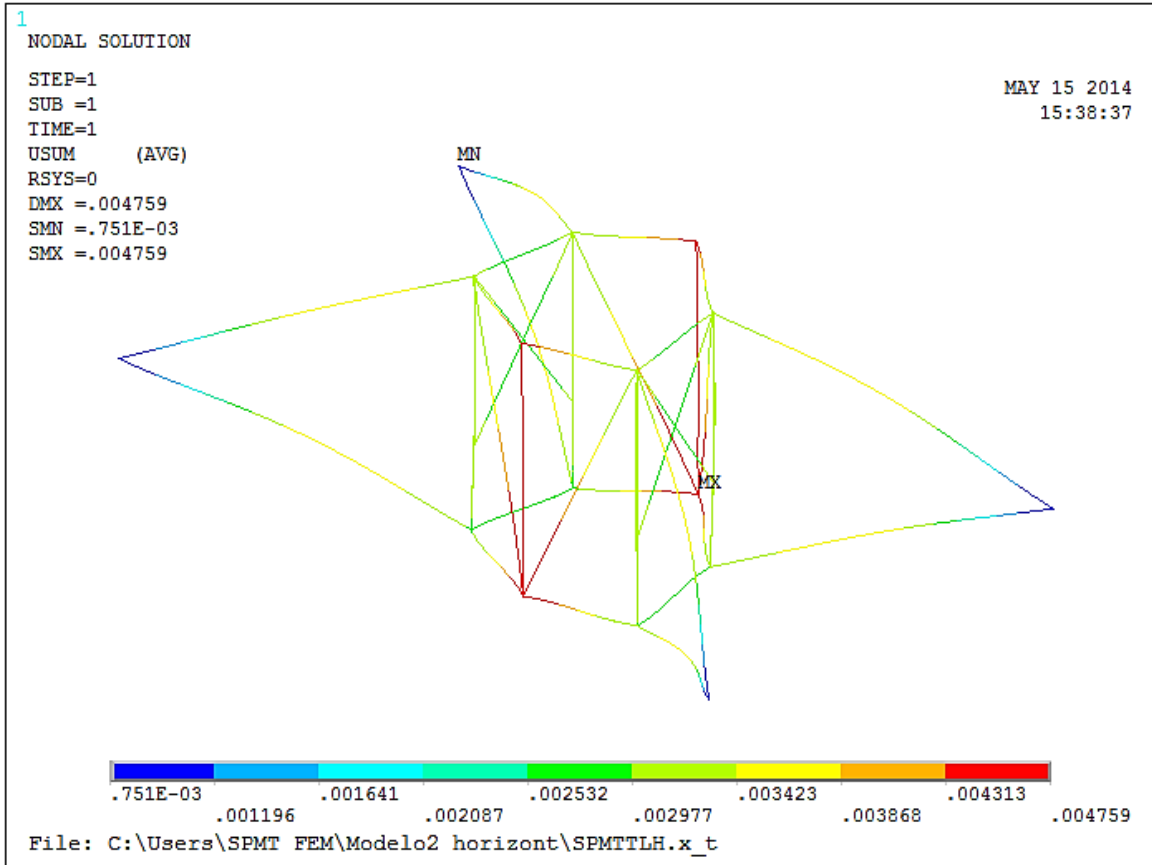



Figure 6-21 Displacements in the spider.

In Figure 6-22, the maximum stress in the primary mirror cell is 11.1 Mpa, comparing the stress ASTM A36 material which is 250 Mpa, can see that is within the safe area of design with a load factor of 22.52, due to this very conservative load factor is possible to decrease the thickness of the plate to redistribute the load and on the component stress to improve performance and optimize the use of materials.

	<p>SPMT</p> <p>SPMT Conceptual Design Pre PDR</p>	<p>Code: TRP/TELE/001-R</p> <p>Issue: 1.C</p> <p>Date: 24/06/2014</p> <p>Page: 127 of 152</p>
---	--	---

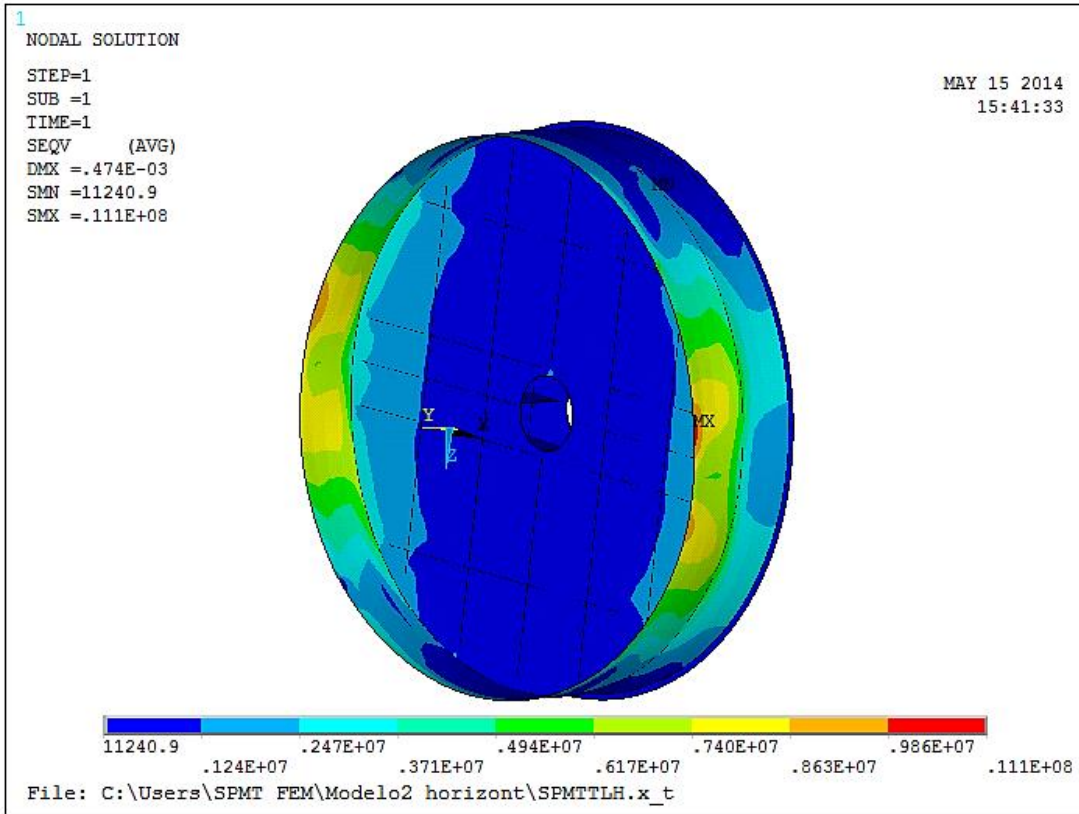


Figure 6-22 Stress in Primary mirror cell.

In Figure 6-23, we can notice that the maximum displacement is at the base of the cell where it will be placed the primary mirror due to buckling caused by the weight of the mirror, which is reflected in a shift of 0.474 mm in the most critical part.

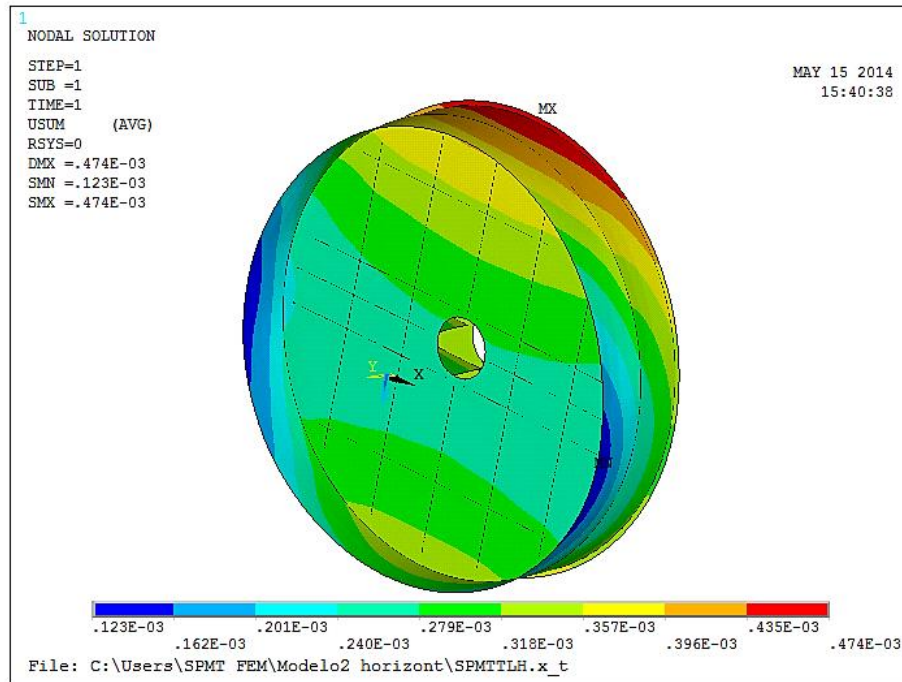



Figure 6-23 Displacements in Primary mirror cell.

6.1.2 Modal analysis

Modal analysis to obtain the results shown below for each vibration mode was performed:

SET	TIME/FREQ	LOAD STEP	SUBSTEP	CUMULATIVE
1	2.3845	1	1	1
2	5.7864	1	2	2
3	7.2095	1	3	3
4	8.1412	1	4	4
5	9.2154	1	5	5
6	11.157	1	6	6
7	11.318	1	7	7
8	11.636	1	8	8
9	11.867	1	9	9
10	12.128	1	10	10

	<p>SPMT</p> <p>SPMT Conceptual Design Pre PDR</p>	<p>Code: TRP/TELE/001-R</p> <p>Issue: 1.C</p> <p>Date: 24/06/2014</p> <p>Page: 129 of 152</p>
---	--	---

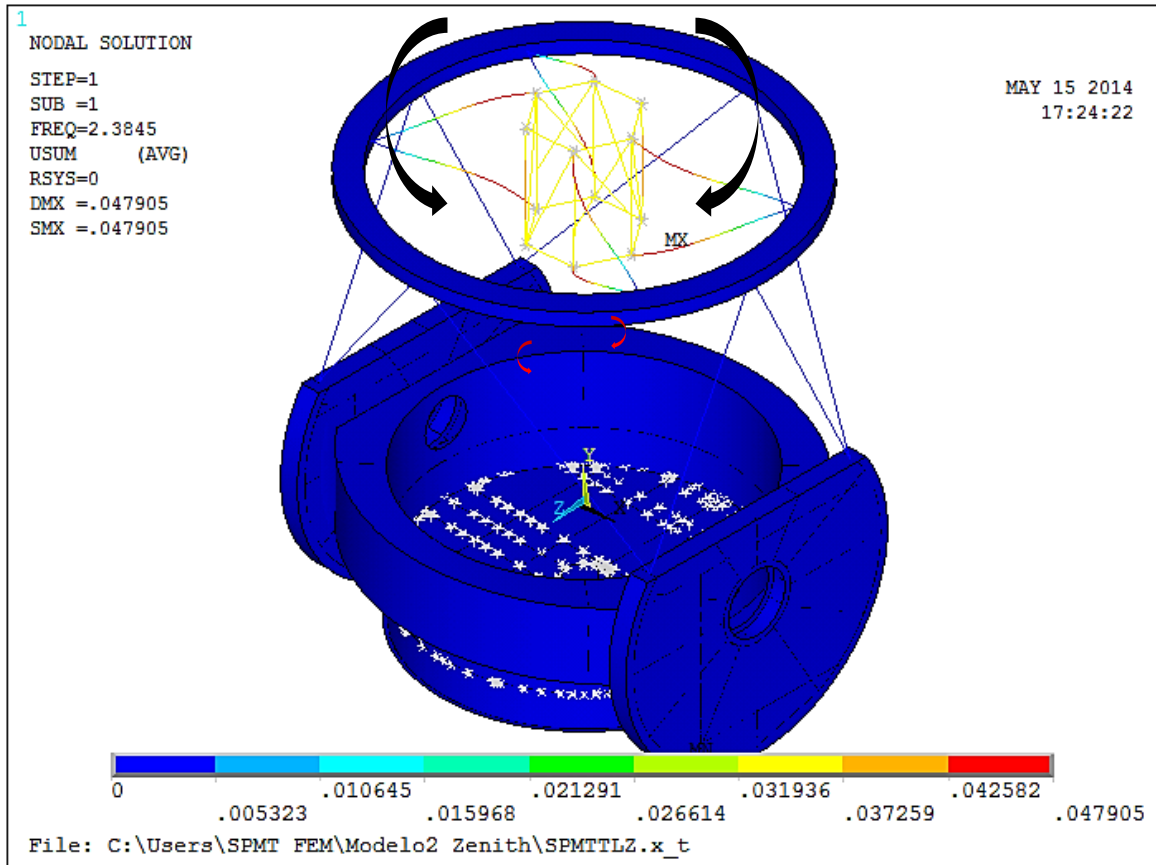


Figure 6-24 Mode 1.

Mode 1: Torque on the shaft and around the telescope but higher torque are presented in the spider, where the unions of the vanes with the basket of the secondary mirror.

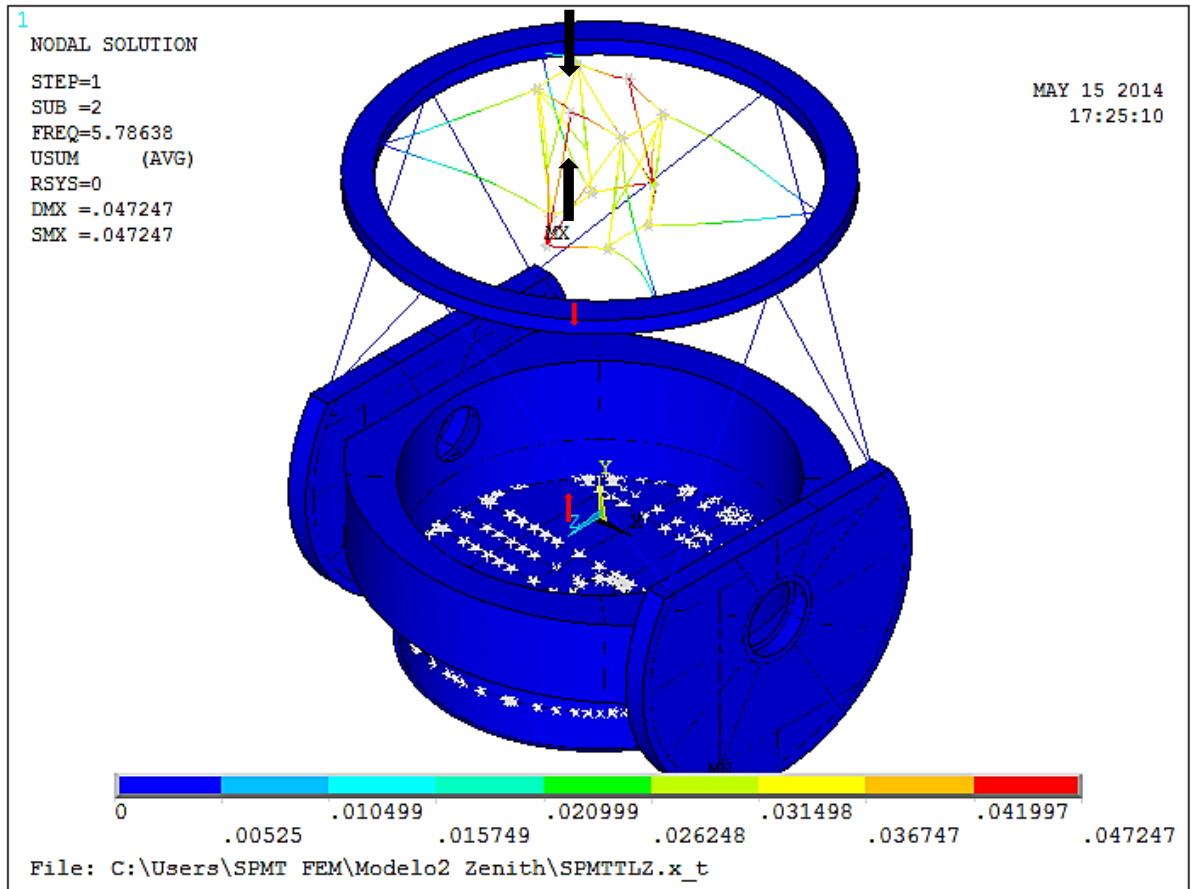



Figure 6-25 Mode 2.

Mode 2: the telescope up and down on the y axis, presenting greater movement in the less rigid part (Spider) and almost zero in the rest of the telescope offset.

	<p>SPMT</p> <p>SPMT Conceptual Design Pre PDR</p>	<p>Code: TRP/TELE/001-R</p> <p>Issue: 1.C</p> <p>Date: 24/06/2014</p> <p>Page: 131 of 152</p>
---	--	---

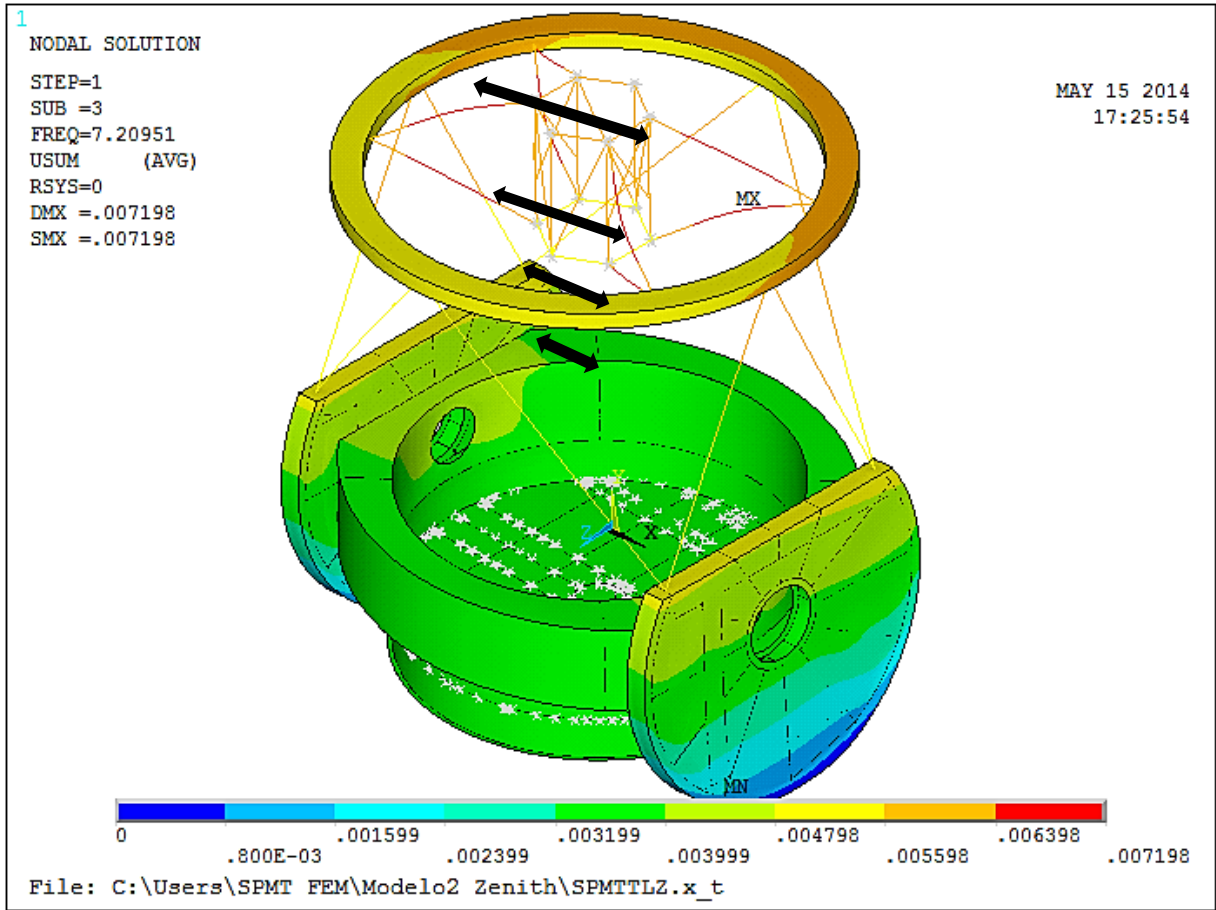



Figure 6-26 Mode 3.

Modo 3: Displacement in the x axis direction, increasing the displacement while the point is further from the constraints.

	<p>SPMT</p> <p>SPMT Conceptual Design Pre PDR</p>	<p>Code: TRP/TELE/001-R</p> <p>Issue: 1.C</p> <p>Date: 24/06/2014</p> <p>Page: 132 of 152</p>
---	--	---

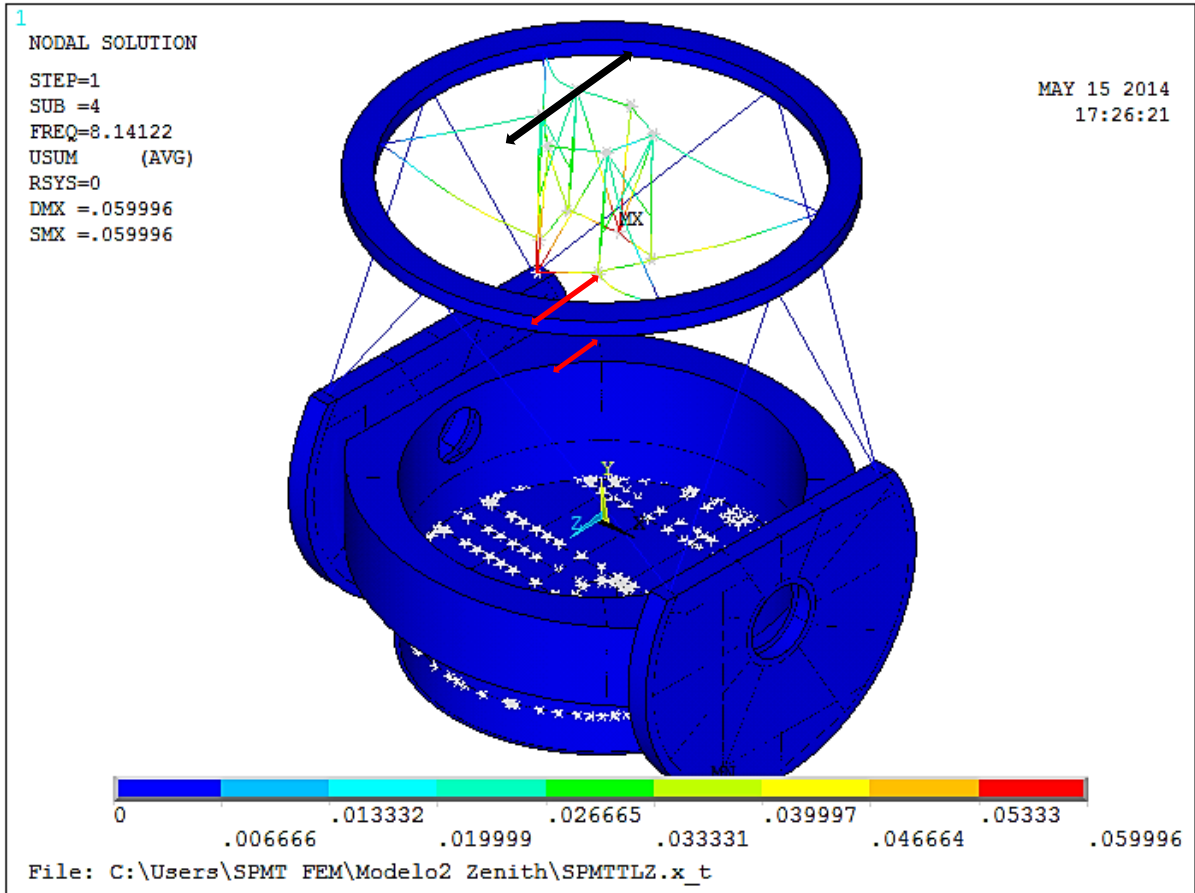



Figure 6-27 Mode 4.

Mode 4: Displacements along the z axis, presenting major shifts in the spider on the lower joints of the basket of the secondary mirror.

	<p>SPMT</p> <p>SPMT Conceptual Design Pre PDR</p>	<p>Code: TRP/TELE/001-R</p> <p>Issue: 1.C</p> <p>Date: 24/06/2014</p> <p>Page: 133 of 152</p>
---	--	---

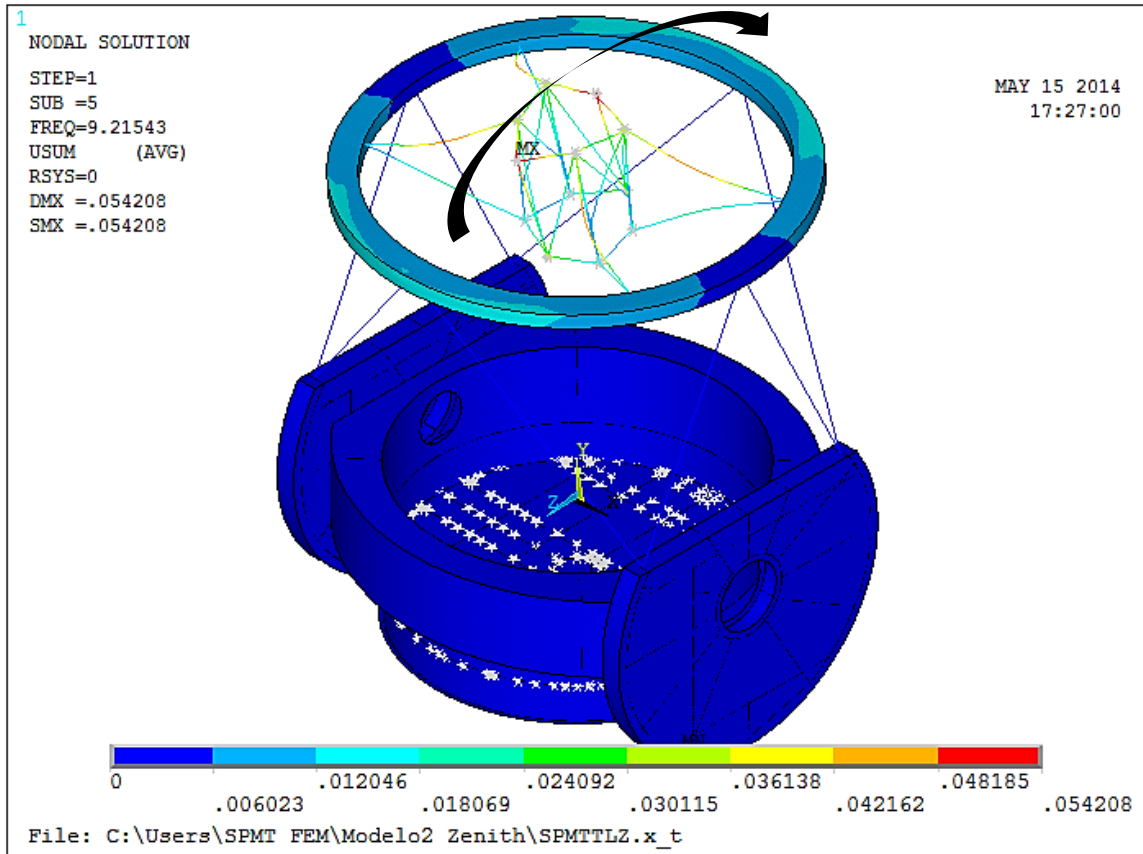



Figure 6-28 Mode 5.

Mode 5: Twist the top ring together with spider presenting the biggest shifts in the upper joints of the basket of the telescope on the x axis.

6.1.3 Analisis conclusions

In both positions of telescope analyzed analysis can be seen that stresses exceed the yield strength of ASTM A36. This can be diminish, because stress is focus on four points in the elevation system, due to modeling, and this are the points of contact between the system and the telescope tube in the results shown as large stress concentrations. All the weight of the upper ring and the whole system of the secondary mirror, is transmitted at these points when, in fact, the area where the force is exerted by the load is greater .This points at the surface are placed plates of the same material and with a thickness, this make the stress located at this points spread in this plates (this will be confirmed in future analysis). So considering that the obtained value of stress

	<p>SPMT</p> <p>SPMT Conceptual Design Pre PDR</p>	<p>Code: TRP/TELE/001-R</p> <p>Issue: 1.C</p> <p>Date: 24/06/2014</p> <p>Page: 134 of 152</p>
---	--	---

compared to the yield strength not exceeding this value much we can say that increasing the contact area is reduced stress.

In the analysis of the stress in the zenith position most of the telescope's stress are in a range from 0 to 29.5 MPa so the design is in the safe area of design.

The Zenith position is where the largest displacements of the telescope which appear in the spider, reducing these, we can use different the cross-sectional areas and moments of inertia to achieve more stiffness in this part of the telescope.

In this same position to analyze the primary mirror cell, stress obtained compared to the yield strength of the material are very low with a load factor of 5.18 to be in a safe area of design which can reduce and optimize thicknesses materials. The movements in the cell due to the weight of the mirror are very low and therefore can further optimize the whole cell.

The results obtained in the horizontal position of the telescope with respect to stress are generally in the range of 0 to 45.7 MPa but even these being higher than those found in the zenith position, they do not exceed the yield strength of the material and therefore the design is still in the safe zone.


In this horizontal position of the telescope the maximum displacements continue to occur in the spider but are much lower than in the Zenith position thus stiffens if the spider is further reduced displacement in this position.

The primary mirror cell in the horizontal position overall the results are very good compared to the properties of the material because the stresses and displacements are reduced much more in this position than in Zenith, therefore can further optimize this cell .

The horizontal position has greater stress but minor displacements. Zenith position has less stress and greater displacement.

7. SAN PEDRO MARTIR TELESCOPE CONTROL ARCHITECTURE


SPMT is conformed by several subsystems that must be controlled and monitored. The observatory control system includes software, computers, communications, electronics and industrial devices needed for control of the telescope, instruments, and supporting systems.

	<p>SPMT</p> <p>SPMT Conceptual Design Pre PDR</p>	<p>Code: TRP/TELE/001-R</p> <p>Issue: 1.C</p> <p>Date: 24/06/2014</p> <p>Page: 135 of 152</p>
---	--	---

Each subsystem will be controlled by a local control; they will require software for configuration, control, diagnostics, and engineering work. Instruments will have specific internal software developed with the instruments but will use a common interface to the observatory control system.

In the past, many different combinations of software environments, operating systems, hardware platforms, and communications protocols, have been used successfully for astronomical telescope control systems. For SPMT it is important to choose a flexible system architecture that can be supported for most of the life of the telescope. Considerations:


- Use existing, well developed solutions.
- Implement transparent distributed control for remote operations.
- Construct a mostly homogenous system to reduce maintenance costs but allow some variations in order to most efficiently integrate other practical solutions.
- Use software and hardware systems with broad industry support, cross platform capability, and the likelihood of continued support in the future.
- Use applications software environments that are simple, well known, stable, and easily documented.
- Use well known operating systems available for a variety of hardware platforms.
- Use communication protocols with adequate bandwidth and wide compatibility with different devices.
- Use robust, cost effective hardware with a wide range of available plug-in accessories, including motion controllers, data acquisition cards, GPS timing hardware, etc.
- PC hardware platforms. These are cost effective, are easily built or modified to provide specific capabilities where needed, are available in numerous configurations from many vendors, have well understood architectures, and are capable of operating either Windows or Linux.
- National Instruments LabVIEW for applications development.

	<p>SPMT</p> <p>SPMT Conceptual Design Pre PDR</p>	<p>Code: TRP/TELE/001-R</p> <p>Issue: 1.C</p> <p>Date: 24/06/2014</p> <p>Page: 136 of 152</p>
---	--	---

This graphic programming environment was developed specifically for instrument, process, and machine control.

- It allow's the rapid development of GUIs.
 - implements transparent distributed control
 - Is available for several platforms, capable of rapid implementation of legacy code.
- Fast Ethernet communications with multiple backbones to separate data traffic from control and support communications.
 - A separate timing bus for synchronization.
 - Motion control cards protocols to transfer data like position, velocity, time and configuration commands. All the servo systems (mount, secondary hexapod, tertiary rotator, primary surface, and enclosure) will have similar interfaces, but with different update rates and different packet contents.
 - General purpose monitoring and control. This will be a slow (a few samples per minute), distributed, industrial I/O system.
 - Instruments will have their own protocol. All instruments will follow the same basic interface strategy, but they will have different command sets and register maps that will be defined in configuration files. An instrument will try to connect to the control system, and if it is successful its commands and registers will be available to scripts and the command line interface. Physical connections between control system components on the telescope will be ethernet. Connections off the telescope will be multimode fiber.
 - Weather station. This will be a slow update rates providing meteorological data to the control system.

NI PXI Express platform, driven by LabVIEW is the heart of the architecture.

	SPMT	Code: TRP/TELE/001-R
		Issue: 1.C
	SPMT Conceptual Design Pre PDR	Date: 24/06/2014
		Page: 137 of 152

PXI Express and FPGA Architecture provides rapid prototyping to facilitate hardware integration, and allows maximal code reuse for the final application. LabVIEW Real-Time runs on the real-time controller to provide deterministic coordination and supervisory control functionality.

The PXI Express (PXIe) bus provides a powerful mechanism for management of high-bandwidth data in the event that multiple FPGAs are required to meet evolving algorithmic requirements. National Instruments provides chassis support for up to 2 GB/s per-slot bandwidth, with significant growth potential.

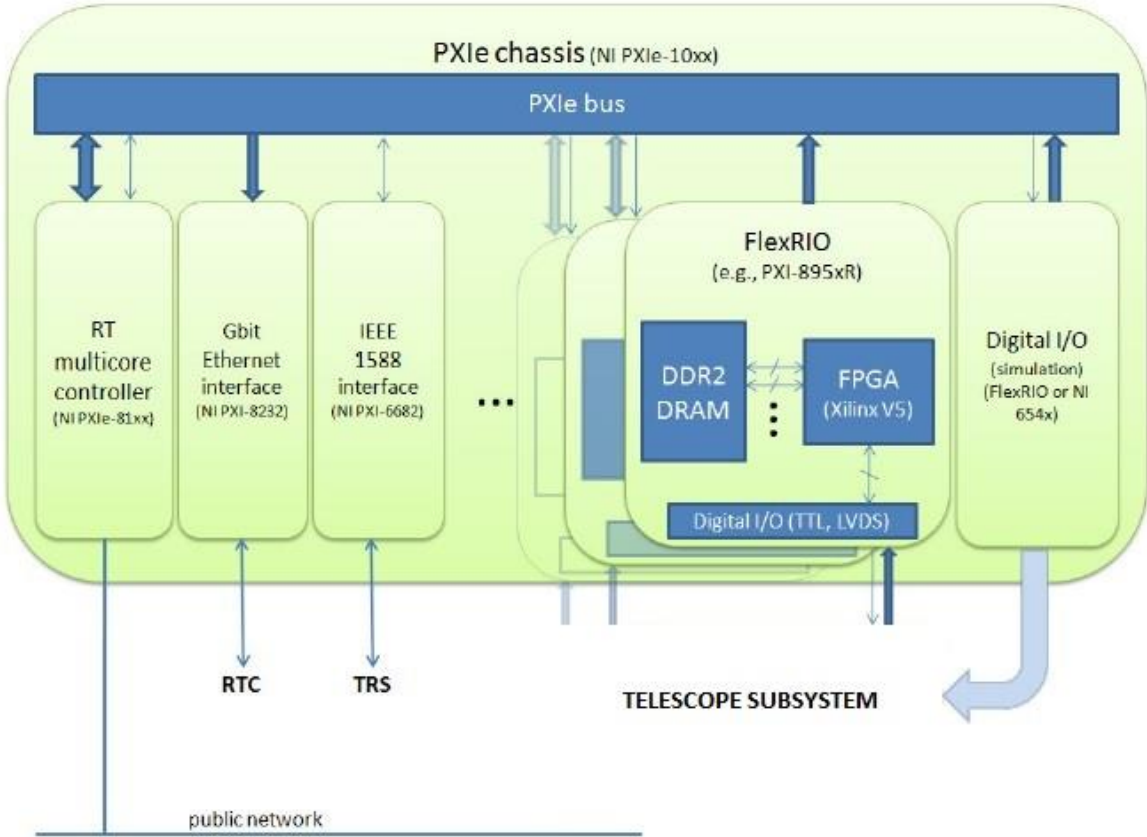



Figure 7-1 Time-stamping in LabVIEW Real-Time

	<p>SPMT</p> <p>SPMT Conceptual Design Pre PDR</p>	<p>Code: TRP/TELE/001-R</p> <p>Issue: 1.C</p> <p>Date: 24/06/2014</p> <p>Page: 138 of 152</p>
---	--	---

All subsystems use the system timing engine built into LV. The engine, referred to as “nano-second engine,” controls all timing in the system and can also be synchronized to an external timing source such as GPS, IEEE 1588, custom FPGA clock, etc. The resolution of the time stamps is user selectable to be in milli-, micro-, or nano- seconds.

7.1 Network reliability.


In general, deterministic systems running on a tight schedule do not retransmit data on the application or software protocol level in order to avoid interfering with the transmission of the new data. One can potentially send each packet twice (duplicate) to increase the chances of delivery but that will come with the penalty of longer communication time. Using a PCIe infrastructure can resolve some of these problems as this bus supports retransmission at the lowest level.

Ethernet is on a 10 us level a deterministic bus. The main causes of non-determinism are IP/TCP/UDP stacks used to send data, non-determinisms in the underlying OS, and the fact that networks themselves are not carefully time-managed. NI uses their own Level 2 protocol, but can, without problems, receive/generate IP/UDP-based packets sent from arbitrary platforms.

Using 10Gb/s Ethernet adapters will simplify the network layout .It’s also expect further reduction in latency.


Hardware list:

- National Instruments Platform:
 - Chassis
 - PXIe - PXI Express
 - Controller
 - PXIe - Windows OS running LabVIEW
 - PXIe - RTOS (Real-Time Operating System) running LabVIEW Real-Time
 - Data acquisition cards
 - PXIe - X Series
 - I / O analog voltage

	<p>SPMT</p> <p>SPMT Conceptual Design Pre PDR</p>	<p>Code: TRP/TELE/001-R</p> <p>Issue: 1.C</p> <p>Date: 24/06/2014</p> <p>Page: 139 of 152</p>
---	--	---

- Digital I / O
 - FlexRIO - R Series
 - FPGA Cards, defined by the adapter module
 - Digitizers
 - Digital I / O for high-speed motion control
 - PXI - Communication Protocols
 - CAN communication cards
 - RS-232 communication cards
- Communication Bus:
 - DDS - Data Distribution System for RT Systems to connect the systems running RTOS.
 - Ethernet, to be used to communicate all the subsystems of the telescope, with the exception of RTOS.
- Timing:
 - Quartz oscillator for GPS.
 - Reference time
 - Synchronization signal for the complete system
 - Using the IEEE 1588-2008 protocol over Switched Ethernet
- High Performance PCs:
 - Dedicated to high processing capabilities and resolution algorithms
 - Hardware-in-the-loop simulation of the telescope and control system
 - Processor: Intel® Core™ 2 Quad processor Q9100 (2.26 GHz quad core processor), Memory: 1GB RAM (normally comes standard with 2G or 4G) L2 cache: 12 MB; 6 MB shared between cores 0 and 1, 6 MB shared between cores 2 and 3
 - TRS connection: NI PXI-6682 (IEEE 1588)
 - Network (public): Gigabit Ethernet (on controller)
 - Network (deterministic): NI PXI-8232, Gigabit Ethernet

The previous hardware can be adapted and particularized to each subsystem of the telescope (active optics, thermalization, alt-azimuth motion control, etc.) once that elements of the subsystems are defined.

	<p>SPMT</p> <p>SPMT Conceptual Design Pre PDR</p>	<p>Code: TRP/TELE/001-R</p> <p>Issue: 1.C</p> <p>Date: 24/06/2014</p> <p>Page: 140 of 152</p>
---	--	---

The control system will:

- Take commands from a GUI.
- Move the telescope and its enclosure to pointing and guiding
- Maintain the profile of the primary surface and the alignment with the secondary mirror.
- Set the configuration of the telescope and instruments
- Display information about the telescope and instruments
- Execute configuration commands from the control system.
- Return monitor values requested by the control system for display purposes.
- Return data from instruments.
- Archive data and status.

The control system functions include:

Telescope Control

- Pointing and tracking
- Primary mirror active surface control
- Secondary mirror positioning and active control
- Optics alignment
- Safety interlock monitor

Enclosure Control


- Shutter open and close
- Safety interlock monitor

Environmental Monitoring

- Site meteorology
- Dome and telescope temperature monitors
- Weather forecasts

Instrument Control

- Configuration, tuning, etc.

	<p>SPMT</p> <p>SPMT Conceptual Design Pre PDR</p>	<p>Code: TRP/TELE/001-R</p> <p>Issue: 1.C</p> <p>Date: 24/06/2014</p> <p>Page: 141 of 152</p>
---	--	---

- Observing synchronization
- Diagnostics
- Data readout and storage

Observation Control

- GUI
- Remote observing
- Queue scheduling and autonomous observations
- Instrument data quick look display

Data Management

- Instrument data archiving, cataloguing, retrieval, and distribution
- Operations logging
- Maintenance logging and scheduling

Network infrastructure


Next, the components to complement the network infrastructure for each of the sections that form the San Pedro Martir telescope are described.

Observation room

At the observation room are considered 8 Pc's to control the telescope and subsystems and 2 printers connected to the network center with communication with the engineering room. Similarly 8 nodes are considered for video surveillance cameras 4 indoor and 4 external, 5 nodes to control access to the dome (if required).

Components list required to installation of switch at this building.

- 25 category 6 A nodes
- 1 cabinet for active equipment

	<p>SPMT</p> <p>SPMT Conceptual Design Pre PDR</p>	<p>Code: TRP/TELE/001-R</p> <p>Issue: 1.C</p> <p>Date: 24/06/2014</p> <p>Page: 142 of 152</p>
---	--	---

- PoE 48 ports Switch
- 8-nodes for cameras
- 5 nodes for access control
- 10 nodes for Pc's
- 1 UPS 3KVA
- 2-node for printing system
- 2 phone lines
- 10Gbps fiber connections

3.5.3 PLANO DE PLANTAS GENERALES

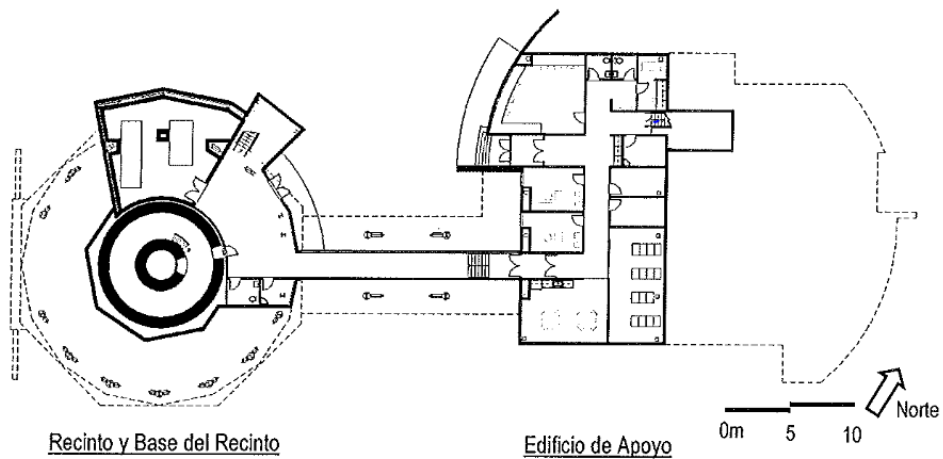



Figura 3.5.3.1 Plano de Planta General – Planta Baja

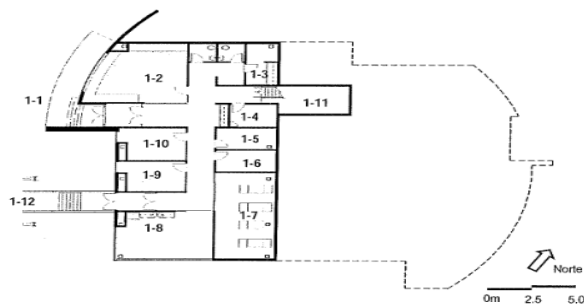
Figure 7-2 First Floor

	SPMT	Code: TRP/TELE/001-R
	SPMT Conceptual Design Pre PDR	Issue: 1.C
		Date: 24/06/2014
		Page: 143 of 152

On the ground floor are being considered 29 network nodes and access points to have wireless network (if necessary).

Components list required to infrastructure installation at this part of the building.

- 16 user nodes
- 10 phone extensions
- 3 access control nodes
- 4 nodes for video surveillance cameras fixed (indoor)
- 2 nodes for access points
- 1 PoE SWITCH with 48 10Gbps uplink ports
- 4 nodes for the printing system
- 10 Gbps fiber connections



1-1	Entrada Principal del Edificio de Apoyo	1-7	Sala de Computo
1-2	Sala de Control	1-8	Cuarto del Observador
1-3	Clinica	1-9	Oficina No. 1
1-4	Armario de Intendencia	1-10	Oficina No. 2
1-5	Almacón	1-11	Circulación Vertical
1-6	Sala de Sistemas	1-12	Acceso al Recinto

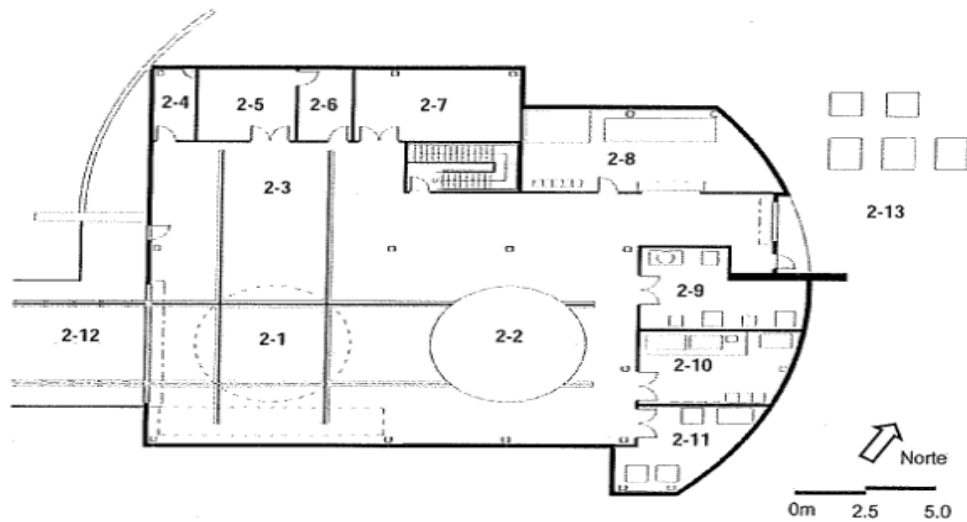
Figure 7-3 Auxiliary building

In this part of the building nodes will change by the number of computers installed.

Second Floor


At the second floor are considered 16 nodes which are as follows:

- 2 nodes for users
- 6 nodes for access control
- 7 nodes for security camera (5 external, 2 internal)
- 2 phone extensions



2-1	Lavado de Espejo	2-8	Sala de Equipos TSPM
2-2	Aluminizado de Espejo	2-9	Cuarto de Maquinaria
2-3	Laboratorio de Instrumentación	2-10	Cuarto Eléctrico
2-4	Armario de Intendencia	2-11	Equipo para Lavado y Aluminizado
2-5	Cuarto de Limpieza	2-12	Puente al Recinto
2-6	Vestíbulo al Cuarto de Limpieza	2-13	Entrada de la Planta Alta y Equipo Exterior
2-7	Almacén de Herramienta		

Figure 7-4 Auxiliary buiding second floor

	SPMT SPMT Conceptual Design Pre PDR	Code: TRP/TELE/001-R Issue: 1.C Date: 24/06/2014 Page: 145 of 152
---	---	--

SITE

To complement the network the following equipment which will be included on the SITE


- Server for the surveillance system
- Access Control Server
- 10 Gb Switch core
- Firewall
- Internet Server
- Server for IT services
- Telephony Server.
- Storage server

Document management

Points to consider in the selection of a document management

User features:


- System storage and management of data and documents
- Database [type] .
- Security storage. Backups [without stopping the system] .
- Access Control roles and stages of development .
- Distributed storage system , there is no single location for all data , however each data is located in one place.

	<p>SPMT</p> <p>SPMT Conceptual Design Pre PDR</p>	<p>Code: TRP/TELE/001-R</p> <p>Issue: 1.C</p> <p>Date: 24/06/2014</p> <p>Page: 146 of 152</p>
---	--	---

- Process and workflow
- Defining workflows.
- Changes authorization control.
- Workflow control , process monitoring .
- Management of product structure
- Create and manage product configuration .
- Classification and Standardization
- Several classification procedures for defining families of elements .
- Management Programming
- Planning, monitoring and control of activities and resources .

Services features


- Communication and reporting
- System Event Notification to the people involved.
- Data Transport
- System allows connectivity between computers, manipulate data without knowing where they are. The user does not need to know the operating system or network system. Type web browser.
- Data Translation
- System Administration

	SPMT SPMT Conceptual Design Pre PDR	Code: TRP/TELE/001-R Issue: 1.C Date: 24/06/2014 Page: 147 of 152
---	---	--

- Access management, change permissions, authorizations, approval procedures, backup and data files.

Management and control of documents proposal, OpenKM, is one of the most recommended on Linux. OpenKM is an open source document management system.

OpenKM is a Java J2EE application running on a JBoss application server, and database repository can store it in MySQL, PostgreSQL, Oracle and others. The hardware requirements for a small company with 25 users and a repository between 10 and 60 GB are 1 GB of RAM, but recommended for best performance 2 to 4, a Dual Core 2 or similar processor and a SATA hard drive between 150 and 250 GB.

	<p>SPMT</p> <p>SPMT Conceptual Design Pre PDR</p>	<p>Code: TRP/TELE/001-R</p> <p>Issue: 1.C</p> <p>Date: 24/06/2014</p> <p>Page: 148 of 152</p>
---	--	---

7.2 Site Dimensions

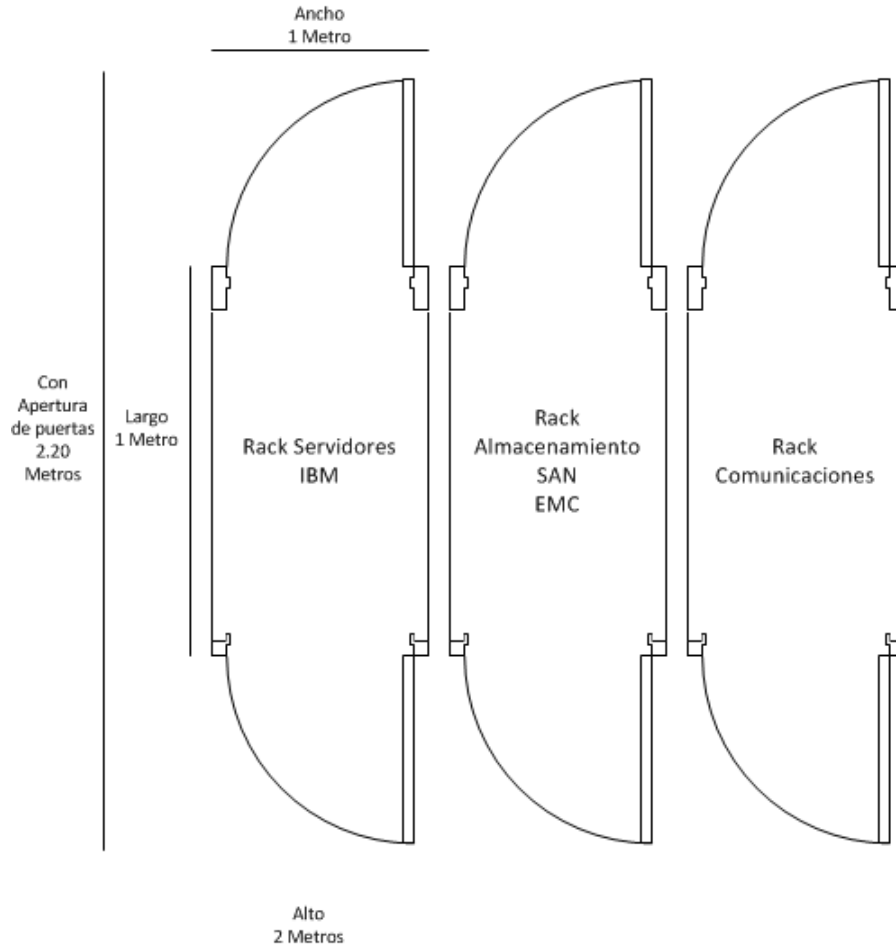



Figure 7-5 Site Dimensions

Length: 6 Meters, contemplating three racks and aisles 1.5 meters laterals

Width: 5 meters, contemplating opening rack and 1.5 meters hall, front and back.

Height: 3.20 meters, contemplating false ceiling 0.50 cm and 0.50 cm false floor, allowing 2.20 meters height working area.

	<p>SPMT</p> <p>SPMT Conceptual Design Pre PDR</p>	<p>Code: TRP/TELE/001-R</p> <p>Issue: 1.C</p> <p>Date: 24/06/2014</p> <p>Page: 149 of 152</p>
---	--	---

Servers:

- Communication and reporting
- Rack for IBM BladeCenter.
- IBM BladeCenter
- 3 IBM Blades as minimum to ensure high availability of systems. (Quantity, capacity and speed depends on the subsequent requests)
- LAN Switching and Optical Fiber communication

Information Security

- information backups system

Communication


- Switch
- Router
- Filtering or Content
- Firewall or
- Distribution Panels
- Telephony
- Fiber Panels

Security

Access Controls

Prevention and Response Systems

- ofire system
- smoke detectors and sprinklers Gas fire spread

	SPMT SPMT Conceptual Design Pre PDR	Code: TRP/TELE/001-R Issue: 1.C Date: 24/06/2014 Page: 150 of 152
---	---	--

- Alarm Control Panel
- temperature detectors
- Humidity detectors

Energy

- UPS Systems
- Emergency plant
- Energy Regulator
- Independent boards or UPS for redundancy
- PDUs for distribution of energy in Racks
- Physical or Earth System

Temperature


- Air Conditioning System
- Hot Air Extraction
- Temperature Controls
- Grilles and Air Distribution false floor

Licenses

- Virtualization vmware
- Operating System (Windows, Linux, etc.)
- Design

Additional Recommendations:


- It is recommended the site is on a second floor
- It is recommended that the walls are smooth

	<p style="text-align: center;">SPMT</p> <p style="text-align: center;">SPMT Conceptual Design Pre PDR</p>	<p>Code: TRP/TELE/001-R</p> <p>Issue: 1.C</p> <p>Date: 24/06/2014</p> <p>Page: 151 of 152</p>
---	--	---

- False ceiling and floor made of fire retardant materials.
- Fire retardant paint.
-

Electrical substation and air conditioning for IT site.

- 225 A switch
- 150 KVA Power plant with a cylinder of at least 16 liters of diesel.
- Isolated ground system
- Three 5KVA UPS system and a peak suppressor
- For the air conditioning system, equip of 6 tons of refrigeration (2 equip of 3 tons each) is contemplated.

	<p style="text-align: center;">SPMT</p> <p style="text-align: center;">SPMT Conceptual Design Pre PDR</p>	<p>Code: TRP/TELE/001-R</p> <p>Issue: 1.C</p> <p>Date: 24/06/2014</p> <p>Page: 152 of 152</p>
---	--	---

8. APPENDIX 1

The following table shows the design alternatives resume.

- SPMT 3D model